ZINC ELECTRODE PERFORMANCE

IN

MODIFIED ELECTROLYTE

by

KEVIN BASS

A DOCTORAL THESIS

Submitted in partial fulfillment of the requirements for the award of Doctor of Philosophy of the Loughborough University of Technology, June 1990

Supervisor: Dr P.J. Mitchell

Industrial Sponsor: Lucas Automotive Research Ltd.

"There are three ways to ruin yourself: gambling, women and technology. Gambling is the fastest. Women are the most pleasurable. Technology is the most certain."

President Pompidou.

ACKNOWLEDGEMENTS

I would like to express many thanks to Dr Philip Mitchell for his constant enthusiasm, encouragement and guidance during the course of this work. I also gratefully acknowledge the invaluable financial support given to me by Lucas Automotive Research and the Science and Engineering Research Council.

As for my fellow research students of the Chemistry department, and in particular the electrochemistry group (both past and present), I thank you for making my time spent at Loughborough both interesting and enjoyable. Thanks must also go to other friends in and around Loughborough, especially Cathy, not least for tolerating me during the preparation and writing of this thesis.

Finally I must give special thanks to my parents who have given me their continued support and encouragement throughout my education.

SUMMARY

The high degree of dissolution that zinc undergoes in alkaline electrolytes is widely acknowledged as being a major cause of the problems encountered in secondary battery systems viz. shape change and dendrite growth. Attempts to alleviate these problems have usually centered on modifications to the electrode, electrolyte and/or separator. This thesis describes the effects of modifying the electrolyte on the electrochemical properties of the electrode.

Preliminary evaluation of a number of different electrolyte additives was performed using the classical electrochemical techniques of galvanostatic polarisation, cyclic voltammetry and rotating disc experiments. These methods provided both a quick screening test for assessing a variety of additives, as well as yielding fundamental electrochemical information of the system.

Long term cycling experiments were performed on actual battery electrode pastes in the modified electrolytes which exhibited the most promise in initial screening. These trials revealed that a trade-off in utilisation, cycle-life and dendrite growth prevention has to be made inorder to optimise the system. Addition of fillers, causing an increase in the surface area of the electrode, was found to improve results, P.V.A. proving to give most benefit. Typical cycle-life performance of a zinc electrode with a 10% P.V.A. addition, in a borate modified electrolyte, revealed that even after seventy C/5 charge-discharge cycles, retention of over 50% of initial capacity was obtained, with no dendrite growth.

One electrode additive which did not prove to be succesful was that of graphite, due to excessive hydrogen evolution on recharge. Further investigation of this problem indicated that when zinc can undergo dissolution into solution, and eventually deposit onto the graphite surface, no problem should arise. However in the case of the modified electrolytes, soluble zinc species is minimised, leaving exposed graphite from which hydrogen evolution can occur.

CONTENTS

CHAPTER 1

GENERAL INTRODUCTION AND HISTORICAL BACKGROUND

The principal commercial use of zinc is in the corrosion prevention of iron and steel (galvanising), where zinc is used as a sacrificial anode. Another important application is in electrochemical energy power sources, again operating as the anode. The earliest reported use of zinc in this context was made by Volta [1], in 1800, when he constructed his 'pile' from alternate discs of silver and zinc, separated by absorbent paper or cloth soaked in an electrolyte of caustic or brine. Volta also demonstrated a multi-cell arrangement which consisted of a number of individual cells connected in series. This so called 'crown of cups' set-up, acted as the power source used in the experiments of the pioneer researchers who developed the fundamental electrochemical principles.

Since Volta, the utilisation of zinc electrodes in both primary and secondary cells has continued to develop up to the present day. A brief history is presented here.

The first major advance in the evolution of the zinc anoded battery came in 1836, when Daniell produced his primary cell [2]. This consisted of an amalgamated zinc rod in an electrolyte of dilute sulphuric acid surrounded by a porous pot, which in turn was immersed in a copper cup containing a copper sulphate solution. The cell gave a potential of 1.08V, which was far superior to any previously used, and many variations of it were developed.

One of these variations was the Grove cell [3]. This employed a platinum positive plate in nitric acid and an amalgamated zinc negative in dilute sulphuric acid, separated by a porous clay pot.

Grove also experimented with other electrolyte systems, and was one of the first to investigate alkaline electrolytes.
Another system developed around this time was that of the Leclanché cell, in 1866 [4]. This consisted of a mixture of manganese dioxide and carbon which was packed around a carbon rod current collector, a zinc anode and an electrolyte of ammonium chloride. One obvious advantage this cell had was its cell potential of 1.5V. Improvements made to this system have subsequently led to the extensively utilised zinc-carbon battery.

All the cells described so far have been of the primary type; that is, they can be discharged but not recharged electrically. The first rechargeable system, the lead-acid battery, was also introduced at this time by the French physicist Planté, in 1859 [5]. Although this battery is recognised to suffer from a number of drawbacks such as low power and energy densities, it still continues to dominate the secondary battery market.

In 1881, Lalande and Chaperon [6] patented a cell, which could be credited as being the first alkaline cell. Although the ultimate aim was probably to produce a rechargeable cell, this proved difficult due to solubility problems with copper and zinc in the electrolyte. However, the cell found widespread utilisation as a replacement for the Daniell cell.

The first rechargeable zinc battery system was patented in 1887, by Dun and Hasslacher [7]. They proposed various cathode materials, such as silver oxide and nickel oxide, to be used in conjunction with zinc electrodes.

Michalowski [8] also worked on a similar nickel-zinc secondary system, in the late 1800's. Nevertheless it was not until the time of Junger [9] and Edison [10], that successful secondary alkaline systems became a commercial reality. Working independently of each other, they pioneered the nickel-cadmium and nickel-iron systems respectively. Both of these workers also performed trials

with zinc electrodes, but the high solubility of the zinc caused them to utilise the better alternatives.

This solubility problem promoted the unpopularity of secondary zinc systems for many years to come, although Drumm [11] did have some success in the 1930's, with a zinc-nickel oxide cell providing propulsion for an electric tram.

It was not until 1941 that André reported the next important development for secondary zinc cells [12]. He found that the cycle-life of silver oxide-zinc cells could be greatly improved by the use of appropriate semi-permeable separators, which were based on cellulose. With these membranes the short circuits due to zinc 'trees' were minimised. Thus their introduction must be considered extremely important, with regard to the development of rechargeable zinc cells.

Since then there have been extensive research programs devoted to exploiting the advantages, and overcoming the problems, of secondary zinc electrodes.

Zinc possesses a range of properties which makes it a favourable material for use in electrochemical energy conversion. One of these is the large standard reduction potential for the reaction:

$$Zn \quad \text{--->} \quad Zn^{2+} + 2e^- \qquad E^{\ominus}_{298K} = -0.763V \text{ (vs s.h.e.)}$$

Because this reaction delivers two electrons per atom and the relatively low molecular weight of zinc, the gravimetric energy density is found to be quite high, i.e. 374 Wh kg^{-1}. Zinc is also relatively cheap and non-toxic. These factors have led to the widespread use of primary zinc systems, along with repeated attempts to develop a successful secondary zinc cell. The poor behaviour of zinc as a secondary electrode can be ultimately attributed to its high solubility in strong alkaline electrolytes.

The following are considered to be the most serious obstacles to the adoption of the rechargeable zinc electrode:

i. Dendrite Growth

On discharge a high degree of zinc dissolution occurs, which on subsequent charge does not deposit evenly all over the electrode. Dendrites tend to grow at points of high charge density. These can then pierce the separator, touch the counter electrode, and thus lead to an internal short circuit.

ii. Shape Change/Densification

On repeated cycling, a redistribution of zinc active material from the edges, to the centre of the electrode plate occurs. This process leads to a reduction in the surface area, and capacity, of the electrode, and therefore results in a loss in cycle-life.

Various workers have investigated the causes and effects of shape change, and two mechanisms have been proposed [13-15]. McBreen [13] suggested that concentration cells, generated by differences in secondary current distribution, caused this relocation effect. Choi et al [14,15] proposed an alternative model based on mathematical predictions. This model stated that a convective flow was set up as the result of electro-osmotic phenomenon across the separator. Hendrikx et al [16] have recently reported that neither of the above schemes is completely satisfactory and proposed that shape change is caused by a combination of both these effects.

iii. Nickel Poisoning

On continued cycling at deep discharge, zincate penetrates into the nickel electrode and eventually reprecipitates onto it, as zinc oxide. This results in pore blocking of this electrode, and hence a loss in capacity. Pocket-plate type electrodes suffer the

greatest from this phenomenon. Little research has been performed on this problem, and as yet no remedy has been found.

iv. Zinc Corrosion

This reaction occurs irrespective of whether or not, the cell is being worked. It basically involves zinc reacting with hydroxyl ions to produce zincate and liberate hydrogen. The capacity is thus reduced and serious gassing problems can also arise. The primary battery industry has minimised this effect by amalgamation [17], or more recently by the use of surfactant materials to raise the hydrogen overvoltage e.g. ethoxylated fluoro-alcohols [18].

In spite of these problems the zinc electrode continues to be the object of many investigations, as it still offers a source of relatively cheap power. Various approaches in minimising these problems have been tested and are reviewed in the following chapter.

1.2 Objectives

The principal aim of the work described in this thesis was to develop a secondary zinc electrode which would give good cycle-life, preferably without the need for expensive separators. In order to accomplish this, the problems of shape change and dendritic growth had to be overcome.

The system recently patented by Lucas Industries Ltd. [19], claimed that the incorporation of graphite into the zinc electrode paste made it much less susceptible to shape change and dendritic growth. However, this system is still far from desirable as these problems are only suppressed, rather than removed. Dendrite growth was combatted by use of multi-layer separators, but this is very expensive, and consequently reduces the commercial

viability of the system. Therefore to keep the cost of the system down, the necessity to employ separators should be eliminated.

One possible method of achieving this goal, is to minimise the amount of free zinc species in solution, and retain the 'discharge' product within the vicinity of the electrode. This mechanism is the one which operates in other successful secondary anodes such as lead in sulphuric acid, and cadmium in potassium hydroxide, (though to a lesser extent). Dunning [20] et al has shown that, to effectively store solid reaction products within a porous electrode, operating by a solution diffusion mechanism, the solubility should be around the order of 10^{-4}M. Lower solubilities yield transport rates too low to maintain reaction rates required by most practical applications. Higher solubilities (as in the case of zinc in 7M potassium hydroxide) allow too much mobility on cycling, and hence shape change.

The reduction in solubility of reaction products is generally achieved in secondary batteries, at the expense of active material utilisation. This is because the discharge product is insulating and ultimately passivates the working surface. Therefore to achieve the required capacity of secondary batteries, a large porous electrode, with a high surface area, is required.

This thesis describes the search, and testing, of electrolyte additives to reduce zinc solubility. The application of some of these additives to porous electrode structures in a pre-production evaluation programme was also performed.

CHAPTER 2

GENERAL ELECTROCHEMICAL THEORY

2.1 Electrode - Electrolyte Interphase

On placing an electrode in an electrolyte, a breakdown of electrical neutrality at the phase boundaries occurs. Two layers of opposite electrical charge separated by a few tenths of a nanometre are formed, producing a potential difference across the interphase. This interphase is so called because it is the region between two phases in which the properties have not yet attained those in either bulk phase. Electrode kinetics are greatly influenced by the nature of the electrode-electrolyte interphase, as it is in this region where electrochemical reactions occur.

The earliest, and simplest, model used to describe the electrical conditions across the interphase was proposed by Helmholtz in 1879 [21], who regarded the interphase as two rigidly held planes of equal charges. This model has been modified by various workers to give a much more accurate, but complex, representation.

Helmholtz's model suggested that the solvated ions lined up along the surface of the electrode, and were held away from it at a fixed distance equivalent to the size of their hydration spheres. This structure of charge distribution is analogous to a parallel plate capacitor, and is shown in Fig. 2.1.1.

In his model of the 'double layer' Helmholtz needed to assume that the separated charges were in electrostatic equilibrium, and that the charge in solution near the interphase changed with potential. He also had to assume that changes in the electrode

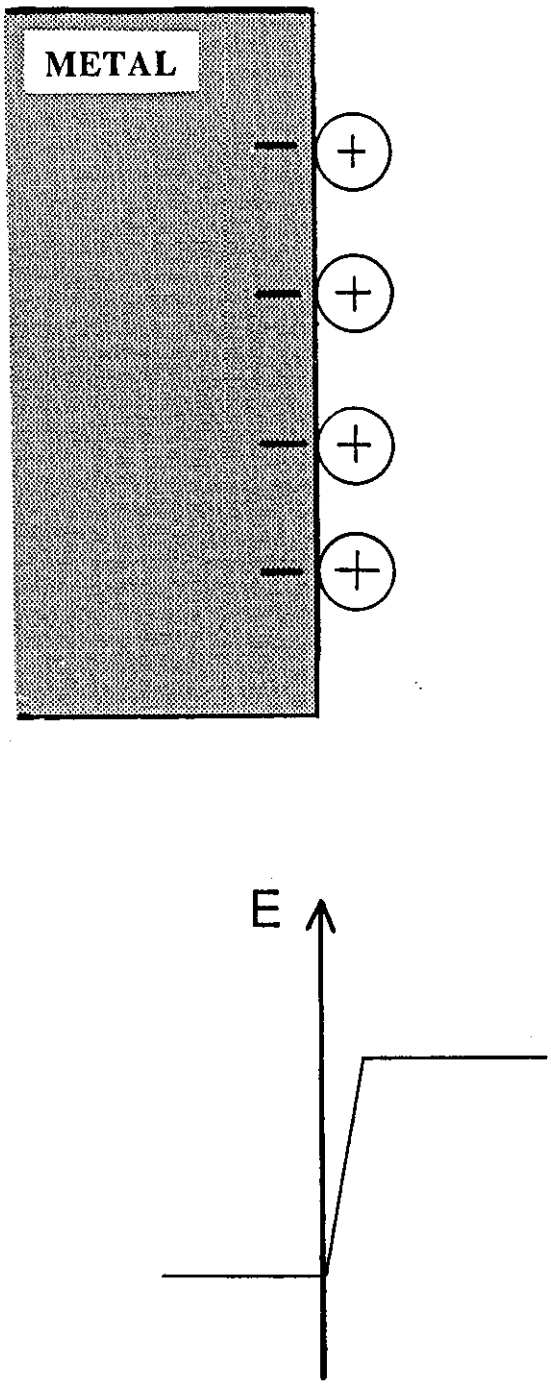

Figure 2.1.1. Helmholtz model of electrode-electrolyte interphase.

potential did not cause charge transfer to occur across the interphase. The implication of these assumptions is that the double layer is purely capacitive, and as such is only applicable to electrodes which are 'ideally polarisable'. The only practical system which approaches this condition is that of the mercury electrode in 1 $mol\,l^{-1}$ HCl between 0.9V (s.h.e.) and the reversible hydrogen potential. The model also proposes that the capacitance is independent of both the potential, and the electrolyte concentration, neither of which is correct.

The Helmholtz model was modified by Gouy [22], who stated that the electrostatic interaction between the field and the charges on the ions would be counteracted by disordering due to random thermal motion. Thus the solution side of the double layer has a diffuse structure in which there is a non-linear fall in potential away from the electrode, as shown in fig. 2.1.2. A similar theory was proposed independently by Chapman [23].

Although this model represented a substantial improvement over the Helmholtz model, discrepancies between the experimental variation of the double layer capacity with concentration and those predicted by theory were found to exist, the later being larger. The reason for these discrepancies was that Gouy and Chapman had considered ions as point charges, which could approach the electrode surface to within infinitely small distances.

The model was further modified by Stern, in 1924 [24], who considered the finite size of the ions. He also recognized the role that ionic adsorption could play at the interface, and proposed a more satisfactory model for the double layer, by using a combination of the concepts of Helmholtz and Gouy. In his model, Stern stated that the ions nearest the electrode are held in a fixed (Helmholtz) plane, to a monolayer thickness. Beyond this plane these ions are dispersed as in the Gouy-Chapman model (i.e. a diffuse layer which extends into the bulk).

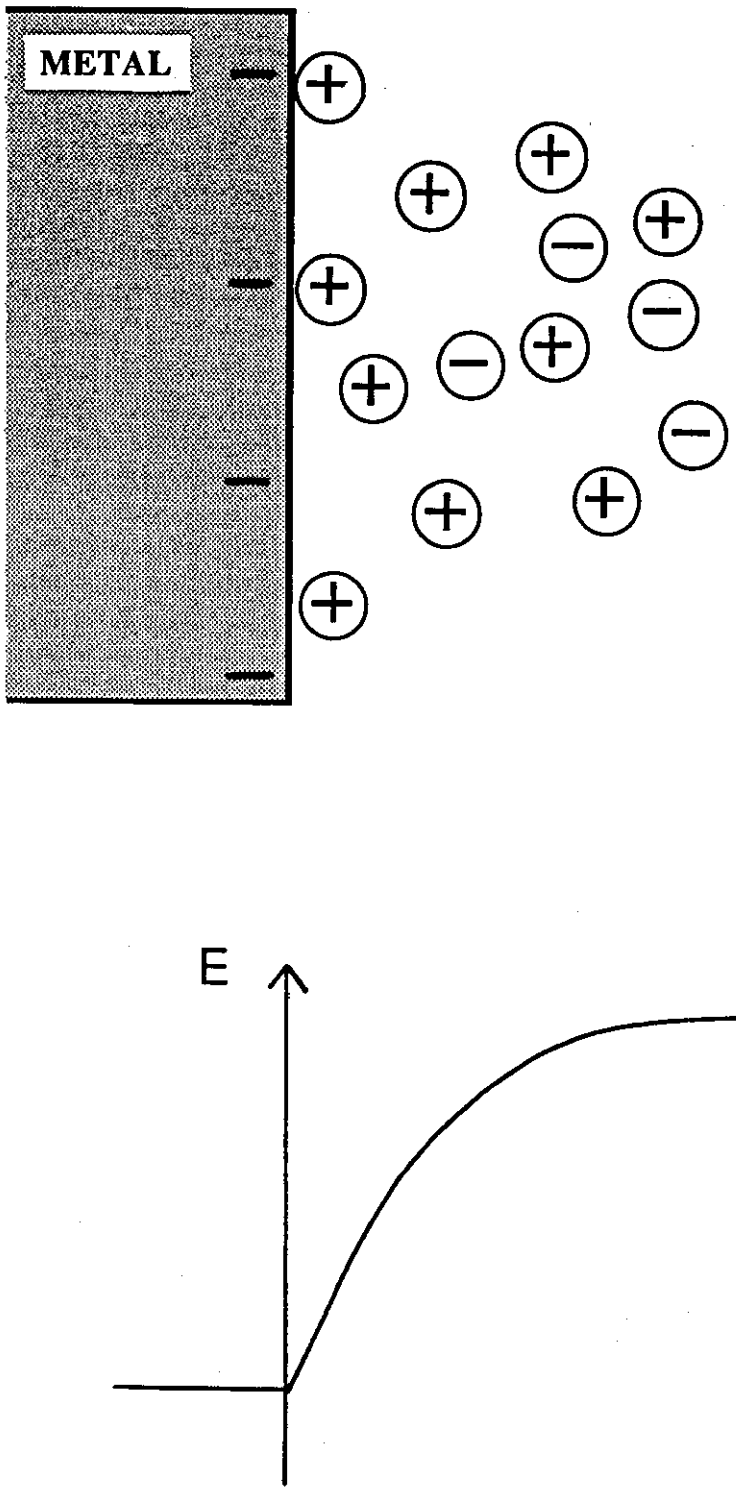

Figure 2.1.2. Gouy-Chapman model of Double Layer.

The compact layer was itself subdivided by Grahame into an inner and outer compact (Helmholtz) plane, as shown in Fig. 2.1.3. The inner Helmholtz plane passes through the centres of specifically adsorbed ions, and the outer Helmholtz plane passes through the centre of the hydrated ion at their distance of nearest approach. Grahame [25] showed that the total double layer capacitance (C_{dl}) could be calculated by considering it as two capacitors in series, such that:-

$$\frac{1}{C_{dl}} = \frac{1}{C_{\text{compact}}} + \frac{1}{C_{\text{diffuse}}} \qquad \text{eq 2.1.1.}$$

It follows that in a dilute solution, and at potentials close to the point of zero charge (p.z.c.), the double layer capacitance is essentially that of the diffuse layer. Whilst at higher concentrations the diffuse layer capacitance is large, and C_{dl} equates to that of the compact (Helmholtz) layer.

More recently Devanathan et al [26] have further developed the Stern model of the double layer, and have postulated the structure shown in Fig. 2.1.4. In this they suggest that the electrode surface is covered by an orientated layer of water molecules, but on certain sites penetration by specifically adsorbed ions, without a hydration shell, may occur. The next layer consists of ions which retain their hydration shell. Thus the inner and outer Helmholtz planes are still defined, although the outer Helmholtz plane is further removed from the electrode, due to the presence of the primary hydration sheath.

2.2 The Charge - Transfer Process

Electrode processes are heterogeneous reactions that occur at the electrode-electrolyte interphase, accompanied by the transfer of charge across the region of the double layer. This charge transferral causes oxidation or reduction to occur and thus can be represented by the general equation:-

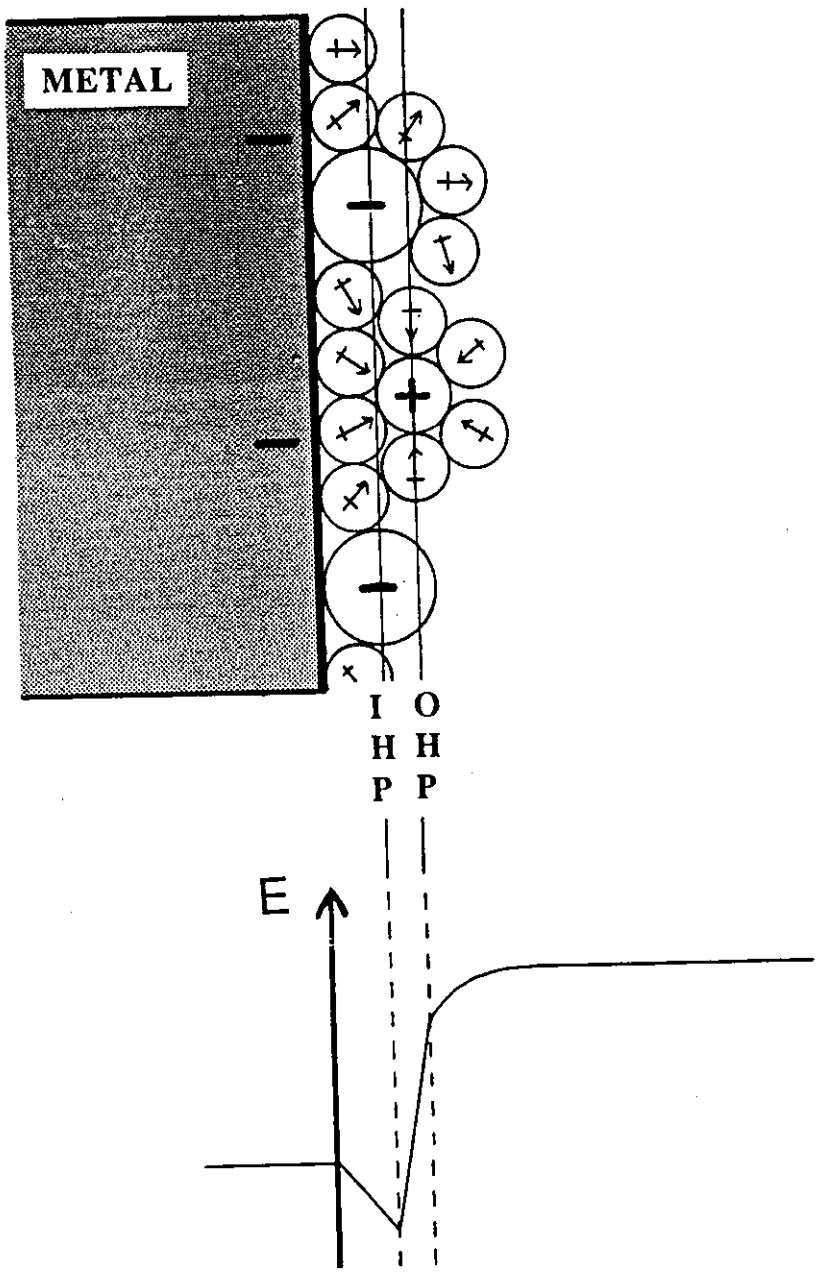

Figure 2.1.3. Grahame model of Double Layer.

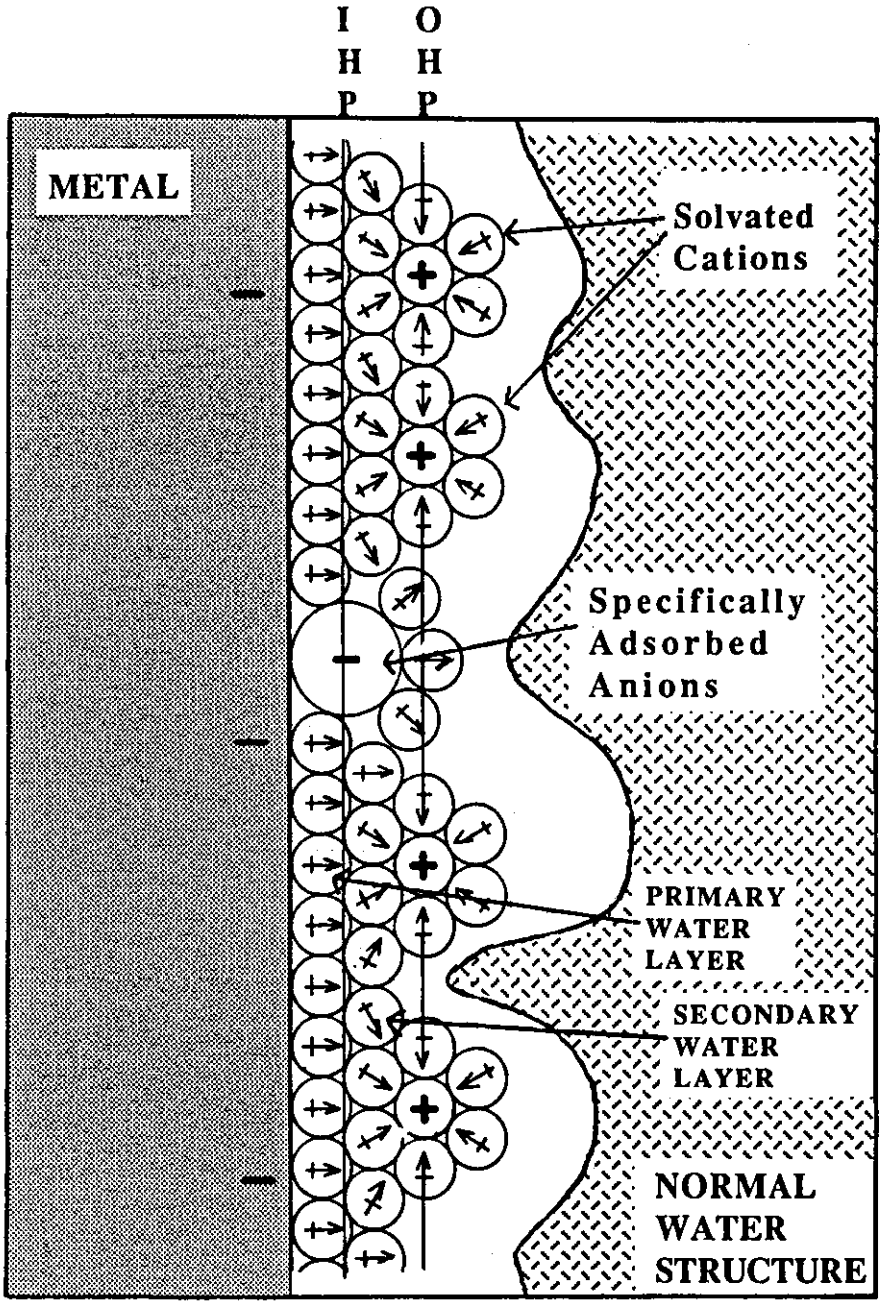

Figure 2.1.4. Devanathan model of the Double Layer

$$O + ze^- \underset{k_b}{\overset{k_f}{\rightleftharpoons}} R \qquad \text{eqn 2.2.1.}$$

where k_f and k_b are the rate constants for the forward and back reactions respectively. If no current has been passed, the surface and bulk concentrations are equivalent, and the equilibrium is characterised by the Nernst equation;

$$E_{eq} = E^{\ominus} + \frac{RT}{zF} \ln \frac{C_o^{\infty}}{C_R^{\infty}} \qquad \text{eq 2.2.2.}$$

where E_{eq} is the equilibrium, or reversible, potential. $E^{\ominus}$ is the standard electrode potential, z is the number of electrons, e, transferred across the interphase, and C_o^{∞} and C_R^{∞} are the bulk concentrations of the oxidised, O, and reduced, R, species respectively. When using the Nernst equation one should correctly use activities rather than concentrations,however so long as this limitation is recognised then concentrations are usually accepted.

The Nernst equation is derived from thermodynamic principles and any consideration of kinetic parameters must predict the same result.

For electrode reactions we require to be able to predict the way in which k_f and k_b vary with potential. One method of achieving this is to consider the shape of the free energy profile, as in Fig. 2.2.1.

If we assign some arbitrary scale to which we can refer, then when E = O the forward and backward activation energies, at this potential, are ΔG^{o}_{f} and ΔG^{o}_{b} respectively. The energy barrier to the reaction is due to the re-orientation, and ultimate removal, of the hydration shell.

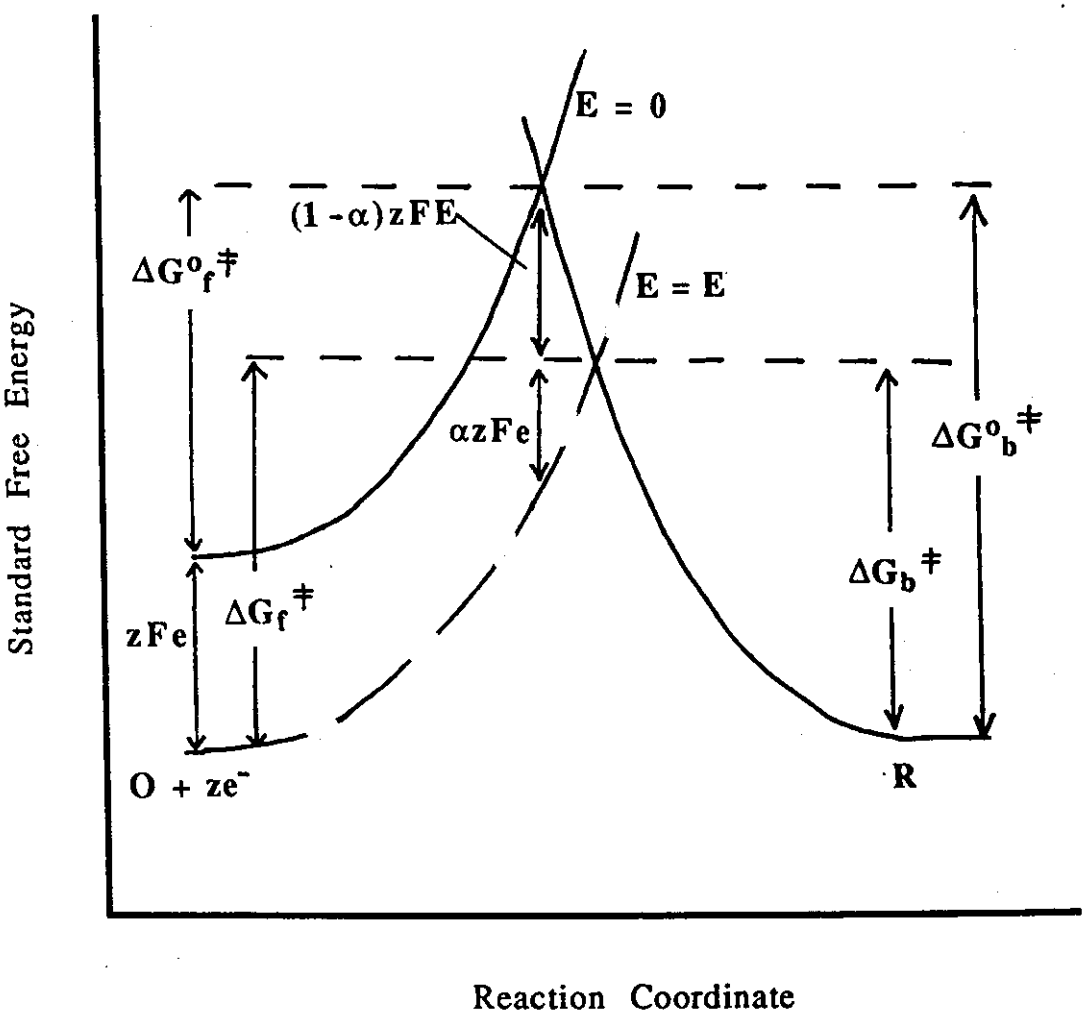

Figure 2.2.1. Potential energy profile for simple redox reaction : $O + ze^- \rightarrow R$

On polarisation to a potential E, the relative energy of the electron on the electrode will change by -zFE. From Fig. 2.2.1. it can be seen that after a positive shift in potential (dashed line) the energy for the forward process is greater than for the backward one. Thus a symmetry factor or charge transfer coefficent, α, must be introduced to account for the variation in energies. The value of α is constant and characteristic of the reaction being considered. It is in the range $O < \alpha < 1$, but it is often close to 0.5 [27].

The Gibbs free energy change of activation for the forward reaction is given by:

$$\Delta G_f^{\ddagger} = \Delta G^{o}_{f}{}^{\ddagger} + \alpha zFE \qquad \text{eqn 2.2.3.}$$

similarly for the reverse reaction:

$$\Delta G_b^{\ddagger} = \Delta G^{o}_{b}{}^{\ddagger} - (1-\alpha)zFE \qquad \text{eqn 2.2.4.}$$

assuming k_f and k_b have an Arrhenius form, both processes can now be expressed as:

$$k_f = A_f \exp^{-}(\Delta G_f^{\ddagger}/RT) \qquad \text{eqn 2.2.5.}$$

and

$$k_b = A_b \exp^{-}(\Delta G_b^{\ddagger}/RT) \qquad \text{eqn 2.2.6.}$$

Expansion of these rates in terms of activation energies gives:

$$k_f = A_f \exp - (\Delta G^{o}_{f}{}^{\ddagger}/RT)_{\exp} -(\alpha zFE/RT) \qquad \text{eqn 2.2.7.}$$

and

$$k_b = A_b \exp - (\Delta G^{o}_{b}{}^{\ddagger}/RT)_{\exp} (1-\alpha)zFE/RT) \qquad \text{eqn 2.2.8.}$$

These expressions have both potential dependent and independent terms. When E = O (on our arbitrary scale), the potential independent terms are equal to the rate constant, and are represented by k_f^o or k_b^o, giving:-

$$k_f = k_f^o \exp^{-\alpha zFE/RT} \qquad \text{eqn 2.2.9.}$$

and

$$k_b = k_b^o \exp(1-\alpha)\, zFE/RT \qquad \text{eqn 2.2.10.}$$

When the electrode is in equilibrium with a solution which has $C_o^\infty = C_R^\infty$, then $E = E^\ominus$ and $k_f C_o^\infty = k_b C_R^\infty$. This implies $k_f = k_b$ and that:

$$k_f^o \exp -\alpha zFE^\ominus/RT = k_b^o \exp (1-\alpha)zFE^\ominus/RT = k^\ominus \qquad \text{eqn 2.2.11.}$$

where $k^\ominus$ is known as the standard or intrinsic rate constant and is the value of k_f and k_b at $E^\ominus$, its size being a measure of the rate equilibrium of a system will be attained. Substitution for this term allows the removal of the potential independent term thus:

$$k_f = k^\ominus \exp^{-\alpha zF(E-E^\ominus)/RT} \qquad \text{eqn 2.2.12.}$$

and

$$k_b = k^\ominus \exp(1-\alpha)zF(E-E^\ominus)/RT \qquad \text{eqn 2.2.13.}$$

In electrochemistry it is generally easier to deal in terms of current rather than rate constants.

$$i = zFkC \qquad \text{eqn. 2.2.14.}$$

However only the net current is measured, which is a result of

contributions from both the forward and reverse reactions thus:

$$i = i_f - i_b \qquad \text{eqn 2.2.15.}$$

substitution yields:

$$i = zF\,(k_f C_{ot} - k_b C_{Rt}) \qquad \text{eqn 2.2.16.}$$

where C_{ot} and C_{Rt} are the concentrations of the oxidised and reduced species at the electrode surface at time t. Hence

$$i = zF[k^{\circ} C_{ot} \exp(-\alpha zF(E-E^{\circ})/RT) - k^{\circ} C_{Rt} \exp((1-\alpha)zF(E-E^{\circ})/RT)] \qquad \text{eqn 2.2.17.}$$

This is known as the Butler-Volmer equation and it, or a variation, is extremely important in electrochemical kinetics.

At the equilibrium, E_{eq}, of a system the net rate of reaction and the current, is zero. (It must be remembered that this is a dynamic equilibrium, and that charge is being donated and accepted by the system continuously). Therefore:

$$i_o = i_f = i_b \qquad \text{eqn 2.2.18.}$$

where i_o is the exchange current density, and is a measure of the electrode reversibility (high i_o = very reversible), also $E - E_{eq} = \eta$, the overpotential.

Substitution for all these factors simplifies eqn 2.2.17 greatly, giving the Erdy-Gruz and Volmer equation:

$$i = i_o\,[\exp -\alpha zF\eta/RT - \exp(1-\alpha)zF\eta/RT] \qquad \text{eqn 2.2.19.}$$

This applies when a solution is well stirred or when the currents are kept low, so that the surface concentrations do not differ appreciably from the bulk.

The Erdy-Gruz and Volmer equation can be further simplified by considering different overpotential situations:

a) low overpotentials

For an electrode at a very low overpotential ($\eta \leq 10$ mV),

$$\eta << \frac{RT}{\alpha z F} \quad \text{or} \quad \eta << \frac{RT}{(1-\alpha) z F}$$

The current density is a linear function of overpotential. Since α is small, the exponential in eqn 2.2.19. may be expanded using the series $e^x = 1+x$. Using just the first two terms (as the remaining ones become insignificant) gives:

$$i = i_o [1 + (-\alpha z F \eta/RT) - i_o (1+(1-\alpha) z F \eta/RT)] \qquad \text{eqn 2.2.20.}$$

Hence $i = i_o \frac{(-z\eta F)}{RT}$ eqn 2.2.21.

Therefore $i_o = -\frac{RT}{zF} \cdot \frac{i}{\eta}$ eqn 2.2.22.

The net current is thus a linear function of both exchange current and overpotential

b) high overpotentials

At high overpotentials ($\eta > 100$ mV),

$$\eta >> \frac{RT}{\alpha z F} \quad \text{or} \quad \eta \gg \frac{RT}{(1-\alpha) z F}$$

thus only one term in eqn 2.2.19. is significant.

At high cathodic (negative) overpotentials the second term in the Erdy-Gruz and Volmer equation becomes negligible, therefore:

$$i = i_o \exp^{-\alpha zF\eta/RT} \qquad \text{eqn 2.2.23.}$$

and by taking logarithms gives

$$\ln i = \ln i_o - \alpha zF\eta/RT \qquad \text{eqn 2.2.24.}$$

Thus

$$\eta = \frac{RT}{\alpha zF} \ln i_o - \frac{RT}{\alpha zF} \ln i \qquad \text{eqn 2.2.25.}$$

which may be written in the form of a Tafel relationship

$$\eta = a + b \ln i \qquad \text{eqn 2.2.26.}$$

Thus a plot of ln i vs η, a so called Tafel plot, is linear with slope , b , equal to $-\frac{\alpha zF}{RT}$ and intercept , a , equal to $\ln i_o$.

Similarly at high anodic (positive) overpotentials

$$i = i_o \exp (1-\alpha)zF\eta/RT \qquad \text{eqn 2.2.27.}$$

which gives

$$\eta = \frac{RT}{(1-\alpha)zF} \ln i_o + \frac{RT}{(1-\alpha)zF} \ln i \qquad \text{eqn 2.2.28.}$$

with slope equal to $\frac{(1-\alpha)zF}{RT}$ and intercept as before ($\ln i_o$).

It must be remembered that the equations presented above will

only apply when electron transfer is the sole determining step in the overall reaction sequence.

2.3. Mass Transport Processes

The redox reaction at an electrode surface can be represented by the general equation:

$$O + ze \underset{k_b}{\overset{k_f}{\rightleftharpoons}} R \qquad \text{eqn 2.3.1.}$$

This process can be considered to occur in three stages:

i. $O_{bulk} \longrightarrow O_{electrode}$ eqn 2.3.2.

ii. $O_{electrode} \longrightarrow R_{electrode}$ eqn 2.3.3.

iii. $R_{electrode} \longrightarrow R_{bulk}$ eqn 2.3.4.

If the slowest step is that of electron transfer i.e. eqn 2.3.3., then the reaction is charge transfer controlled, and the reaction is governed by the kinetic factors outlined previously.

If however the rate of removal from, or supply to, the electrode surface of a species is the slowest step, then the overall reaction is mass transport controlled or limited. Occasionally none of the above processes are as slow as a chemical transformation of an

electroactive species, which then becomes the rate determining step.

Three forms of mass transport are normally considered:- migration, diffusion and convection. The Nernst-Plank equation can be used to define the mass transport parameters, such that:

$$J_j = - D_j \bar{\nabla} c_j - \frac{z_j F}{RT} D_j c_j \bar{\nabla} \phi + C_j \upsilon \qquad \text{eqn 2.3.5.}$$

Diffusion Migration Convection

where J_j is the flux of species j (mol s^{-1} cm^{-2}), D_j is the diffusion coefficent (cm^2 s^{-1}), ϕ is the electrostatic potential, z_j and c_j are the charge and concentration of species j respectively, and υ is the velocity profile (cm s^{-1}). $\bar{\nabla}$ is the vector operator and is defined as

$$\bar{\nabla} = \frac{i\partial}{\partial x} + \frac{j\partial}{\partial y} + \frac{k\partial}{\partial z} \qquad \text{eqn 2.3.6.}$$

i, j and k being the unit vectors.

For this discussion it is better to deal with each mass transport mode separately.

a. Migration

This is the movement of a charged particle in the influence of an electrical potential gradient. The contribution of migration can be greatly reduced by the use of a large excess of inert supporting electrolyte, which carries most of the current. This causes the transport numbers of the electroactive species in solution to effectively become zero. Therefore the $\bar{\nabla}\phi$ term in eqn 2.3.5. is negligible.

b. Convection

Convection generally arises in two distinct ways. It may be free (natural) or forced.

Natural convection will always occur, to some extent, in a solution undergoing electrolysis. It arises from local density changes within the vicinity of the electrode, causing an influx of ions from the surrounding electrolyte. These density changes may have both thermal and mechanical contributions.

Forced convection can be achieved by agitating the electrolyte in some way, such as stirring, bubbling gas, rotating the electrode etc. This minimises natural convection as it ensures thorough mixing of any local density differences.

c. Diffusion

This is the movement of a species under the influence of a concentration gradient. Since such a gradient develops as soon as an electrode reaction begins, diffusion will occur in all such reactions, to some degree.

Diffusion is described by Fick's Laws:-

When considering a planar electrode immersed in a static electrolyte (free from both migration and convection) undergoing a redox reaction, the number of molecules of O which diffuse past cross-sectional area, A, in time, dt, is proportional to the concentration gradient of the diffusing species. This is a statement of Fick's first law:

$$\frac{dN}{dt} = A D_O \frac{\partial C_O}{\partial x} \qquad \text{eqn 2.3.7.}$$

D_o is the diffusion coefficent, and its magnitude depends on the size of the diffusing species and the velocity of the solvent.

$\frac{dN}{Adt}$ is known as the flux, q eqn 2.3.8.

Fick's second law relates non-steady-state, i.e. time dependent conditions; and describes the rate of change of concentration $\frac{\partial C_o}{\partial t}$, at a point x thus:

$$\frac{\partial C_{o(x,t)}}{\partial t} = D_o \frac{\partial^2 C_{o\,(x,t)}}{\partial x^2} \qquad \text{eqn 2.3.9.}$$

Boundary conditions can be applied to this equation in order to determine the value of $\frac{\partial C_o}{\partial t}$. These are:-

i $C_{o\,(o,t)} = 0$ at $t > 0$

ii $C_{o\,(x,t)} \dashrightarrow C_o^{\infty}$, as $x \dashrightarrow \infty$

iii $C_{o\,(x,t)} = C_o^{\infty}$ at $t < 0$

where C_o^{∞} is the bulk concentration of 0 and $C_{o\,(o,t)}$ is the concentration at the electrode surface.

Solution of the differential equation 2.3.9. with these boundary conditions ultimately yields the Cottrell equation:

$$i_d\,(t) = \frac{zFAD_o^{1/2} C_o^{\infty}}{\pi^{1/2} t^{1/2}} \qquad \text{eqn 2.3.10.}$$

which shows how the diffusion limited current at a stationary planar electrode varies with time.

2.4. Electrocrystallisation

The formation of a solid phase occurs in many electrode reactions. Either as the result of reduction of ions in solution (as in the case of metal deposition) or by oxidation of the electrode and subsequent reaction with ions present in the electrolyte to form an anodic film. The term given to such phenomena is electrocrystallisation.

In these processes either a new solid phase is formed, or one already present grows or disappears. To account for these processes one must also take into consideration factors such as crystallisation, as well as the electrochemical kinetics described previously.

The process of deposition proceeds via two distinct phases. Initially the deposition must occur on the surface of a substate which may be different to the depositing layer. Thickening of this layer then follows which eventually leads to a macrodeposit. These two stages will be discussed separately.

Electrocrystallisation has features analogous to other kinds of crystallisation, for example the electrode overpotential replacing the solution supersaturation required to bring about the stability needed for crystal formation. The nucleation and early stages of growth of the deposit are very important, since they determine the structure of the initial layer and hence influence the final electroplate morphology and properties.

The growth of crystals occurs by the incorporation of atoms into the crystal lattice. This process is dependent on the crystallographic character of the growing surface and is largely affected by the surface structure itself. The surface of a solid metal electrode is very complex in character, with crystal defects, adsorbed molecules, oxide layers etc all being present to some

extent. Thus for ease of understanding the processes involved it is best to assume, to begin with, perfect crystal structure.

Kossel [28] proposed a model of crystal growth based on a "Kink Site" model. This model states that growth occurs by atoms adsorbing onto the regular crystalline lattice, diffusing along the surface as an adsorbed species, or adion, until it reaches a step on the surface. This adion then travels along the step until it meets a kink, and it is here where the atom adds into the surface lattice. Stranski [29] further developed this model into the kink site model, as illustrated in Fig. 2.4.1.

From this model it is clear that the incorporation of atoms are most probable at a kink site (where the atom can interact with three neighbours). Some incorporation may also take place at edge sites, where there are two neighbours. Adatoms have only one neighbour and thus generally redissolve. Therefore an essential condition for crystal growth is the generation of an edge at which growth can proceed. In general, this requires the formation of nuclei so that growth can occur at their peripheries.

The kink site model developed by Kossel and Stranski does not fully cover the situation of electrochemical nucleation. This is because, in this case, it is possible that the charge transfer reaction will produce a species which carries some residual charge, for this reason lattice growth must involve the surface diffusion of these.

However the main problem of this model is that the surface of a real solid is not perfect, and contains many defects, as already mentioned. Frank [30] was first in recognising that screw dislocations are one of the most important defects involved in crystal growth. These dislocations are the cause of the crystal face being deformed in such a way that a monatomic step originates from a point in the face where the screw-dislocation line intersects the surface at the crystal face. During the crystal growth the shape of the dislocation is preserved, only its direction

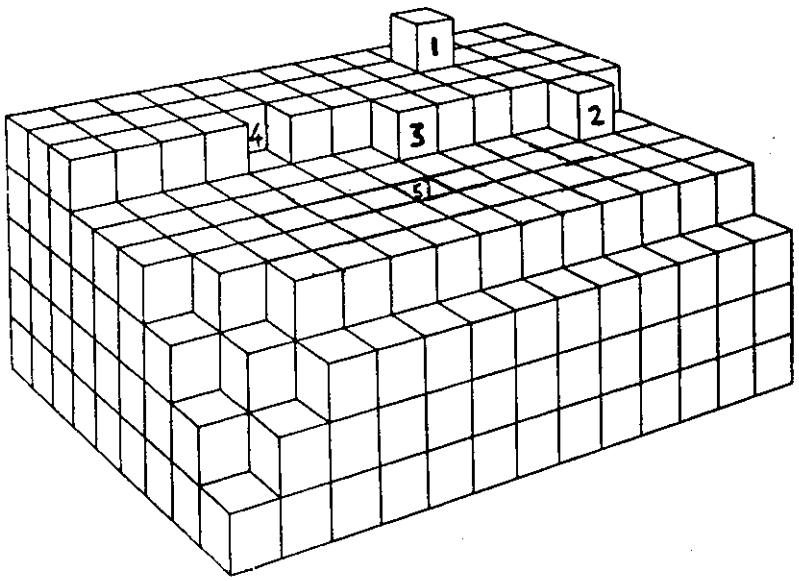

1. Adsorbed atom at surface site.
2. Edge (step) site.
3. Kink site.
4. Edge vacancy.
5. Surface vacancy.

Figure 2.4.1. Kossel-Stranski model of crystal growth.

changes. Together with Burton and Cabrerà's [31] analysis of the atomic nature of the growing surface, the theory of crystal growth at screw dislocations was soon developed - this process is illustrated in fig 2.4.2.

Fleischman, Thirsk and Harrison [32,33], extended this theory to the electrochemical case. They studied the deposition of a new phase under potentiostatic conditions and found that two types of nucleation are distinguishable; instantaneous and progressive. Instantaneous nucleation occurs when all possible sites for nucleation are taken up at the beginning of the electrolysis and further nucleation can be ignored i.e. nucleation time short compared to growth. Progressive nucleation consists of nuclei appearing continually with time, at a constant rate of formation. Since the adoption of this model, the theory of electrochemical nucleation has virtually remained the same.

Following nucleation the growth of a layer can be regarded to consist of at least three steps:-

i. Mass transport of the metal-bearing species to the surface.
ii. Formation of an adion by an electron transfer process
iii. Diffusion of an adion across the surface to a position within the lattice.

The relative rates of (ii) and (iii) largely determine the structure of the growing layer. The current density also effects the structure of this layer. At high current densities surface diffusion (iii) is no longer fast when compared to electron transfer, and the layer becomes less ordered, giving a mossy or dendritic growth.

In the case of anodic dissolution, films are often formed on the metal surface, film growth following the same pattern as metal deposition with nucleation and spiral growth playing analogous roles. The films can either be discontinuous, which are often

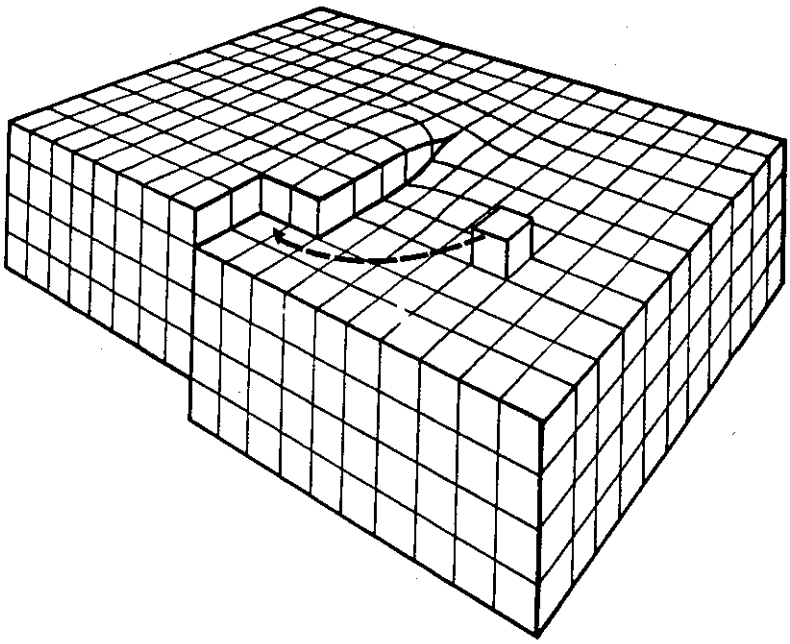

Figure 2.4.2. Screw dislocation model of crystal growth

formed by the precipitation of insoluble salts on the surface of the electrode, or continuous.

Continuous films are characterised by their small thickness (10^{-4} cm) and high specific resistance (10^{-6} Ω cm). Both types of film inhibit metal oxidation, particularly continuous ones, and cause so-called passivation.

2.5. Linear Potential Sweep and Cyclic Voltammetry

This technique involves the sweeping of the electrode potential from an initial value E_1, to another potential E_2, at a known rate, υ, by the application of a linear potential time sweep. At any time between these limits the potential is given by:-

$$E = E_1 - \upsilon t$$

The resultant i - E responses are noted. If the sweep is halted at potential E_2 the technique is known as linear sweep voltammetry (L.S.V.), however if the sweep is reversed (and may be repeated) the technique is known as cyclic voltammetry (C.V.).

The technique was first utilised by Matheson and Nichols [34] and the fundamental equations relating to it have been developed by Randles [35] and Sevcik [36]. More recently Nicholson and Shain [37] have considered the theoretical aspects of the technique in great detail. The technique is often used for the preliminary investigation of a new electrochemical system, as it is a simple and easy procedure to perform, which can provide details of charge transfer reactions and their mechanisms.

The generation of a current peak at a characteristic potential for the reaction occurring, is the basis of the whole technique. The position and shape of the peak is dependent on many factors, such

as sweep rate, electrode and solution composition, and their concentrations, under steady state conditions Sweep rates can vary greatly from only a few mV s^{-1} to a few hundred V s^{-1}. The slow sweep rates allow surface relaxation to occur so that a true 'steady-state' is approached. Very high sweep rates are used to detect the existence of any short lived species in the system.

Linear potential sweep experiments can be used to obtain accurate quantitative kinetic information. This is not so for cyclic voltammetry, where complex concentration gradients arise, invalidating the derived equations, which apply only if there are no gradients prior to sweeping. For this reason cyclic voltammetry is better suited to a qualitative role of identification and detection of species during the reaction. Nicholson and Shain have reviewed the various reaction schemes [37].

On following the i - E response (voltammogram) for a simple reversible reaction of the following type:-

$$O + ze^- \quad \longrightarrow \quad R$$

Assuming O is initially present in solution, on shifting the potential we obtain a resultant profile as in Fig. 2.5.1. Before point A the potential applied too low to cause the reduction of any of O. When the electrode potential reaches the vicinity of E_o, point A, the species begins to be reduced and the current rises rapidly in accordance with the Erdy-Gruz and Volmer equation. Thus kinetic parameters can be derived at the base of the peak. As the potential continues to grow more negative, the diffusion processes begin to limit the current (as the ions are reduced at a faster rate than they can be supplied to the electrode surface).

This situation continues until the depletion in the surface concentration effectively reaches zero and the concentration gradient starts to decrease, giving a peaked response.

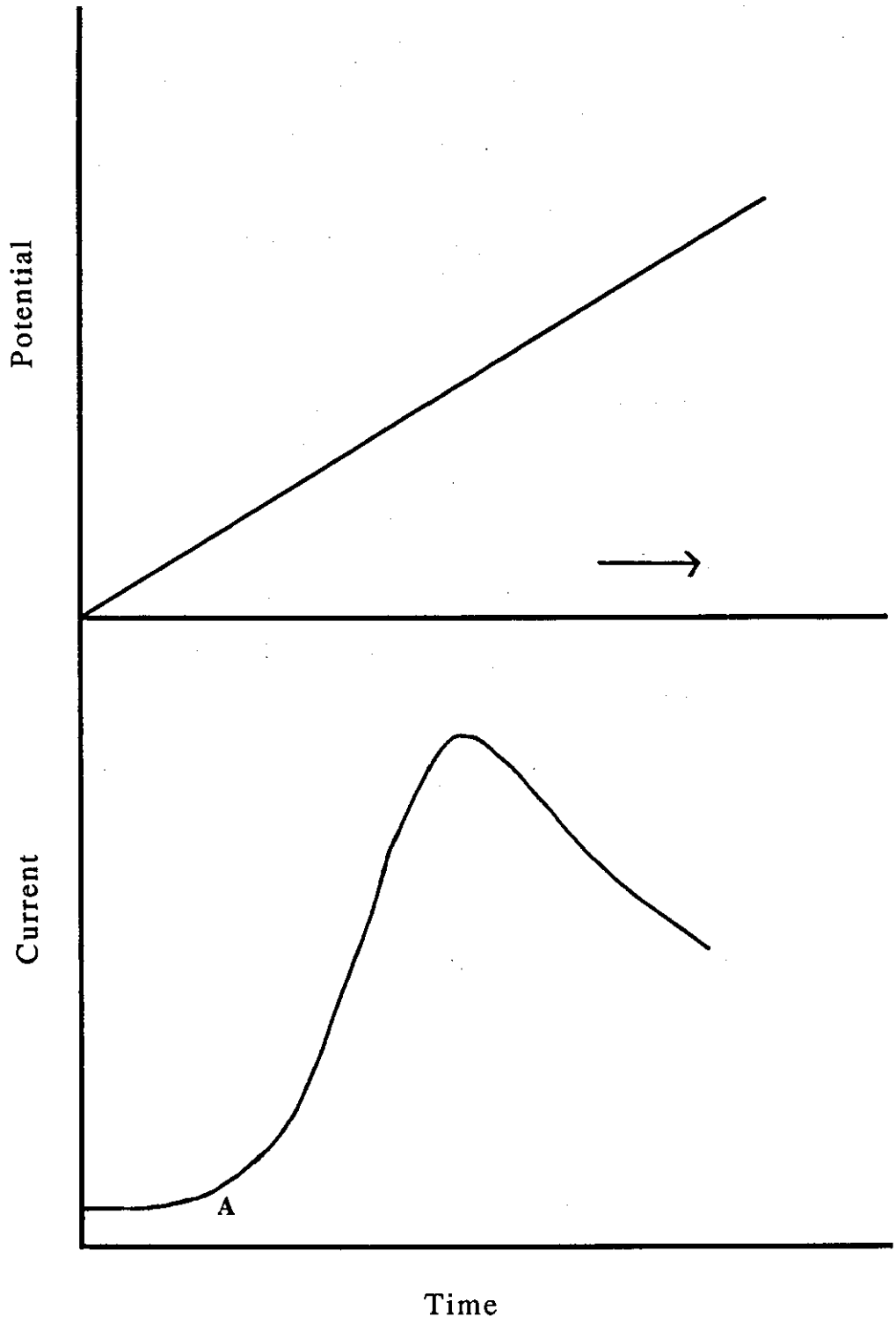

Figure 2.5.1. Typical i-E response for a simple redox reaction.

For a simple electron transfer process, increasing the sweep rate causes the peak current density, i_p, to also increase, at the corresponding potential, E_p. If the rate of charge transfer at the electrode surface is fast enough to maintain the Nernst equilibrium, then we call the reaction reversible. For this case the peak current density (A cm^{-2})for a cathodic sweep is given by the Randels - Sevcik equation:

$$i_p = - 2.69 \times 10^5 z^{3/2} C_o^{\infty} D^{1/2} \upsilon^{1/2} \quad \text{(at } 25^o \text{ C)} \qquad \text{eqn 2.5.1.}$$

where C_o^{∞} is the concentration of oxidised species in the bulk solution (mol cm^{-3})
and D is the diffusion coefficient (cm^2 s^{-1})

For reversible reactions it is also noted that the peak potential, E_p, is independent of sweep rate i.e. completely diffusion controlled. The peak potential is related to the polarographic half-wave potential by:

$$E_p = E_{1/2} - \frac{1.109\ RT}{zF} \qquad \text{eqn 2.5.2.}$$

where $E_{1/2}$ is the potential at $i - i_{p/2}$

If a reverse sweep is made, the separation between the cathodic and anodic peaks is governed by the number of electrons transferred, thus:

$$\Delta E_p = E_p{}^A - E_p{}^C = 59/z \ \text{mV} \qquad \text{eqn 2.5.3.}$$

Another characteristic feature of a reversible reaction is that :

$$i_p{}^A / i_p{}^C = 1$$

Under totally irreversible conditions the reaction rate is slow compared to the sweep rate, and the Nernstian response can no

longer be assumed. The peak current position can thus change with varying sweep rate and the Randels-Sevcik equation is modified to:

$$i_p = -2.99 \times 10^5 z \left(\frac{2.3RT}{bF}\right)^{1/2} D^{1/2} C_o^{\infty} \upsilon^{1/2} \qquad \text{eqn 2.5.4}$$

where b is the Tafel slope.

As already stated the peak potential can vary with sweep rate and is given by:

$$E_p = E_{1/2} - b\,(0.52 - 1/2 \log \frac{b}{D} - \log k_S + 1/2 \log \upsilon) \qquad \text{eqn 2.5.5.}$$

where k_S is the specific rate constant at the standard electrode potential.

The dependence of E_p on υ is therefore very useful in determining the reversibility of the system. These relationships all hold for continuous cycling of the electrode, although as stated earlier, all quantitative measurements should be made from the first sweep at a clean electrode, since the n th sweep may differ significantly from the first; hence cyclic voltammetry's qualitative nature.

2.6. The Rotating Disc Electrode

The rotating disc electrode technique is particularly useful in discriminating between the rate controlling factors of mass transport and charge transfer (or associated chemical reactions).

The technique is one of the few forced convective electrode systems for which a complete solution of the hydrodynamic equations has been made.

The electrode consists of a disc of the material under study embedded in a rod of insulating material. The disc, as the technique's name implies, is rotated setting up a steady-state where electrolyte is continually being brought to, or away from, the electrode surface. Thus a well defined diffusion layer is created.

Levich [38] showed that for laminar flow the boundary layer thickness, δ, was dependent on the angular velocity of the electrode, ω, such that:

$$\delta = 1.61\ D_o^{1/3}\ \upsilon^{1/6}\ \omega^{-1/2} \qquad \text{eqn 2.6.1.}$$

where ω = angular frequency, rad s^{-1}

D_o = Diffusion coefficent, $cm^2\ s^{-1}$

υ = Kinematic viscosity (viscosity/density), $cm^2\ s^{-1}$

Hence, as the angular velocity increases the boundary layer thickness decreases. The relationship holds between 100 - 10,000 r.p.m. At lower values of ω natural convection becomes significant, whilst at higher values turbulence becomes problematic.

As stated above the rotating disc is capable of distinguishing between mass transport and charge transfer control. For the reduction of species, O:

$$i = \frac{zFC_o^{\infty} k_f}{1 + 1.61\ k_f\ \omega^{-1/2}\ \upsilon^{1/6}\ D_o^{-2/3}} \qquad \text{eqn 2.6.2}$$

At large overpotentials mass transport is the controlling process and the current is dependent on the rotation speed, and is given

by the Levich equation:

$$i = 0.621\ z\ F\ D_0^{2/3}\ \upsilon^{-1/6}\ C_0^{\infty}\ \omega^{1/2} \qquad \text{eqn 2.6.3.}$$

Thus a plot of i vs $\omega^{1/2}$ is linear and passes through the origin.

At small values of k_f electron transfer becomes the rate determining step and eqn 2.6.2 becomes:

$$i = zF\ k_f\ C_0^{\infty} = i_{\infty} \qquad \text{eqn 2.6.4.}$$

i_{∞} = current at infinite rotation speed.

Thus current is independent of rotation speed.

For cases when mixed control occurs then the full form of eqn 2.6.2. must be used, though it is usually rearranged as:

$$-\frac{1}{i} = \frac{1}{zFk_f\ C_0^{\infty}} + \frac{1.61\ \upsilon^{1/6}}{zFD_0^{\ 2/3}\ C_0^{\infty}\ \omega^{1/2}} \qquad \text{eqn 2.6.5.}$$

A plot of $-i^{-1}$ vs $\omega^{-1/2}$ should be linear and the value of k_f obtained from the intercept.

Thus using these solutions the rotating disc electrode technique can determine kinetic data from experimental results.

CHAPTER 3

REVIEW OF METHODS FOR THE ELIMINATION OF SHAPE CHANGE AND DENDRITE GROWTH

3.1 Introduction

The reactions and electrochemistry of zinc in alkaline electrolytes has been the subject of a number of previous reviews [39-44]. Some of the properties that make zinc such an attractive material in primary system have, however, hindered its adoption in secondary systems. The main cause of these drawbacks is the high solubility of zinc in the strong alkaline electrolyte normally employed in these secondary systems. This problem manifests itself in two main forms of failure mechanism, i.e. shape change (a redistribution of active material culminating in capacity losses) and, dendritic growth promoting eventual cell failure due to short circuiting. These drawbacks lead to poor cycle-life, particularly when compared to rival systems such as lead-acid and nickel-cadmium.

Considerable research effort has been spent on discovering ways of either eliminating, or at least minimising, the effects of these problems. The research can be divided into four distinct categories, viz:-

i.) Additions to the electrode
ii.) Additions to the electrolyte
iii.) Development and improvement of separators
iv.) Miscellaneous techniques such as; pulse charging, vibrating the electrode, flowing electrolyte

This review will attempt to indicate which methods have found most favour in the battery industry in recent years. Although, it must be noted that many of the approaches have been employed, in some form or another, for several years. At the same time, the

electrochemistry and theory behind certain methods will be explained.

i. Electrode Addition

The incorporation of an additive within the active material of the electrode, during its fabrication, is an extensively used method of zinc cycle-life enhancement. One of the most commonly used additives, in both primary and secondary systems, is that of mercury [17,40,45]. It has long been known that in aqueous alkali, dissolution of zinc and the evolution of hydrogen occur simultaneously (as the anodic and cathodic reactions responsible for 'self-discharge'). This corrosion of the zinc active material is obviously detrimental to the performance of the battery, causing a reduction in capacity, and therefore has to be minimised. This can be achieved by the addition of an inhibitor which possesses a hydrogen overvoltage which is higher than that of zinc.

Mercury is one such additive chosen to perform this role, typically 1-4% of the paste weight, in the form of the oxide (HgO). For the purpose of inhibiting self-discharge, mercury has been found to be extremely effective [45-48]. Unfortunately the effect of amalgamation has also been found to be detrimental on the cycling performance of zinc anodes. In particular, it has been reported that the rate of shape change increases with the addition of this metal. Thus, a considerable amount of research has been undertaken into finding a suitable substitute for mercury, that would also be capable of reducing the rate of self-discharge whilst not accelerating the rate of shape change (and hopefully retarding it) [48,49].

The effect of various additives in pasted zinc electrodes has been studied in great detail by McBreen et al [50,51]. He found that the most successful additives were heavy metals (e.g. Pb, Cd, Tl and In), added to the paste mix in the form of their oxide/hydroxides,

(which are reduced to the metal prior to the reduction of zincate). The beneficial effect of these additives on shape change was attributed to a substrate effect, and that additives such as PbO, $In(OH)_3$ and Tl_2O_3 increase the polarisability of the electrode, which in turn improves current distribution and decreases shape-change. The adverse effect of HgO was attributed to a decrease in polarisability.

Himy and Wagner [48,49] also found that mercury greatly increased shape change, and that lead, cadmium and thallium decreased it in agreement with the results of McBreen et al [50,51]. In addition they performed tests on paste formulations which contained two additives in combination with each other. Using such mixtures shape change considerably decreased, due to a synergistic relationship occurring with these binary compounds. Despite these findings, and the drawbacks associated with mercury, it still finds a high level of use due to its excellent corrosion inhibiting properties. The latter effect usually outweighing any deleterious effects on shape change. However, there is currently a trend amongst battery manufacturers to replace mercury with other metals such as thallium and indium [48-50].(See also; tables at end of this chapter).

Another series of additives which have received attention in recent years, is that of the alkali earth metal oxides or hydroxides. Of these the most promising, at the present time, is calcium. The chemistry of zinc electrodes containing calcium hydroxide has been the subject of many investigations [52-57].

The improvement in cycle-life observed in calcium containing electrodes can be attributed to the formation of calcium zincate, $Ca(OH)_2.2Zn(OH)_2\ 2H_2O$, which is insoluble [55]. Thus, the migration of zincate away from the electrode is minimised, which in turn decreases shape change. However, the incorporation of $Ca(OH)_2$ can result in a decrease in zinc utilisation, and it has been reported that for optimum efficiency the molar ratio of

$Ca(OH)_2$ to ZnO is greater than 0.5 to one [56]. Magnesium and aluminium hydroxides are also thought to function in a similar manner to calcium i.e. by forming an insoluble species which prevents migration of the zincate species.

Another electrode additive which has been found to give beneficial effects on cycling is up to 10% bismuth oxide, Bi_2O_3 [58-60]. McBreen [58] suggested that one reason for this improvement was due to the crystal growth at the electrode surface being influenced by the bismuth to such an extent that an active deposit is made, and maintained. In conjunction with this, it was also suggested that bismuth provides a conductive matrix of needle-like deposits, within the electrode during cycling, hence preventing densification.

One final inorganic additive which has received attention in recent years is that of titanium salts, usually as the oxide or titanate [61,62]. In particular, Berchelli [61] patented an electrode which specified using between 0.2 and 1.8% wt/wt of titanate mixed homogeneously throughout the electrode, in the form of fibres, which also improves the mechanical strength of the electrode. Charkey [62] observed that potassium titanate created a stable concentration gradient of $Zn(OH)_4^{2-}$ within the electrode pores, and as such resulted in improved capacity retention.

Organic additions have also received considerable attention during recent years, and of these polymeric additives have dominated. Their main advantages are essentially mechanical, i.e. binding the electrode, and also structural by providing a stable network to retain the zinc active material, thus slowing shape change.

The most extensively used polymeric addition is that of polytetrafluoroethylene, P.T.F.E. [63-66]. Small additions of this polymer have been shown to engender a high degree of mechanical stability, whilst still maintaining an open network. Other polymer systems have been utilised, though to a lesser

extent. Of these, polyvinyl alcohol [40,67], and polyethylene [68] have received the most attention. Hampson and McNeil [69-71] have recently performed a large study of polymer bound zinc electrodes, observing both potential and cycle-life parameters. In high concentration, >10%, all polymers tend to shield the active material, and as a result reduce the electrode cycle life and capacity. Of the polymers studied by these workers only polycarbonate was found to be competitive with p.t.f.e., in terms of cycle-life performance.

The addition of a polymer alone does not engender any electrical conductivity to the matrix. Therefore, other additions have been made in order to rectify this situation. In particular, various carbons and graphites have been investigated for this purpose, due to their conducting properties. Duffield et al [72-74] carried out work with graphite additions and found that the cycle-life could significantly be improved, in contrast to results obtained by Sandera et al [75]. Duffield attributed this difference to the particle size of graphite used by Sandera, which was large, 150μm. Duffield found that the smaller the particle size used, the better the performance of the cell. He postulated that the beneficial effect was due to a physical entrapment of soluble zincate species, during discharge, within the electrode matrix. This occurs until a super-saturation takes place and precipitation of zinc oxide follows. Thus it can be seen that the graphite/P.T.F.E. matrix acts more as a retardant to shape change, rather than a complete prevention (as zinc will eventually escape into the solution).

Other organic additives which have been successfully utilised in secondary zinc cells are surface active agents, such as emulphogenes [76]. These tend to reduce shape change and densification by being adsorbed onto the zinc surface.

ii. Electrolyte Addition

An alternative way of improving the cycle-life of the zinc electrode is to incorporate additives in the electrolyte. It is obvious that in this situation the concentration of the additive is also determined by its own solubility, hence with some materials only small additions can be made. Consideration must also be given to the effect that the additive will have on the performance of the counter electrode. Electrolyte additions promote improvements to cycle-life by similar mechanisms to those of electrode additions, namely: reduction of electrode corrosion, shape change and dendritic growth.

Electrolyte additives are used extensively in the metal finishing industry to modify deposit characteristics. One would therefore expect that the exchange of knowledge and information from one technology to another would readily occur. However, this is true to only a limited extent, as most plating baths operate at much less concentrated solutions than those encountered in battery systems (e.g. 2M sodium hydroxide solution compared to 6-7M potassium hydroxide). This difference helps explain why certain levellers and brighteners, which work exceedingly well in the metal finishing industry, fail to be of any significant use in modifying zinc deposits in battery systems.

The addition of lead ions to the electrolyte has long been used as a method of influencing the zinc deposit morphology. Mansfeld and Gilman [77] reported that lead inhibited the growth of dendrites by blocking the sites which were active for dissolution and deposition. Thus, dissolution only occurs at macroscopic crystal defects. The morphology of the deposit was found to be affected by lead, in that it consisted of smooth rounded dendrites of many small crystallites, as opposed to the classical side-branched monocrystal dendrites obtained in lead free electrolyte. Diggle and Damjanovic [78-80] found that the effectiveness of lead was

potential dependent (suggesting that the inhibiting species was partially charged), and at high enough concentration ($>10^{-4}M$) could totally suppress dendritic growth.

Tin salts have also been investigated in a similar way and have been found to exhibit properties favourable for deposit morphology enhancement [81-83]. The effect was attributed to blocking of active sites, similar to the mode of action of lead.

Lithium hydroxide is a very common addition to the electrolyte, to extend the capacity of the nickel counter electrode. However, Flerov [84,85] believed that the presence of LiOH also had a beneficial effect on the zinc electrode, as it could stabilise supersaturated zincate solutions and therefore prevent zinc passivation.

Numerous other electrolyte additives have been suggested, and their respective patents applied for. These include: silicate [85 - 87], ferro or ferricyanide [88], phosphate [89-91], borate [89], arsenate [89], and fluoride [91-92]. Silicate is thought to inhibit the dissolution of zinc by adsorbing it on to its surface, thus reducing the amount of charge needed to cause passivation. The other additives listed above all cause a reduction in the solubility of the discharged zincate species either by reducing the number of free hydroxyl ions, as with the fluoride, or by causing precipitation of zinc oxide within the vicinity of the electrode. Thornton and Carlson [93] investigated a number of alternative electrolytes, and found that there were no zinc anions which formed insoluble zinc compounds at pH values compatible with nickel electrodes. They therefore suggested that the most useful electrolytes were those which could have minimal hydroxyl concentration with the maximum conductivity, usually achieved by the addition of highly soluble salts such as phosphate, borate and fluoride. Nichols et al [94] found that by using fluoride and borate solutions the cycle-life capacity and shape change could indeed be improved by use of such electrolytes. However, increased cell resistance and

lower electrode utilisation were also noted by these workers. This compromise between cycle-life and energy density must thus play a part in selection of additives.

Organic additions through the solution route has also been investigated. In particular quaternary ammonium salts have been reported to influence zinc deposit morphology [78,79,81,95]. The proposed mechanism for this action, stated that the large organic cationic species undergoes specific adsorption at the growth centres, thus blocking deposition at this site. The deposition therefore occurs at another site, hence producing a more even deposit. This in turn leads to an improved cycle-life.

Other organic compounds that have been tested as electrolyte additions include various surfactants [96,97], thiourea [83] and polyethylene glycol [98]. These probably function in a similar manner to that of the quaternary ammonium salts.

One final modification that can be made to the electrolyte is the addition of a cellulose or starch based derivative, to cause a general gellation. The gelled electrolyte will inhibit the rapid movement of zincate species and this should, in theory, cause a reduction in the shape change and dendritic growth. However, problems that may arise with using this system is that the internal cell resistance may be significantly increased, due to the reduced ionic mobility. Primary zinc systems use gelled electrolytes extensively [40,99], and so transfer of technology should be relatively simple.

iii. Separators

Separator material is used in virtually all zinc battery systems, primarily as a means of keeping the positive and negative electrodes apart. Initially separators took the form of a cellulose film, usually wrapped around the electrode two or three times. However as time has progressed the use and complexity of

separator systems has developed to a point where multilayers of differing materials are nowadays in common use. Broadly speaking though, the basic functions of these systems still remain the same as they were in the simple cellulose ones, namely: to act as an electrolyte reservoir and wick, and to interpose a gap between the opposing electrodes thus preventing a direct link between the two. The selection of the correct separator system is therefore of vital importance to the successful operation of a battery. In addition to the basic requirements that a separator must fulfil, listed above, there are also certain others which must also be met if it is to be of use in a battery. These are, that it should be:-

i) resistant to degradation by either the electrolyte and/or active materials
ii) high in ionic conductivity and low in electrical resistance
iii) effective in preventing migration of particules between electrodes
iv) easily wettable by the electrolyte
v) mechanically strong and flexible enough to withstand battery fabrication
vi) preferably relatively inexpensive

Lundquist [100] recently characterised the various types of separators employed in Ni-Zn cells.

As previously mentioned, cellophane was the first material to be successfully employed as a separator in a practical secondary silver-zinc cell [12]. Unfortunately cellophane is not stable in alkaline solutions, and it is also prone to undergo oxidative degradation in silver-zinc cells. This degradation limits battery life and performance. Thus considerable research and development has been undertaken into both improving the properties of cellulosic materials and finding a suitable replacement for it.

Modifications to the cellulose film have included treatment with sodium borohydride [101], to improve chemical stability by reducing the number of aldehyde groups. Anti-oxidants such as phenylene diamine [102] have also been suggested as a method of improving oxidation resistance.

The search for a suitable replacement for cellulose has progressed along two distinct paths, one being the development of grafted and radiation cross-linked polyalkenes [103, 104], the other being the use of inorganic separators [105-107].

The radiation polymers consist of a film of the polyalkene which was then cross-linked to give a uniform three dimensional structure. This structure creates a more tortuous pathway for any species to penetrate i.e. dendrite penetration is delayed. Grafting of the film, and exposing it to radiation was performed to increase conductivity in potassium hydroxide and oxidation resistance. This type of separator has the added advantage over cellulose in that it can withstand the heat sterilisation which is used on some space mission batteries. One disadvantage that these separators have, compared to cellulose, is that they do not swell when wetted - which in turn allows the electrodes themselves to expand on cycling, hence accelerating shape change.

Other non-cellulosic separator systems which have been proposed are polyvinyl-alcohol membranes [104], these do swell in hydroxyl solutions to form a dense gel, but their mechanical strength is poor and consequently their use is mainly in conjunction with other systems. Polymer blends consisting of an aromatic heterocyclic polymer and another polymer have also been investigated with some reported success [108].

The final class of separator system which has been utilised in secondary zinc system is that of inorganic separators. These were developed mainly for silver-zinc cells in space and military applications, their cost would therefore prove prohibitive for

everyday civilian use. Initially, rigid separators were manufactured from alumina silicate compositions [109], but it was soon realised that flexible separators would have a much greater use and appeal. The formulations for these were based upon those developed for the rigid separators, but with a suitable polymer addition to engender flexibility. The initial results showed that rigid separators gave increased cycle-life compared to cellulose types, whereas flexible ones gave slightly less. Further work on the later separators has since improved this situation somewhat.

At the present time the main direction of research into separators is to use a combination of one, or more, of the separator systems mentioned above, hence combining the advantages of each.

The application of certain substances on the surface of the membrane has also been suggested - so called 'coated separators' [110-112]. These include a metallic nickel coating on the zinc side of the separator, causing the dendrites to be destroyed on contact with the nickel [110, 111]. However, this method only delays penetration, it does not totally prevent it. Another coated separator suggested, consists of a copolymer of acrylonitrile and poly (vinyl chloride) with a coating of PVA containing inorganic additions [112]. This separator has been reported to be resistant to zincate ion penetration.

Although separators have progressed greatly with the research dedicated to them, it is probably fair to say that they still have not advanced far enough to meet all the requirements asked of them, in terms of improving cycle-life.

iv. Other Methods

One method of improving the cycle-life of zinc batteries, which has received increasing interest in recent years, is that of modifying the charging current in some way. This can be

achieved in a variety of differing methods viz:- pulsating the current, superimposing a.c. current on d.c., reversing the current, and multi-component pulse charging current.

The reasoning behind why pulse current is successful in the prevention of dendrites has been summarised in the following manner by Bennion [113]. The application of a high current peak creates a high surface overvoltage, and thus activates a large number of nucleation sites. The following rest period allows local zinc concentration gradients to relax by diffusion into the depleted diffusion layer. Thus a more uniform deposit is obtained.

Arouete et al [114] reported that the effect of pulsed d.c. current on the electrodeposition of zinc was to produce a thicker, more compact deposit by appropriate choice of current density and the pulse on : off ratio. Smithrick [115] conducted pulse current charging on zinc-nickel cells, but found no evidence of any improvement over constant current charging. McBreen [116] suggested that at the frequencies employed by Smithrick, double layer effects eliminated any advantages of diffusion relaxation. Wagner [117,118] confirmed this result stating an optimum frequency to be 5-8 Hz, and rest : pulse ratio to be 3 : 1. Katz [119] also reported similar results to this, observing a two to three fold improvement in capacity loss versus constant current charging.

The second modification to the charging regime that could be employed is the superimposition of an a.c. current on a constant d.c. waveform. Chin [120] et al performed such experiments with the deposition of zinc from an acidic zinc chloride solution, finding that the number of nucleation sites increased with the pulse current.

The third alternative of reversing the current is only effective when the deposition is rate determining. When the reaction is activation controlled, little or no effect is obtained. Obviously the

deposition period must last longer than the dissolution one in this method.

The final method of modifying the charging waveform is to use a multi-component pulse current. This consists of a deposition current, a dissolution current, and a rest period. Appelt and Jurewicz [121, 122], and also Binder and Kordesh [123] have claimed beneficial effects when using such a waveform.

It must be remembered, however, that the time required for charging when using these modified waveforms is much longer than using constant current - in the case of the optimised pulse current suggested by Wagner [118], this can be four times longer.

Other miscellaneous ways of improving cell performance are vibrating the electrode [124-125] and flowing (or pumping) the electrolyte. The patented 'Vibrocel' [126] has not found commercial success, probably due to the expense in the construction of the cell. Flowing electrolytes are utilised in zinc-halogen cells, but not in alkaline ones [43]. The mechanism by which both of the above work is mass transport enhancement, also any dendrites formed tend to be broken off by the agitation/circulation of electrolyte.

Summary/Conclusion

The various methods listed in this review have been discussed separately in order to examine the effect of each one independently. However, combinations of methods are more usual today, typified by the work of Sato et al [112]. This combination approach is employed since it is now realised that application of only one of the aforementioned methods can not achieve what is required of the secondary zinc cell. However, using such a complex combination can sometimes lead to a masking of which mechanism is actually causing the greatest beneficial effect.

The following tables list patents which have been filed (mainly in Japan) under the various headings, claiming to give an improvement in cycle-life behaviour.

ELECTRODE ADDITIVES

AUTHOR(S)	COMPANY	BRIEF DETAILS/COMMENTS	PATENT NO.
Ueda T, Ishikura Y, et al	Sanyo Electric Co Ltd	$Ca(OH)_2$ in paste and coated on surface. Paste also contains calcium lignosulphate	JK 63 155 556
Ueda T, Ishikura Y, et al	Sanyo Electric Co Ltd	$Ca(OH)_2$ particle size optimised at 50-250μ	JK 63 126 163
Fujiwara Y, Ishikura Y, et al	Sanyo Electric Co Ltd	In oxide or hydroxide coated with silicic acid	JK 63 26 952
Ishikura Y, Fujiwara Y, et al	Sanyo Electric Co Ltd	Sodium lignosulphonate (4%)	JK 62 287 569
Ueda T, Ishikura Y	Sanyo Electric Co Ltd	Hydroxycarboxylic acids or their salts eg. sodium gluconate (0.5%)	JK 62 241 262
Furukawa S, Inoue K, et al	Sanyo Electric Co Ltd	In oxide/hydroxide plus Sr hydroxide (5%)	JK 62 66 571
Furukawa S, Inoue K, et al	Sanyo Electric Co Ltd	Two layer electrode:zinc powder in surface layer only ;both layers with In_2O_3 and $Ca(OH)_2$	JK 62 11 022
Furukawa S, Murakami S, et al	Sanyo Electric Co Ltd	In or Tl oxide/hydroxide plus oxide/hydrozide of Ga, Cd,Pb,Sn,Bi or Ag	JK 61 96 666
Inoue K, Nogami M	Sanyo Electric Co Ltd	Outer layer having 2-4 times In oxide than inner layer layer improves cycle life over even In distribution	JK 61 101 955
Furukawa S, Murakami S, et al	Sanyo Electric Co Ltd	In oxide plus Ga oxide	JK 61 811 967
Furukawa S, Inoue K	Sanyo Electric Co Ltd	Regenerated cellulose powder	JK 61 91 872
Inoue K, Nogami M	Sanyo Electric Co Ltd	In or Tl oxide/hydroxide plus LiOH (optimised at 0.1 ---> 0.8% wt.)	JK 61 118 968
Shirogami T,Inada K	Toshiba Corp	Paste containing $Ca(OH)_2$ and Bi_2O_3	JK 61 06 500

ELECTRODE ADDITIVES (cont.)

AUTHOR(S)	COMPANY	BRIEF DETAILS/COMMENTS	PATENT NO.
Tsuji H	Furakawa Electric Co	Polyvinyl alcohol plus $Ca(OH)_2$, $Ba(OH)_2$, TiO_2, ZrO_2 and/or MgO	JK 60 20 853
Furukawa S, Murakami S	Sanyo Electric Co Ltd	In and Tl oxide in electrode plus In and Li ions in electrolyte	JK 60 185 372
	Sanyo Electric Co Ltd	Anode having higher binder concentration at edges than at centre	JK 60 08 964
	Sanyo Electric Co Ltd	SBR rubber at edges of electrode	JK 60 97 559
	Mitsubishi Electric Corp	Isoprene-isobutylene rubber binder (5%) instead of p.t.f.e.	JK 60 89 073
	Sanyo Electric Co Ltd	In plus 1 or more oxide of Hg, Pb, Cd, TI, Sn or Bi improved cycle-life	JK 60 84 768
	Mitsubishi Electric Corp	HgO addition plus Al_2O_3	JK 60 56 368
	Sanyo Electric Co Ltd	In concentration higher at edges than centre	JK 60 14 758
	Sanyo Electric Co Ltd	CdO and p.t.f.e. resin which was higher at edges than centre	JK 60 14 757
	Sanyo Electric Co Ltd	In_2O_3 found to improve cycle-life over In metal	JK 59 186 257
	Sanyo Electric Co Ltd	Tl oxide and In oxide plus P.V.A. (1%)	JK 59 189 563
	Sanyo Electric Co Ltd	In_2O_3 addition enhances effect of Tl_2O_3	JK 59 18 956
	Sanyo Electric Co Ltd	In and In hydroxide plus alkaline earth silicate eg calcium silicate	JK 59 71 260

ELECTRODE ADDITIVES (cont.)

AUTHOR(S)	COMPANY	BRIEF DETAILS/COMMENTS	PATENT NO.
	Sanyo Electric Co Ltd	P.V.A. and In found to improve cycle-life	JK 59 66 060
	Toshiba Corp	Chopped polyimide fibres (0.5% wt.)	JK 59 03 027
	Toyota Central R&D	Zinc complexing agent(2,3,7 trihydroxy fluorene)	JK 58 17 895
	Sanyo Electric Co Ltd	Zinc anode with (2-15%) oxide of Sn and In (In:Sn::0.25:10)	JK 58 176 870
	Sanyo Electric Co Ltd	Zinc anode with (2-15%) oxide of Cd and Sn (Cd:Sn::0.25:10)	JK 58 176 871
	Sanyo Electric Co Ltd	Mix of carbon fibre and TiO_2 (1:1 mix)	JK 53 163 172
	Sanyo Electric Co Ltd	In oxide and Sn oxide (Sn inhibits densification of anode)	JK 58 163 158
	Sanyo Electric Co Ltd	Cd oxide and Sn oxide	JK 58 163 159
	Sanyo Electric Co Ltd	In oxide or hydroxide and In metal	JK 58 163 160
	Sanyo Electric Co Ltd	In oxide and carbon fibre	JK 58 163 161
	Sanyo Electric Co Ltd	Ti oxide and Sn oxide/hydroxide	JK 58 163 162
	Sanyo Electric Co Ltd	Expanded graphite	JK 58 165 250
	Sanyo Electric Co Ltd	In hydroxide	JK 58 137 966
	Sanyo Electric Co Ltd	Cd and In compounds coated on edges of electrode	JK 58 137 964

ELECTRODE ADDITIVES (cont.)

AUTHOR(S)	COMPANY	BRIEF DETAILS/COMMENTS	PATENT NO.
	Sanyo Electric Co Ltd	Cu oxide (2-10%) improves battery life. $Ca(OH)_2$ also in paste	JK 58 119 159
	Matsushita Electrical Ltd	Na polyacrylate (0.5%-2.5%) and C.M.C. (2-4%)	JK 58 87 759
	Toshiba Battery Co Ltd	Isobutene-maleic anhydride co-polymer	JK 58 73 954
	Furakawa Battery Co	Cu or Cuo to prevent dendrites	JK 58 71 561
Jones R A	General Motors Corp	$Ca(OH)_2$, Pb_3O_4 and cellulose fibres	US Pat 4 358 517
	Toshiba Corp	Bi_2O_3 (30%) and $Ca(OH)_2$ (10%) added	J.T.K. 82 13 102
Viadyanathan H	Energy Research Corp	ZnF_2 or Zn titante added	US Pat 4 304 828
Witherspoon R R, Meibuhr S G	General Motors Corp	$CaSi_2O_5$ (5-15%)	US Pat 4 312 931
	Tokyo Shibaura Electric Co	Bi, Bi_2O_3 and/or $Bi(OH)_2$ (~3%)	J.T.K. 81 29 345
Sandera J, Touskova A, et al		ZnF_2 and/or Zn oxalate	Czech 184 504
Berchielli A S, Chireau R F	Yardney Electric Corp	Alkali earth titanate compounds (eg Na titanate)	Australian 505 367
Tsuji H	Furukawa Battery Co	TiO_2 (5%) of particle size 0.05μ	JK 79 122 838
Shirokami T, Inada K	Tokyo Shibura Electric Co	$Ca(OH)_2$, Bi_2O_3 and nonionic surfactant (Triton X-100)	JK 79 41 429
Ohsawa K, Fujiwara K, et al	Furukawa Electric Co	Mn or its oxide (0.1 ---> 20%)	JK 79 16 631
Berchelli A S, Chirea R F	Yardney Electric Co	Potassium titanate in silver-zinc cells	US Pat 4 041 221

ELECTRODE ADDITIVES (cont.)

AUTHOR(S)	COMPANY	BRIEF DETAILS/COMMENTS	PATENT NO.
Tsuburaya Y, Maki Y	Hitachi Maxell Ltd	Na polyacrylate (0.7 ---> 2.5 parts/1 part ZnO)	JK 76 142 644
Ohira T, Kumano H	Matsushita Electrical Ltd	$Ca(OH)_2$ added	JK 76 121 741
Takamura T, Kaneda Y	Tokyo Shibura Electric Co	Bi_2O_3, In_2O_3 and poly (acrylic acid) Na salt as binder	JK 74 112 125

ELECTROLYTE ADDITIVES

AUTHOR(S)	COMPANY	BRIEF DETAILS/COMMENTS	PATENT NO.
Furukawa S, Inoue K	Sanyo Electric Co Ltd	Fe^{3+} ions (0.1mM) in electrolyte, In/Tl in electrode	JK 62 110 269
Furukawa S, Inoue K	Sanyo Electric Co Ltd	Ge^{4+} ions (0.1mM) in electrolyte, In/Tl in electrode	JK 62 108 467
Furukawa S, Inoue K	Sanyo Electric Co Ltd	K_3PO_4 (1-7%)	JK 62 165 878
Furukawa S, Inoue K	Sanyo Electric Co Ltd	LiOH (O.5M)	JK 60 225 372
Furukawa S, Murakemi S	Sanyo Electric Co Ltd	$In(OH)_3$ (0.1mM) and LiOH(M)	JK 60 185 372
Furukawa S, Murakemi S	Sanyo Electric Co Ltd	$In(OH)_3$ (0.1mM) and $Co(OH)_2$ (0.1M)	JK 60 185 373
	Pentel Co Ltd	Dithiocarbamic acid or its derivatives eg K N,N'-diethyldithiocarbamate	JK 60 240 639
	Matsushita Electrical Ltd	1 or more compound of Al, Ga, In, Tl (up to 0.8%) in CMC gel	JK 59 103 278
	Fuji Electrochem Co Ltd	Chromate in electrolyte, active material in CMC gel	JK 59 51 476
	Sanyo Electric Co Ltd	CdO ($100gl^{-1}$) addition	JK 58 158 875
	Agency of Industrial Sciences and Technology	Te oxide ($500mgl^{-1}$) and Pb oxide ($500mgl^{-1}$) in 9M KOH	J.T.K. 82 05 025
Carlson E J	General Electric Co	KOH(5-10%) with KF(5-15%) and K_3PO_4 (10-20%)	US Pat 4 273 841
Eisenberg M	Electrochimica Corp	K_3PO_4 or borate salt	UK Pat 4 224 391

ELECTROLYTE ADDITIVES (cont.)

AUTHOR(S)	COMPANY	BRIEF DETAILS/COMMENTS	PATENT NO.
Furuhashi B	Nakamura Kazuo	$Sr(OH)_2.8H_2O$ ($5gl^{-1}$) added for dendrite prevention	JK 78 133 734
Fukuhara R, Oshimura S, et al	Hitachi-Maxell Ltd	Electrolyte containing alkali soluble amine/urea or thiourea derivative having unpaired electrons	JK 78 00 839 78 00 840 78 00 841
Ohsawa K	Furukawa Electric Co	Polycationic polymer	JK 75 43 435
Ikela H, Furukawa N, et al		In and Tl compounds addition	JK 75 65 832
Ikela Y, Ohhira T	Matsushita Electric Co	Benzyldimethyldodecyl ammonium chloride (5%)	JK 75 96 845
Ikeda Y, Ohhura T	Matsushita Electric Co	In and Te ($500mgl^{-1}$)	JK 75 118 231
Ikeda Y, Obhira T	Matsushita Electric Co	Poly(oxyethylene)dodecyl ether and lingosulphonate to electrolyte and/or electrolyte	JK 75 96 844
Ohsawa K	Furukawa Electric Co	Ioene polymer addition (eg N, N' dimethylpiperazine -1,5 dibromo pentane polymer)	JK 75 139 939
Ikeda Y, Ohhira T	Matsushita Electric Co	Fluoride ions ($2gl^{-1}$) additions	JK 75 26 040 041 044

SEPARATORS

AUTHOR(S)	COMPANY	BRIEF DETAILS/COMMENTS	PATENT NO.
Fujiwara Y, Ishikura	Sanyo Electric Co Ltd	Anode sprayed with 1:1 dispersion of MgO:Zn to give 50μ layer	JK 62 22 369
Matsui M		Porous chloroprene-rubber coated on electrode by dipping	JK 60 53 422
Poa S	US Dept. of Energy	Microporous separator of tertiary C_{5-10} alkyl amine)	US Pat 580 982
	Japan Storage Battery Co	Electrode wrapped in teflon - Ni powder coated microporous bag	JK 59 71 258
	Hitachi Maxell Ltd	Vinylon sheet coated with alkali earth hydroxide and p.t.f.e. or polyacrylate	JK 59 16 394
	Japan Storage Battery Co	Two polypropylene bags - inner one coated at edges with Ni	JK 59 83 363
	Sanyo Electric Co Ltd	Polyactelene wrap (CH)x	JK 58 198 855
	Japan Storage Battery Co	Ni-coated separators - carbonyl Ni better than Ni plate	JK 58 126 666 667
	Sanyo Electric Co Ltd	Cd on anode face of separator	JK 57 162 275
	Yuasa Battery Co	Zinc anode covered with dispersion of 80 parts MgO:20 parts p.t.f.e.	JK 57 163 963
	Yuasa Battery Co	Coating of di-Me polysiloxane with hydrophilic groups	JK 82 86 670

SEPARATORS (cont.)

AUTHOR(S)	COMPANY	BRIEF DETAILS/COMMENTS	PATENT NO.
	Toshiba Corp.	Non-woven acrylo-nitro-vinylchloride co-polymer coated with 10% PVA / 1.2% H_3BO_3	JK 82 20 667
Schmidt G F and Weber R E	Kimberly-Clark Corp	Non-woven polyproplylene coated with hydrophilic wetting agent (Strodex PK90), a K salt of organo-phosphoric acid ester, and butyl rubber latex and curred	Fr.Demande FR 2 486 312
Hsu L-C, Phillip W H, et al	N.A.S.A.	Crosslinked copolymer of vinyl alcohol and unsaturated carboxylic acid	US Pat App 282 298
Dodin M G, Charkey A	Energy Research Corp	Polyamide and wettable polymer with filler reactive to zinc eg CeO_2, $Ca(OH)_2$, $Mg(OH)_2$, $Ba(OH)_2$, $Al(OH)_3$, ZnF_2, or $Zn(BO_3)_2$.	Euro. Pat EP 40 826
Sakai T, Furukawa H, et al	Sanyo Electric Co Ltd	Zinc anode coated with a carbon black-$Ca(OH)_2$ mixture	JK 79 129 331
Sekido S, Ohhira T	Matsushita Electrical Co	Ni-Zn cell with separator containing $Ca(OH)_2$	US Pat 3 976 502
Chireau R F	Yardney	Interspacer of separator contains 50-95% of titanate material such as K_2TiO_3	US Pat 4 034 144
Takamura T, Kanada Y, et al	Tokyo Shibura Electric Co	Polyamide separator - electrode contains alkali earth metal oxide/hydroxide	Ger Offen 2 433 487
Ohsawa K	Furukawa Electric	Zinc anode dipped in polycationic polymer eg 20% poly (N,N-dimethyldiallyammonium)chloride	JK 75 77 839
Forst H, Vielstich W		Coat anode with synthetic latex eg styrene - acrylate latex	Ger Offen 2 360 026

OTHERS e.g. Pulse Charging, Flowing Electrolyte

AUTHOR(S)	COMPANY	BRIEF DETAILS/COMMENTS	PATENT NO.
Ando Y	Meidensha Electric Mfg Co	Zinc dendrite inhibitor for electrolyte circulation systems incorporates quaternary ammonium compound	Euro. Pat E.P.101 239

KEY

E.P. European Patent Appliacation

JK. Japan Kohai

JTK. Japan Kohai Tokkyo Koho

CHAPTER 4

EXPERIMENTAL TECHNIQUES

4.1 Electrolytic Cells

Two different designs of cell were utilised in these investigations.

Galvanostatic passivation experiments were performed in a cell similar to that used by Hampson and Tarbox [127], and is illustrated in Fig. 4.1.1. The cell body was made from borosilicate glass with a screw-thread bottom which connected to a detachable polycarbonate nut. The working electrode was placed between this connection. In order to prevent electrolyte leakage, a rubber 'O' ring surrounded by p.t.f.e. was positioned on the upper surface of the electrode. This also provided a simple method of defining the area of the electrode. The potential of this electrode was measured with reference to a mercury-mercury oxide electrode, in conjunction with a luggin capillary positioned ~4 mm above the centre of the electrode.

The upper end of the cell held a nickel gauze counter electrode, positioned 7.5 cm above the surface of the working electrode.

The second cell design was a conventional three-limbed electrolytic cell, again made from borosilicate glass. The cell was used in both potentiostatic passivation and zinc electrodeposition experiments, its construction is illustrated in Fig. 4.1.2. All cell fittings had lubrication-free ground glass joints. The design enabled the passage of nitrogen through the cell prior to, and during, the experiment. The reference compartment terminated in a luggin capillary which was sited directly below the working electrode. The distance between the working electrode and luggin was adjustable, but for all experiments was maintained at 5 mm.

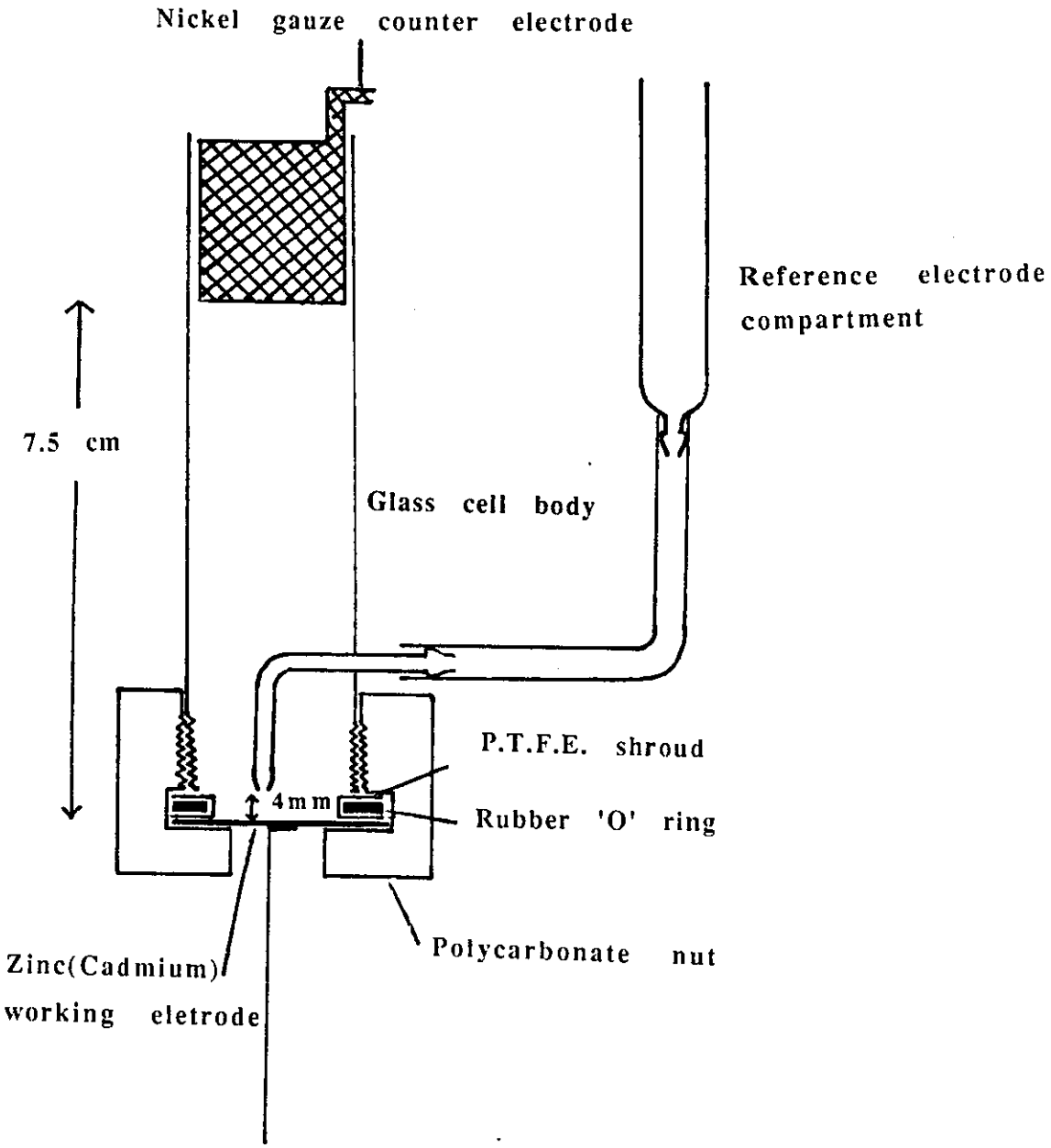

Figure 4.1.1. Galvanostatic passivation electrolytic cell.

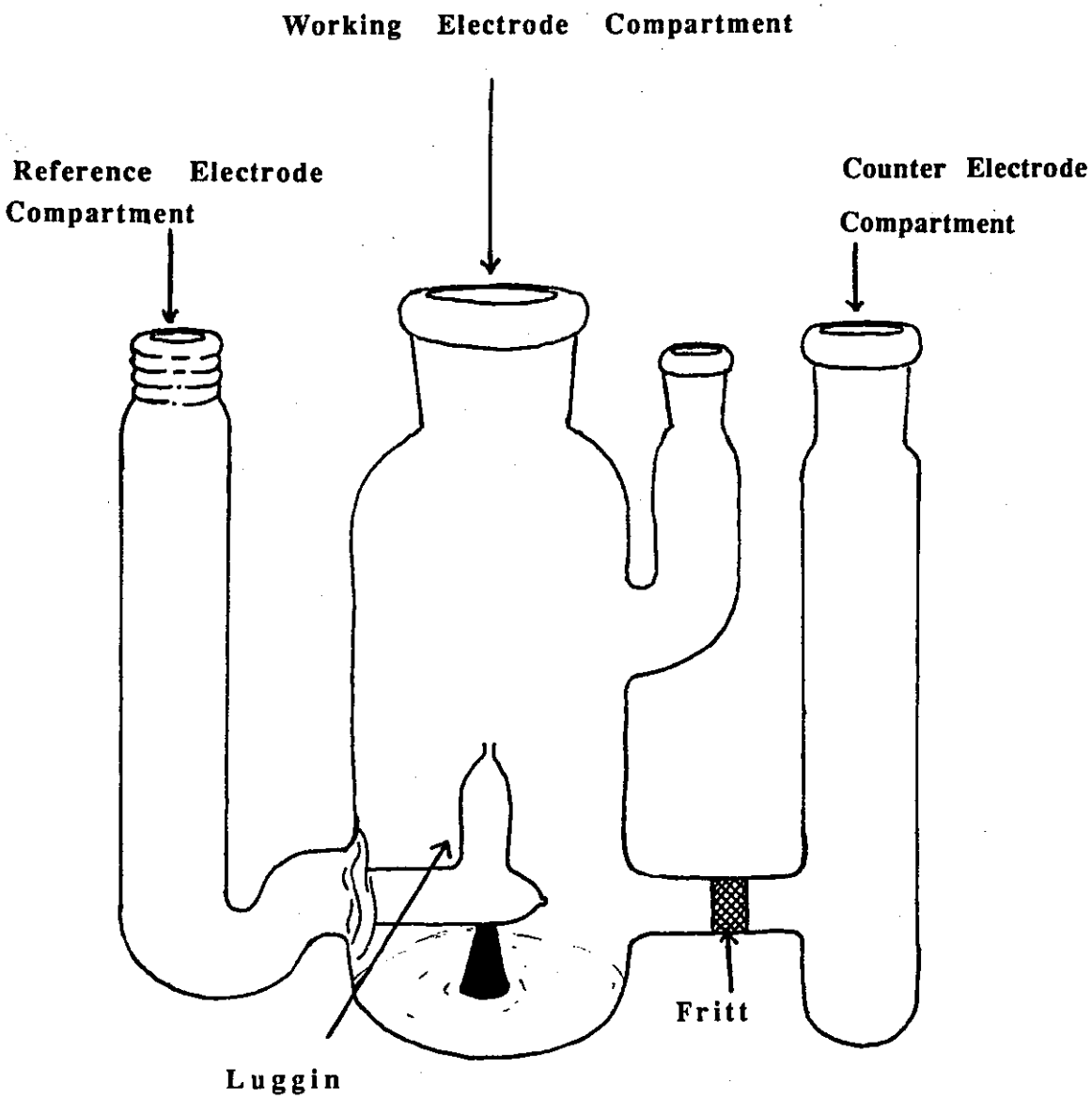

Figure 4.1.2. Conventional three-limbed electrolytic cell.

All glassware used was cleaned by steeping in a 50:50 mixture of nitric and sulphuric acid for several days before use. Thorough washing with triply distilled water was carried out prior to experiments.

4.2. Electrolyte

The electrolyte employed in all experiments was based on a potassium hydroxide solution, of the required concentration. The solutions were made from AR grade pellets (B.D.H.) dissolved in triply distilled water.

A number of additives were also dissolved in the solution in varying amounts. The purity of each additive was analar, or equivalent, where available.

The concentration of each electrolyte mixture will be given in the relevant experimental section of each chapter.

4.3. Working Electrodes

Numerous different types of working electrodes were utilised in these investigations. The section here will give details of their differing constructions; final surface preparation will be found in the experimental sections of the relevant chapter.

For the galvanostatic polarisation experiments the working electrode was either sheet zinc (99.99% BDH) or sheet cadmium (99.85%, Johnson Matthey). The metal was cut to fit in to the polycarbonate nut - the washer defining a circular working surface area of 3.142 cm^2.

Potentiostatic polarisation experiments utilised solid zinc electrodes, the construction of which is shown in Fig. 4.3.1. These were made from zinc rods (99.999% Koch Light), machined to 5mm diameter to give a circular electrode of cross-sectional area

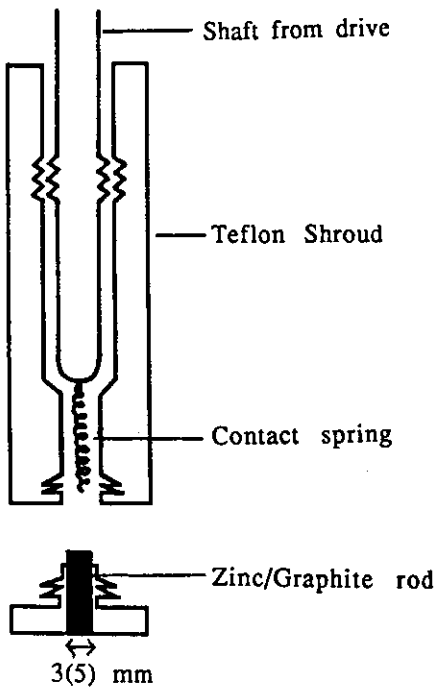

Figure 4.3.1. Solid electrode fabrication.

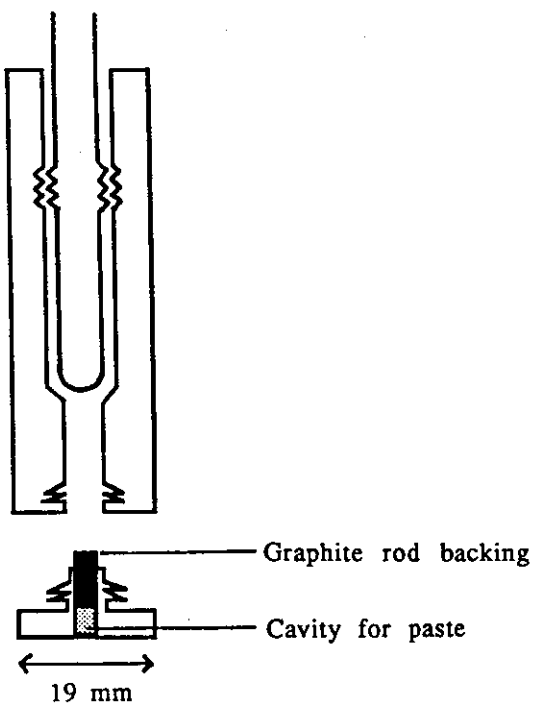

Figure 4.3.2. Porous electrode fabrication.

0.1963 cm^2, which was then cold molded into a teflon shroud. Electrical contact was maintained by way of a spring, which connected to the stainless steel shaft of the rotating disc assembly.

Electrodeposition studies also used a similar zinc electrode, although the diameter was smaller at 3mm, giving a working area of 0.0707 cm^2.

In addition to zinc electrodes, electrodeposition studies also employed two forms of graphite electrode : solid and porous.

The solid electrode was made from graphite (RWO grade, Ringsdorff-Werke) also in rod form and set in teflon - giving an identical cross-sectional area to that of the zinc electrode (0.0707 cm^2).

Porous graphite electrodes were fabricated from a paste mix containing 95% graphite powder (K.S. 2.5, Lonza) and 5% p.t.f.e. suspension in isopropanol (I.C.I.). The paste was mixed and rolled successively to give a tough, fiberous sheet. The alcohol was then driven off by warming in an oven at ~ 100 °C for one hour. The paste was then pressed into a recessed graphite electrode in a teflon shroud, to a depth of 2 mm. Careful trimming of the paste with a clean glass blade followed, until it was flush with the holder surface. Construction of this electrode is shown in Fig. 4.3.2.

Discharge and cycling experiments also utilised pasted electrodes similar to the porous graphite electrodes.
Mixing of the dry components was firstly done to ensure a homogeneous mix. Isopropanol was then added to give a slurry, to which the required amount of p.t.f.e. suspension (Fluon I.C.I. 60% w/w suspension) was incorporated to give a paste which was rolled in a similar manner to the graphite electrodes.

4.4. Reference and Counter Electrodes

The reference electrode employed in all experiments was a Hg/HgO/KOH - the potassium hydroxide concentration being the same as that in the cell. The potential of this couple being + 926 mV vs s.h.e.

Two different constructions were used. The first was a wick type electrode, shown in Fig. 4.4.1., utilised in the 3-limb cell. The second type was slightly different in design as illustrated in Fig. 4.4.2., being used in galvanostatic, discharge and cycling experiments. In all experiments using this design the reference electrode was held in a separate compartment remote from the electrolytic cell.

The counter electrode employed in cycling experiments was a nickel sinter electrode - in all other experiments a high surface area nickel gauze was used.

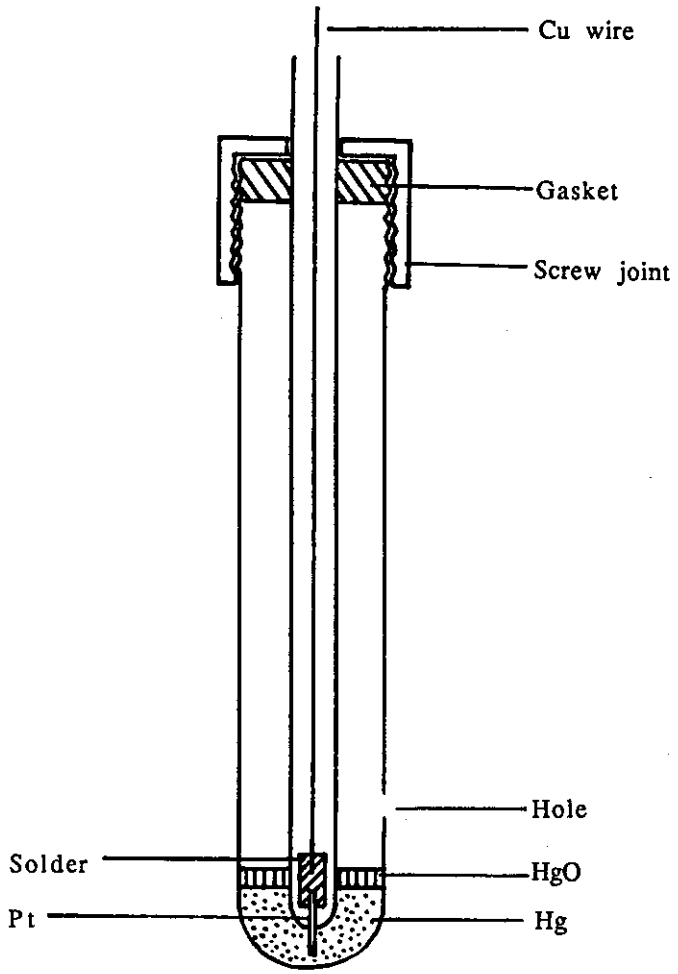

Figure 4.4.1. Wick reference electrode construction.

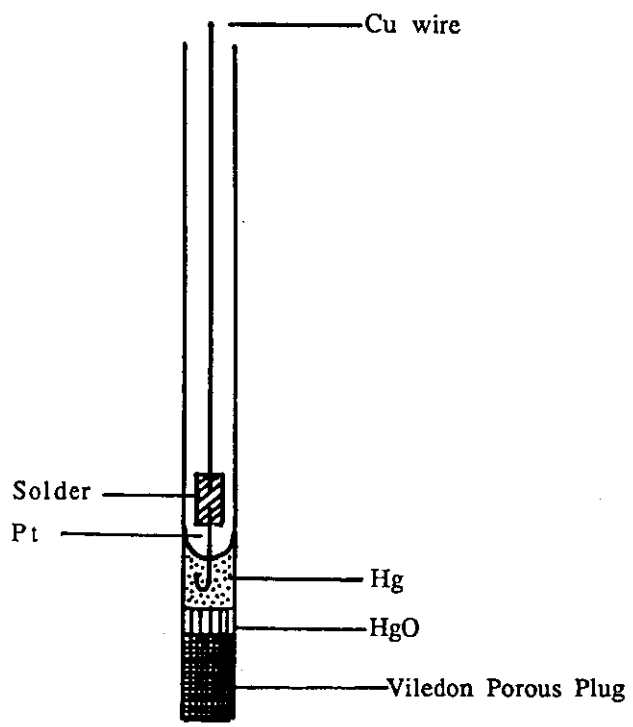

Figure 4.4.2. Inverted reference electrode construction.

CHAPTER 5

GALVANOSTATIC PASSIVATION STUDIES OF ZINC IN ALKALI

5.1. Introduction

As already mentioned in previous chapters the high solubility of the zincate species is responsible for the processes which cause failure of secondary zinc anodes, viz dendrite growth, shape change and densification.

This suggests an obvious approach to solving the problem. This being to reduce the solubility of the discharge product to such a level that there is very little free solution species available at the re-charge stage. Provided that the reaction is reasonably reversible then the localisation of the discharge product will ensure that dendrite growth and zinc redistribution will be minimised. This is the principle of operation of most successful secondary anodes, e.g. Cd - $Cd(OH)_2$, Fe - $Fe(OH)_2$, and Pb - $PbSO_4$.

There are three possible routes to achieving this goal:-

i. change the hydroxyl concentration of the electrolyte
ii. addition of a species which will cause a lowering of the solubility of the discharge product in the presence of hydroxyl ion or
iii. change the electrolyte system from hydroxyl-based completely.

Whichever route is chosen, the electrolyte still has to meet stringent conductivity, self-discharge, utilisation (for both the zinc anode and the counter electrode), and cost requirements.

For the purpose of this investigation, the third of these alternatives was discounted because of the obvious implications for the selection of a suitable cathode material, other than nickel oxyhydroxide.

Examination of the behaviour of zinc in alkaline solutions reveals that the solubility of the oxide and hydroxide increase with increasing hydroxyl concentration, as shown in Fig. 5.1.1. [128]. Concurrent with this are the effects of the solution conductivity as shown in Fig. 5.1.2. [129].

The usual electrolyte concentration employed in primary zinc systems is 7M potassium hydroxide. This choice is made to ensure that the conductivity is at a maximum. It would appear that the developers of the secondary zinc electrode have, to date, mainly followed this lead, and tended to ignore the fact that the solubility of zinc hydroxide (and hence ultimately zincate) is around 1.7 $mol l^{-1}$ @ 25 °C in this concentration of caustic [128].

It has to be realised that for a system which will provide reasonable recharge characteristics then it is necessary to have a trade-off between a high conductivity and low solubility.

It should also be noted that there is a large difference between chemical solubility levels, as shown in Fig. 5.1.1. and that of electrochemical solubility (through anodic dissolution) as obtained in actual operating alkaline cells. In fact electrochemically prepared solutions can often contain as much as twice the amount of zinc in solution, than one which is chemically prepared.

The concentration of hydroxyl which gives a conductivity that is still acceptable for a practical battery system is around 2M. Any further decrease will impair "high" rate performance and introduce the complication of poor performance of the NiOOH electrode. Figures 5.1.1. and 5.1.2. show that in 2M the conductivity is approximately half that of 7M, but the solubility is

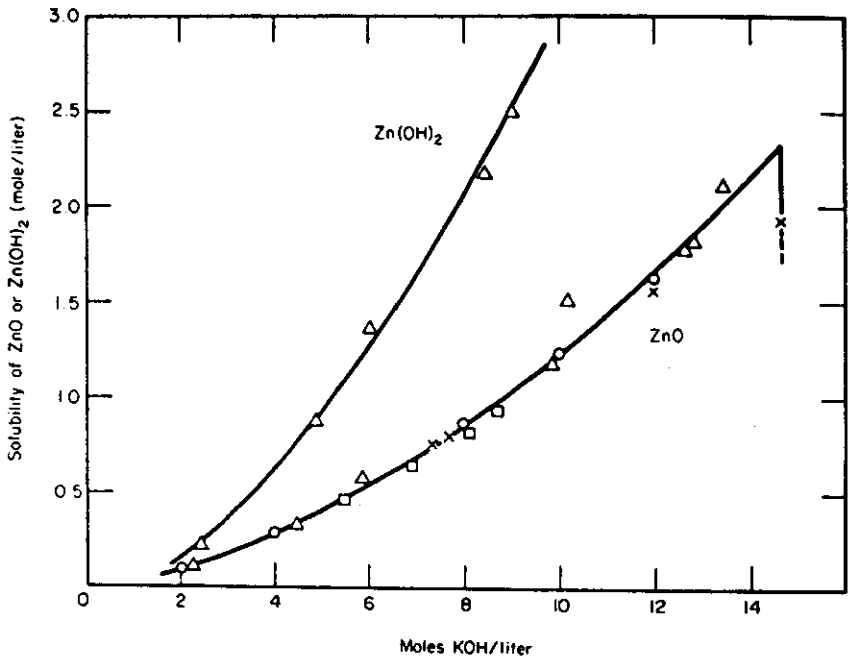

Figure 5.1.1. Zinc oxide / hydroxide solubility variation with hydroxyl ion concentration at 25 °C.

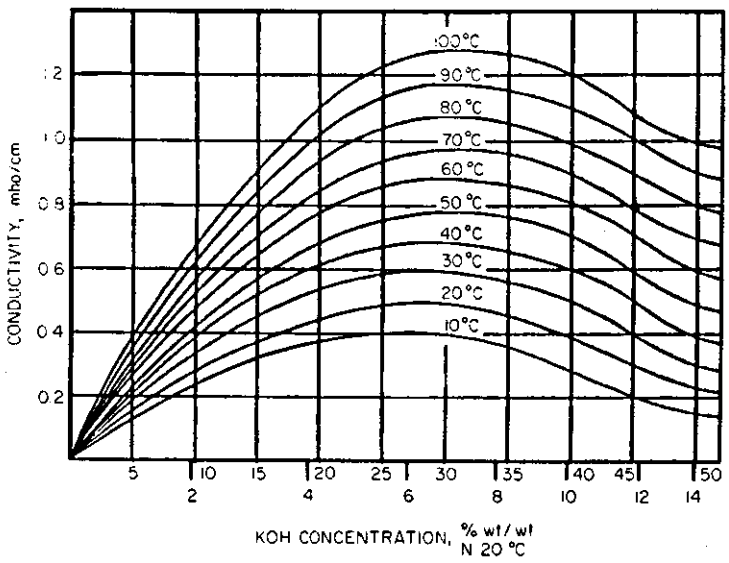

Figure 5.1.2. Conductivity variation with hydroxyl ion concentration.

some three to four times less than that in the higher concentration.

However, the solubility of zincate is still at an unacceptably high level for the successful functioning of a secondary zinc electrode. Thus, a further reduction in the concentration of free zinc species in solution is required. This brings us to the second proposal i.e. addition of a solubility reducing agent to the electrolyte. The type of additive can be divided into one of two distinct groups defined by its mechanism of interaction with the soluble zinc species;

i. those which form a cation-zincate reaction product, and
ii. those which form a zinc-anion reaction product

The solubilities of a number of simple and complex zinc salts are listed in Table 5.1.1. [130]. It must be borne in mind that although solubility is the primary phenomena under consideration, other factors such as crystal morphology and nucleation rate all affect the ultimate packing at the electrode surface. Consequently solubility data is only a rough guide to predicting which additives may prove to be successful for battery systems.

The selected additives could simply be put into actual systems, and their effect on the cell performance monitored. However, this is both very costly and time consuming, and leads to the need for an appropriate technique for screening the additives. Galvanostatic polarisation and the time to passivation was considered to best represent the performance of a simple planar battery electrode.

Many investigators have used this technique to study the anodic behaviour of zinc in alkaline electrolytes. Hampson and co-workers [127,131,132] examined the relationship between passivation times, current density, concentration and temperature for both horizontal and vertical electrodes. They reported that, in

Table 5.1.1. Solubilities of zinc salts.

Zinc Compound	Solubility in grams per 100 ml water
Acetate	30
Aluminate	Insoluble - slightly soluble in alkali
Borate	Slightly soluble
Bromide	447
Chloride	432
Chromate	Insoluble (dissolve in hot water)
Citrate	Slightly soluble
Cyanide	0.0005
Ferrocyanide	Insoluble
Fluoride	1.62
Hydroxide	0.00007 (soluble in alkali)
Nitrate	184
Orthophosphate	Insoluble
Oxalate	0.00079
Oxide	0.00016 (soluble in alkali)
Silicate	Insoluble
Sterate	Insoluble
Sulphate	542
Tartrate	0.055
Tellurate	Insoluble

general, the results conformed to a modified Sand equation of the form:

$$(i - i_L)\, t_p^{1/2} = k \qquad \text{eqn 5.1.1.}$$

k being a constant for a given electrolyte concentration, temperature and electrode orientation. The linear relationship between $t_p^{-1/2}$ and current density being indicative of a diffusion controlled process. The times to passivation for vertical electrodes were found to be considerably longer, due to convective flow of the electrolyte.

Elsdale et al [132] performed similar experiments on porous zinc electrodes, which is a closer approximation to an actual battery situation. He found that the transition time was longer than for a planar electrode, and that horizontal and vertical electrodes had similar passivation times. He also observed that the transition at passivation was gradual, unlike the abrupt change seen with planar electrodes. These findings were explained by the electrode reaction being driven deeper into the electrodes, as the pores became blocked with zinc oxide. However, the general trend of passivation times and their variation with concentration, temperature, etc. is still the same for both planar and porous electrodes. We are, therefore, justified in using planar electrodes in the search for appropriate additives. Comparison of the passivation times, alone, is not enough to assess the usefulness of an additive. A 'benchmark' is required, against which all other results can be judged. This was chosen as the time taken to passivate a cadmium electrode, in 5.3M KOH, as it is this combination which is employed in successful secondary alkaline cadmium systems. The criterion of whether or not an additive was successful, was if it reduced the time to passivation to that approaching a planar cadmium electrode, (of identical area). This would indicate the build-up of an insoluble zinc species within the vicinity of the electrode.

5.2. Experimental

The zinc electrode was cut to the required dimensions before degreasing in acetone. Surface preparation consisted of polishing on 600 and 1200 grade silicon carbide paper, and then etching for 15s in 10% v/v nitric acid (S.G. 1.42). Thorough washing with triply-distilled water followed each stage in the preparation. The electrode was then placed in the cell with a working area of 3.142 cm^2 - as defined by the p.t.f.e. 'O' ring.

The preparation of the cadmium electrode was less complex due to the inherent softness of the metal. It consisted only of degreasing in acetone, and etching in 10% v/v nitric acid for 30s, with a final rinse in triply distilled water before use.

The electrolyte employed in the cadmium passivation experiments was 5.3M KOH, which is the concentration commonly used in secondary Ni-Cd cells.

The zinc passivation experiments used both 7M and 2M KOH as electrolyte, the 2M KOH also had various additions made to it, as detailed in Table 5.2.1.

5.3. Results

The passivation curves obtained were typical of those reported elsewhere, with the potential rising virtually linearly with time until the onset of passivation, at which point it rose rapidly to the oxygen evolution plateau. Table 5.2.1. provides a summary of the passivation times, t_p, and open circuit potentials of the cadmium and zinc electrodes in the electrolytes utilised in the experiments.

The first significant results are those of the passivation times for a cadmium electrode in 5.3M KOH, at varying current densities. Typical passivation curves are presented in Fig. 5.3.1. These

Table 5.2.1. Additives used in Galvanostatic Passivation experiments.

ADDITIVE	Rest Potential / mV Corrosion	PASSIVATION TIMES / s Current Density / mA cm^{-2} 30	15	10	0.25
2M KOH (Zinc)	-1400	299	1114	2299	-
Cd(in 5.3M KOH)	- 900	<-------	Immediately	--------->	~600
$Ca(OH)_2$ sat.	-1378	270	885	2108	
$Mg(OH)_2$ sat.	-1370	280	1018	1890	
Al_2O_3 sat.	-1371	-	999	-	
Sodium boroheptonate					
20 gl^{-1}	-1345	-	881	-	
Potassium orthophosphate					
50 gl^{-1}	-1395	-	856	-	
100 gl^{-1}	-1397	-	887	-	
Potassium ferricyanide					
20 gl^{-1}	-1335	-	886	2042	
Potassium molybdate					
10 gl^{-1}	-1383	-	1000	-	
50 gl^{-1}	-1384	-	950	1760	
Potassium tungstate					
50 gl^{-1}	-1386	-	980	1758	
Potassium chromate					
0.5 gl^{-1}	-1370	-	470	-	-
1 gl^{-1}	-1354	<------	Immediately	------->	2232
2.5 gl^{-1}	-1308	<------	Immediately	------->	85
5 gl^{-1}	-1258	<------	Immediately	------->	15
10 gl^{-1}	-1214	<------	Immediately	------->	8

Table 5.2.1 (cont.) Additives used in Galvanostatic Passivation experiments.

ADDITIVE	Rest Potential / mV Corrosion	PASSIVATION TIMES / s			
		Current Density / mA cm^{-2}			
		30	15	10	0.25
2M KOH (Zinc)	-1400	229	1114	2299	-
Potassium tetraborate					
30 gl^{-1}	-1369	-	-	-	-1324 mV after 100 min
60 gl^{-1}	-1372	-	436	-	-1327 mV after 110 min
100 gl^{-1}	-1368	-	263		-
150 gl^{-1}	-1360	-	50		-1318 mV after 40 min
200 gl^{-1}	-1340	-	9		-1288 mV after 60 min
250 gl^{-1}	-1283	-	Immediately	-	~3120
270 gl^{-1}	-1245	-	Immediately	-	69
300 gl^{-1}	~-1200 (Falling constantly)	-	Immediately	-	~20
Boric acid					
85 gl^{-1}	-1342	-	-	-	24480
90 gl^{-1}	-1330	-	-	-	7422
95 gl-1	-1309	-	Immediately	~3	~1900
100 gl^{-1}	-1283	-	Immediately	Immediately	317
105 gl^{-1}	-1262	-	Immediately	Immediately	69
132 gl^{-1}	-620 (Falling constantly)	-	-	-	-

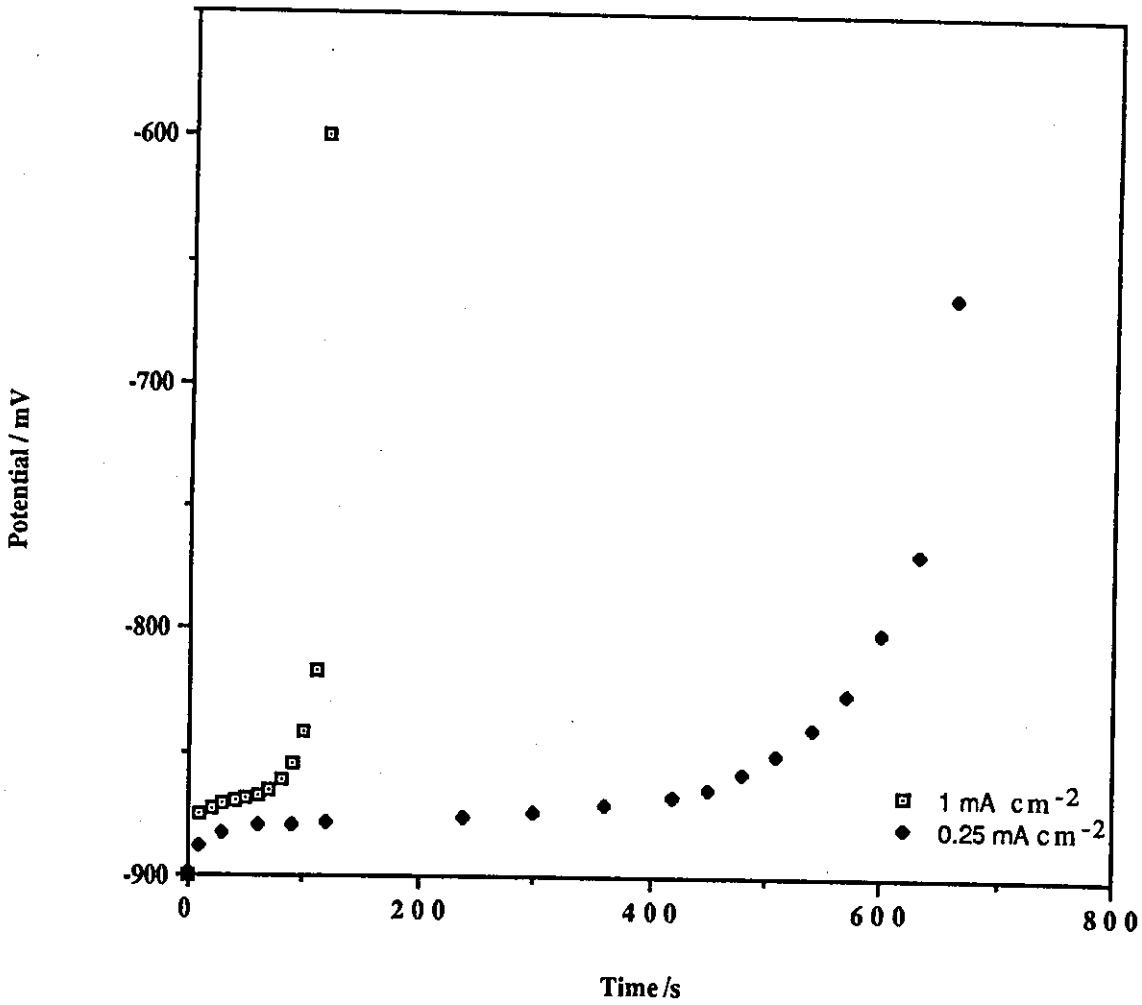

Figure 5.3.1. Typical passivation curves for a cadmium electrode in 5.3M KOH .

compare well with the results of Farr et al [133], any discrepancies can be attributed to variations in temperature and electrode surface preparation. It can be seen that only at very low current densities the passivation times were measurable, as large current densities caused spontaneous passivation. On first sight, this behaviour appears strange, and that cadmium is at all useful in battery applications when it can only deliver such small capacities is surprising. It must be remembered, however, that this result is obtained for cadmium sheet, and that all successful cadmium cells are based on pocket plate, sintered or plastic bonded electrodes. These have highly porous structures, with the large surface areas which are required to produce the desired cell capacity. This is also true for lead-acid cells where it is calculated that the actual current density within such a cell is as low as 2×10^{-5} A cm^{-2} [134]. It can be seen therefore, that the passivation of an electrode is not itself detrimental, so long as the surface area available for further reaction is large.

The time taken for a zinc electrode to passivate in 7M potassium hydroxide solution was excessively long at the current densities employed. This was attributed to the fact that the solubility of the zincate species is sufficiently high at this electrolyte concentration to overcome the accumulation of zincate at the electrode surface which ultimately leads to passivation. The use of 2M KOH was successful in reducing the passivation times to measurable values. However, when compared to the times obtained with the cadmium electrodes, they are still very large, (Fig. 5.3.2.). Fig. 5.3.3. shows a plot of $t_p^{-1/2}$ vs i gives a straight line with a value of k of ~ 0.5, this compares well with work reported by Hampson [127].

Table 5.2.1. also shows the salient data obtained for the additives which form zincate species. The results for this type of addition unfortunately tended to show very little difference in the passivation times to those obtained with no electrolyte addition. A possible explanation for this is that the potassium salts

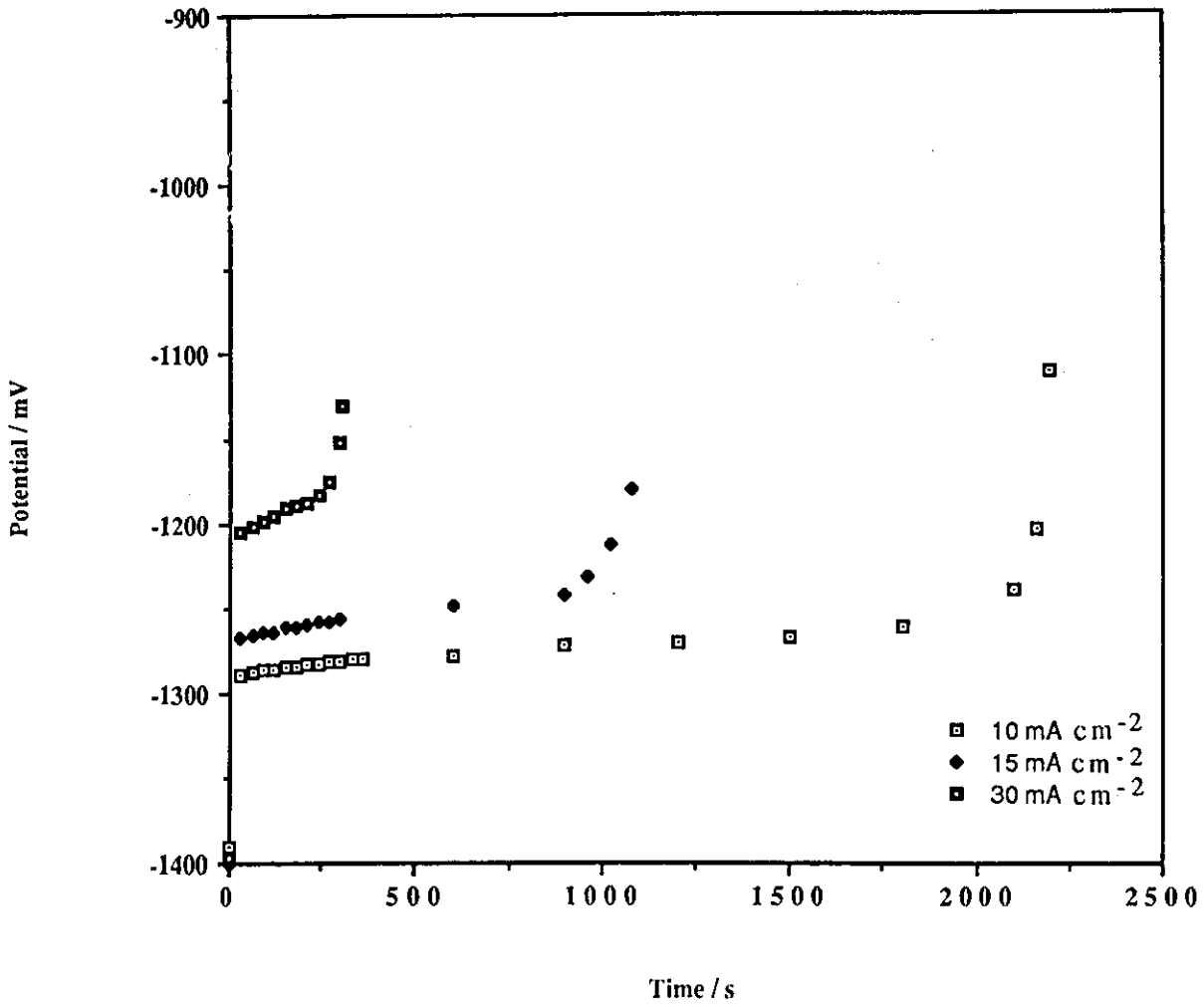

Figure 5.3.2. Passivation curves for a zinc electrode in 2M KOH at various current densities

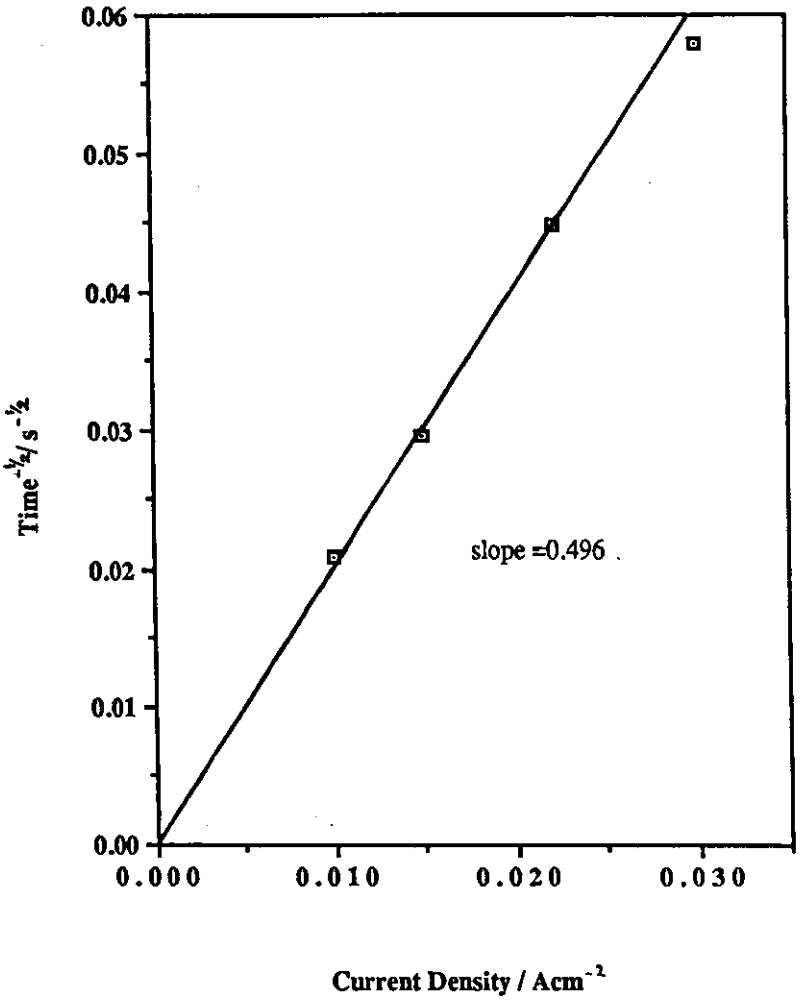

Figure 5.3.3. Plot of $t^{-1/2}$ vs. current density for a zinc electrode in 2M KOH.

themselves were only sparingly soluble in potassium hydroxide, such that not enough of the cation was present to react with all the zincate being discharged into the solution. Thus these additions may prove to be more successful if they are incorporated into the electrode paste during fabrication, as more of the salt could be added. This may also help explain why $Ca(OH)_2$, $Mg(OH)_2$ and $Al(OH)_3$ have been reported to give beneficial effects in the electrode performance data published by other investigators [52-57].

The second group of additives, the zinc-anion reaction products, were found to be more successful, the results are again presented in Table 5.2.1.

The addition of the chromate ion, CrO_4^{2-}, was one example of this type of additive which was found to be very efficient in reducing passivation times, Figs. 5.3.4 and 5. This is not that surprising since chromate is well known for its passivating properties, and is used extensively in the electroplating and metal finishing industry, for the surface protection of metals, particularly iron. Chromate addition to secondary zinc batteries was patented in the early 1900's [135], but the idea was never taken up commercially. Very little of the chromate ion was necessary to cause passivation of the zinc surface. Investigation of the other members of group VIa in the Periodic Table i.e. molybdate and tungstate, revealed that these were much less effective in reducing the passivation time. This was the case even at high concentration, and hence further studies of these salts were discontinued. Although the oxidising properties of the chromate are not as high in basic solutions, compared to acidic conditions, it is still a good oxidising agent:

$$CrO_4^{2-} + 4H_2O + 3e^- \longrightarrow Cr(OH)_3 + 5OH^- \qquad E^\circ = -0.13V$$

This may explain its superiority over the other group members. Auger analysis of the electrode surface after passivation in

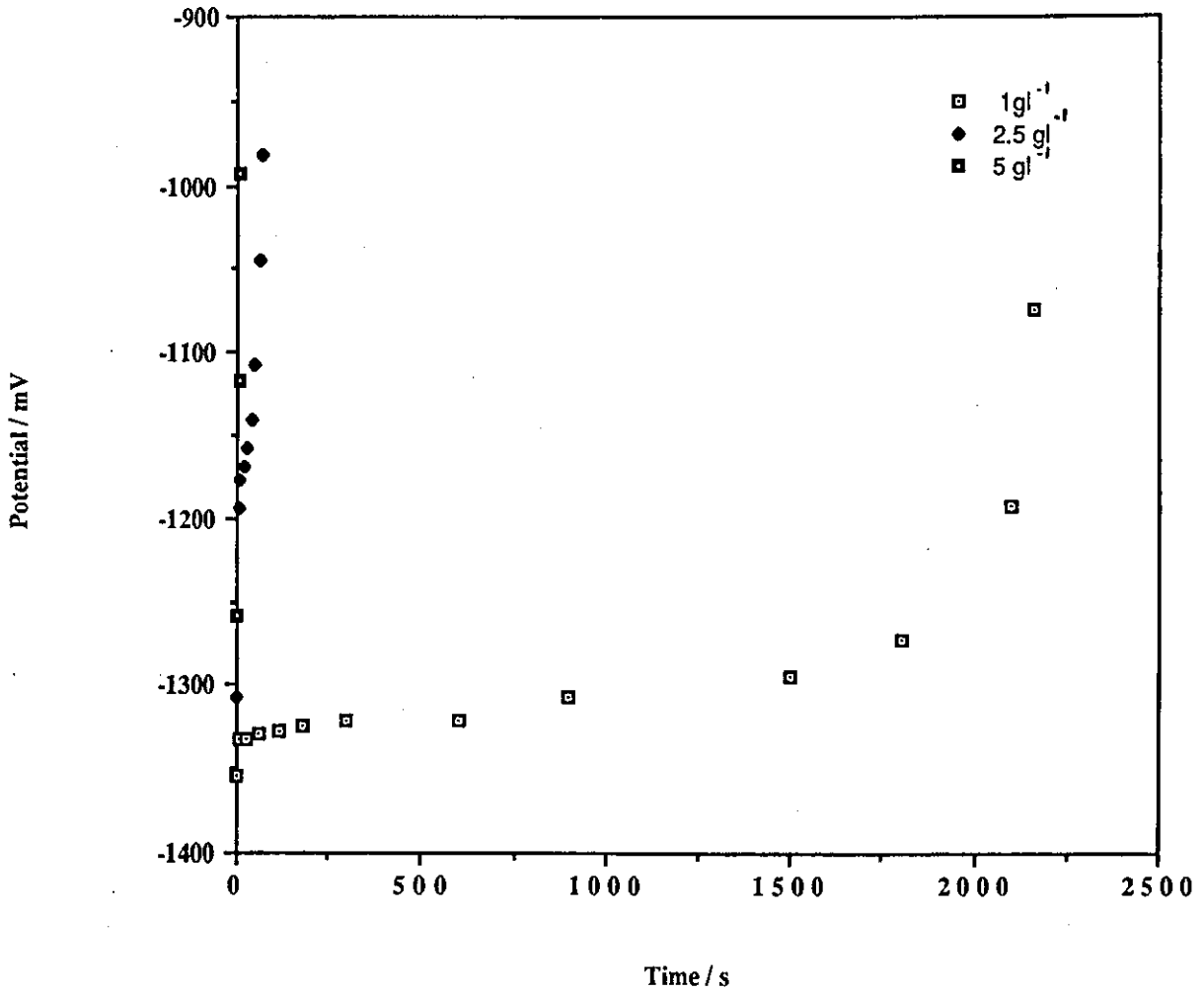

Figure 5.3.4. Passivation curves for a zinc electrode in electrolyte containing chromate ions, at 0.25 mA cm^{-2}

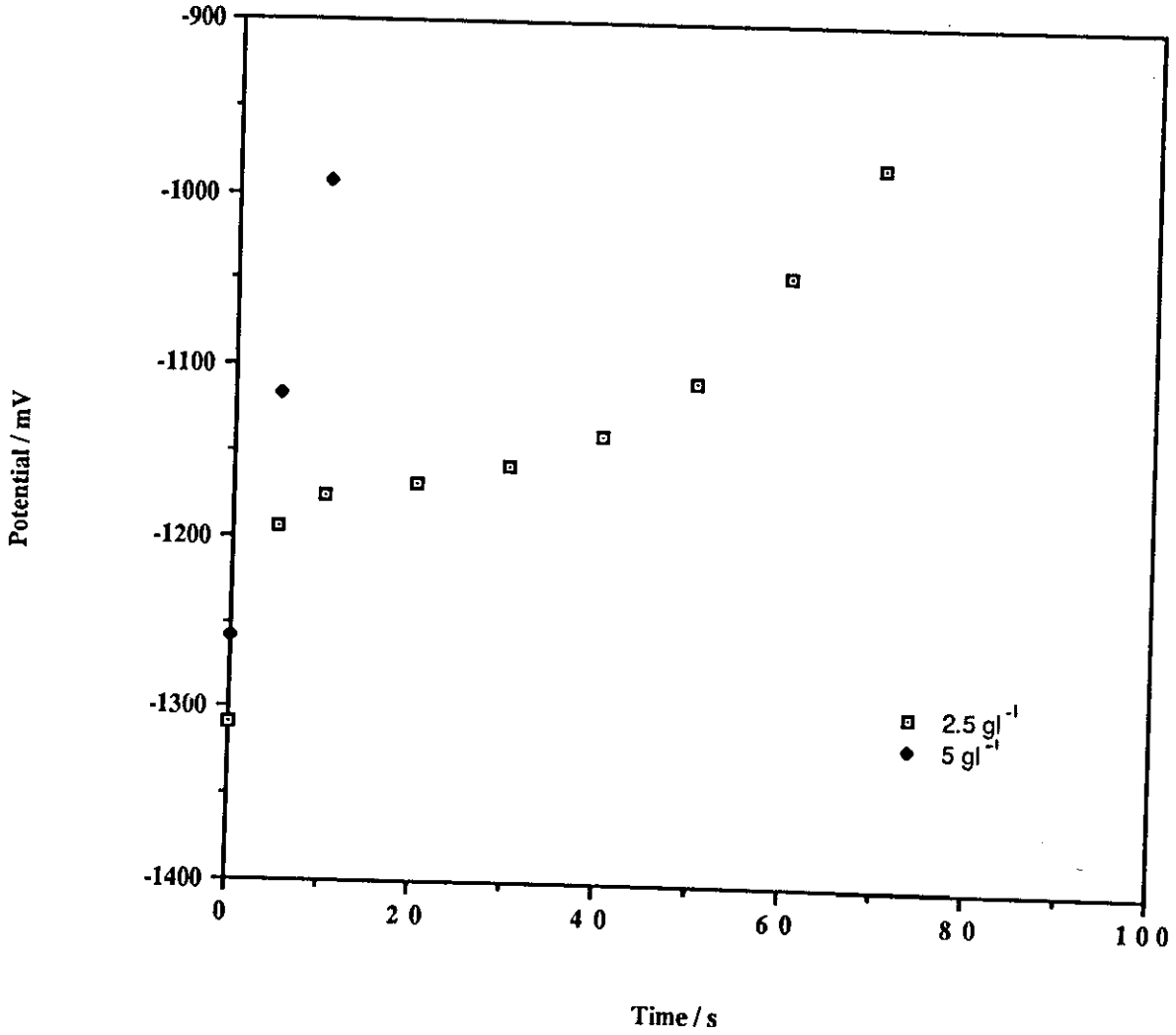

Figure 5.3.5. Passivation curves for a zinc electrode in electrolyte containing chromate ions, at 0.25 mA cm^{-2}.

chromate solution (Figs. 5.3.6. a & b) revealed the passivating layer to contain zinc, oxygen and chromium species only, therefore the layer can be either a mixed oxide (eg Cr_2O_3 and zinc) or zinc chromate. This was still the case after bombarding the surface with a 500 eV Ar ion beam for 30s, indicating the elements detected were not due to surface contamination.

Another anion additive tested was that of the phosphate. This ion has often been suggested as an additive for zinc batteries [89-91]. However, the investigation showed that at the concentrations used, the passivation times for phosphate modified electrolytes were only slightly reduced compared to 2M KOH alone. These findings are in good agreement with those of Morgan [136] who found the rate of dissolution to decrease with phosphate addition.

The final anion additive examined was the borate species; both in the form of orthoboric acid, H_3BO_3, and potassium tetraborate, $K_2B_4O_7.4H_2O$. It was found that by careful variation in the amount of additive it was possible to obtain passivation times of the order to those obtained with cadmium. These results are again presented in Table 5.2.1.

Considerably less boric acid was required to produce the same effect as potassium tetraborate. This can be explained by an examination of the chemistry of the two additions in alkaline conditions:

The tetraborate ion has a structure analogous to the sodium salt borax, $Na_2B_4O_7.10H_2O$, which is slightly basic. It contains two tetrahedral BO_4 and two trigonal BO_3 groups, and so should correctly be written as $K_2B_4O_5(OH)_4.2H_2O$. In alkali solutions the ion hydrolyses to the $B(OH)_4^-$ ion.

Boric acid is a very weak, monobasic, Lewis acid and thus acts as a OH^- acceptor. In alkali it converts by a series of steps to the

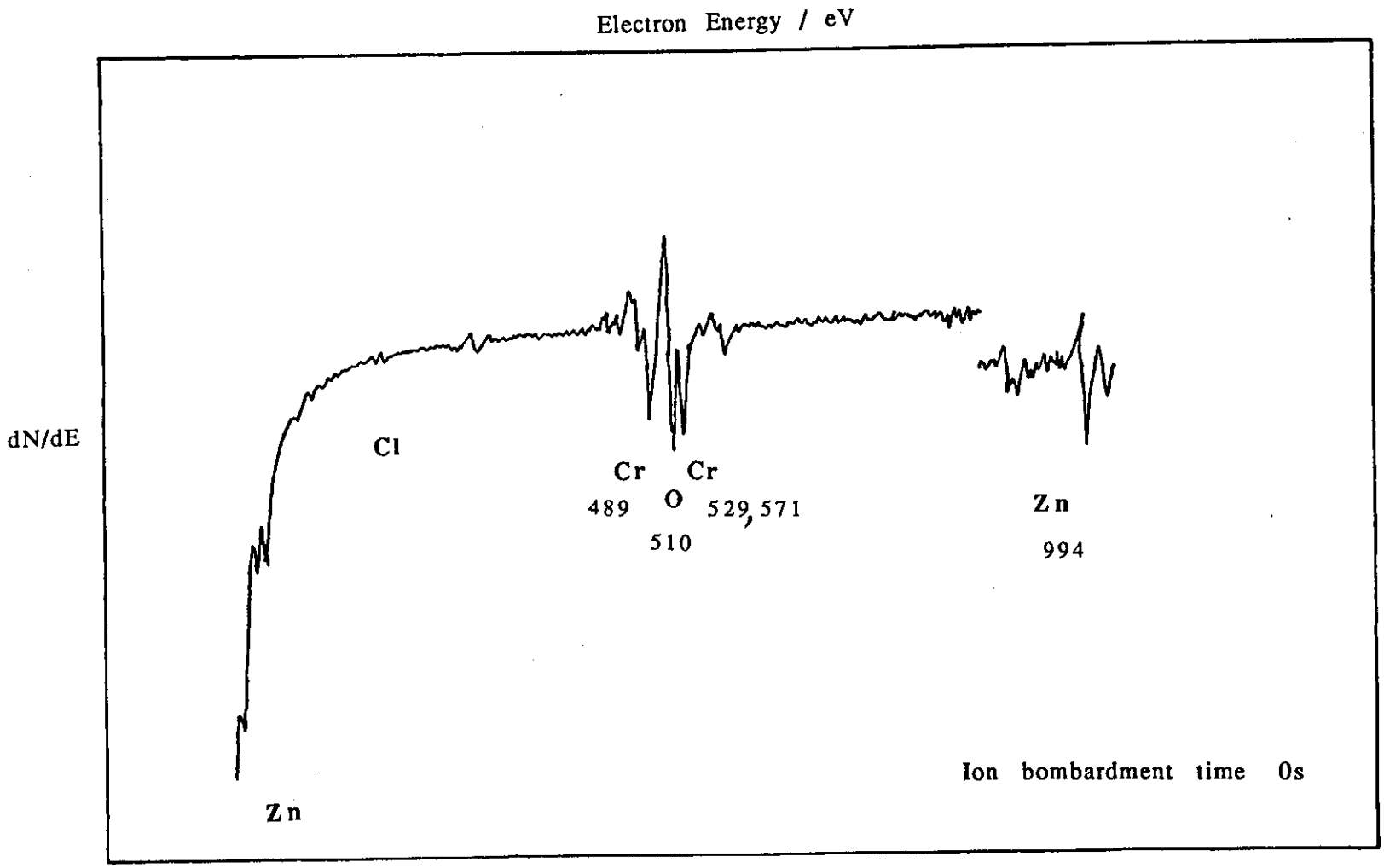

Figure 5.3.6a. Auger analysis of electrode surface after passivation in chromate solution.

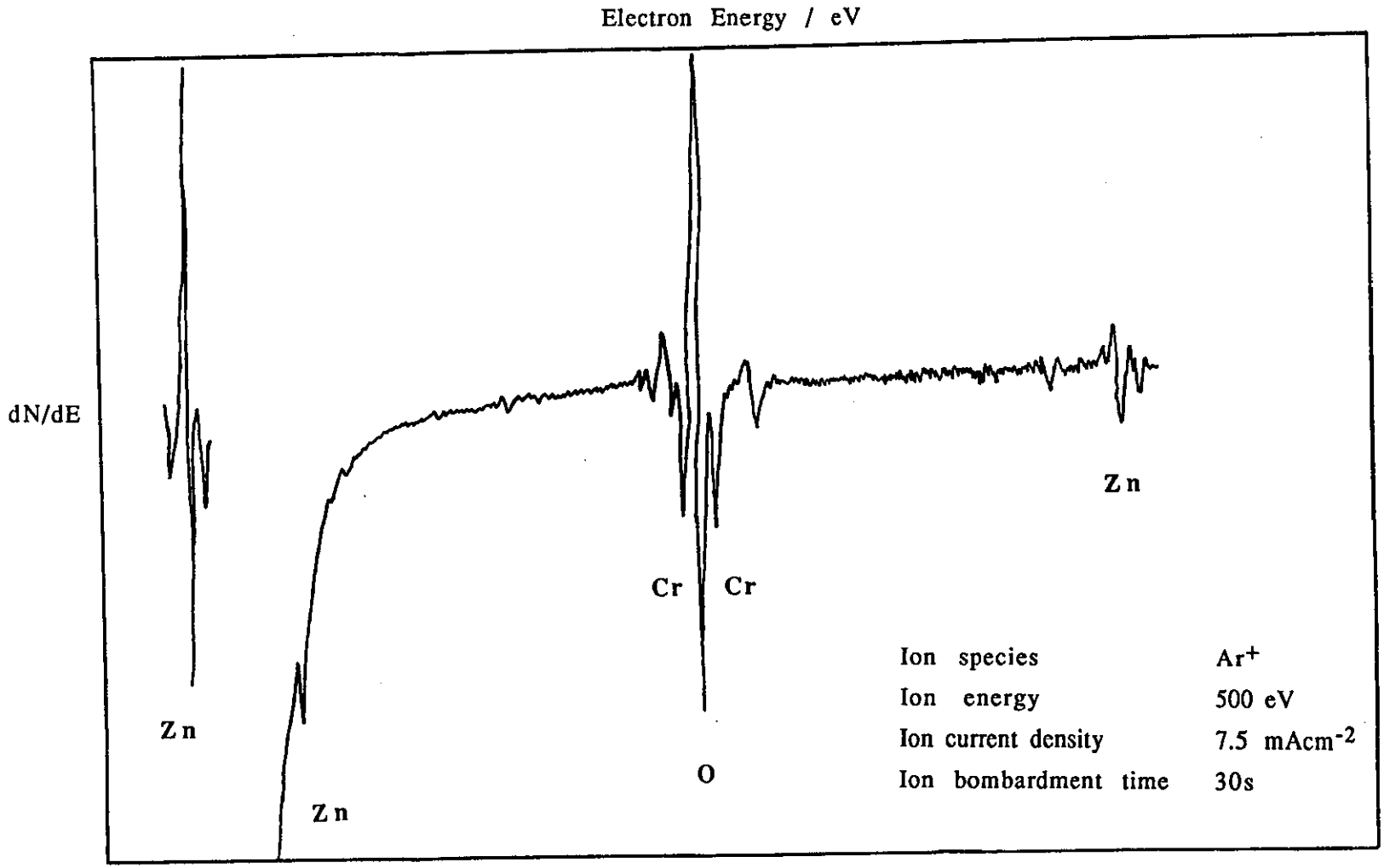

Figure 5.3.6b. Auger analysis of electrode surface after passivation in chromate solution. After 500 eV Ar ion bombardment for 30s.

borate ion $B(OH)_4^-$. These steps have been identified by Ingri [137], as follows:-

$$B(OH)_3 \rightarrow B_5O_6(OH)_4^- \rightarrow B_3O_3(OH)_5^{2-} + B_4O_5(OH)_4^{2-} \rightarrow B(OH)_4^-$$

--------> increasing pH

It can be seen that one of these steps involves the $B_4O_5(OH)_4^{2-}$ ion present in the tetraborate species. Thus on a weight for weight basis boric acid should be more efficient at using up OH^- ions, than the tetraborate species. This indeed was found to be the case as shown in Table 5.2.1. For this reason subsequent investigations of borate additions were thus performed using boric acid.

As already mentioned, the amount of boric acid added was found to be critical to the length of passivation time, Figs. 5.3.7.and 8. This is in agreement with results reported by Schneider et al [138], who considered that the composition of the borate species in solution changed as more boric acid was added. At low additions K_3BO_3 was the predominant species, but as the amount of boric acid gradually increased a transition occurred until at higher concentrations KH_2BO_3 became dominant. Schneider found that a composition between K_3BO_3 and K_2HBO_3 gave optimum results for his bipolar accumulator, in 25% KOH.

Auger analysis of the electrode surface after passivating in borate solution revealed no evidence of a boron species (Figs. 5.3.9.a & b). This finding is in agreement with that reported by Thornton and Carlson [93] who stated that the solubility of zinc was a function of the hydroxyl ion concentration, rather than the formation of an insoluble zinc salt (other than the oxide). This was also found to be the situation by Nichols et al [94].

It was therefore considered important to measure the pH's of the solutions containing borate and chromate, Table 5.3.1.

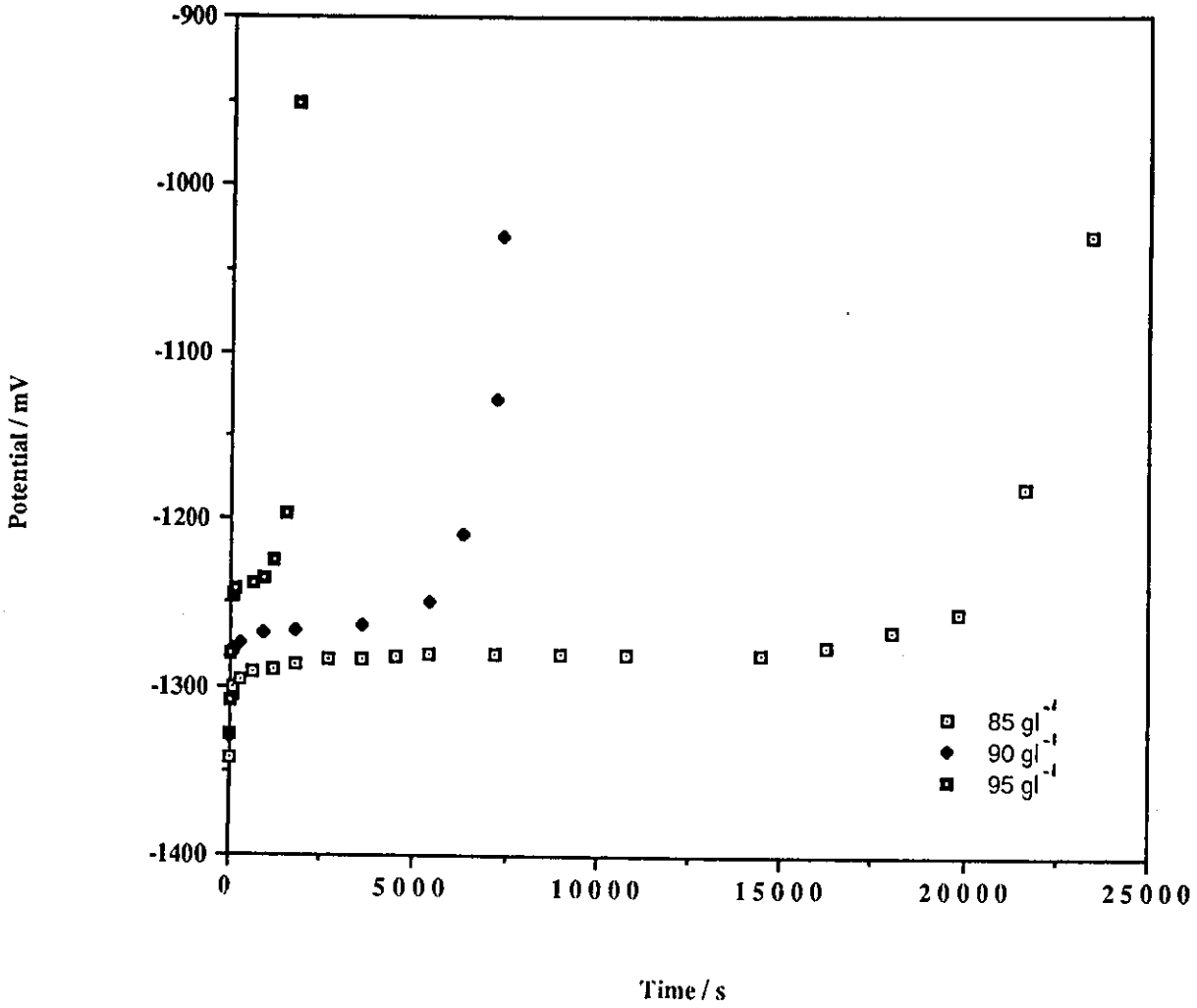

Figure 5.3.7. Passivation curves for a zinc electrode in electrolyte containing borate ions, at 0.25 mA cm^{-2}.

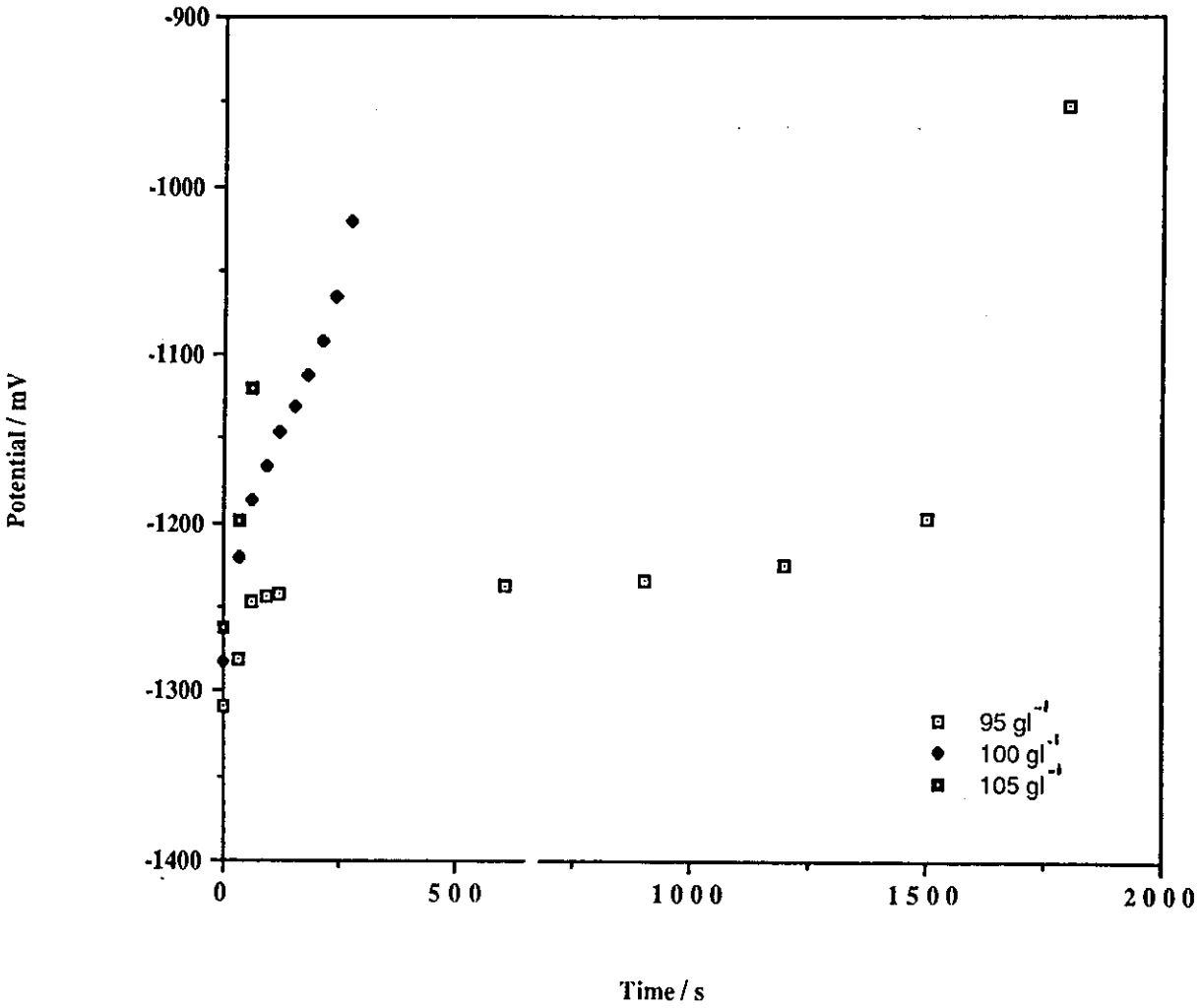

Figure 5.3.8. Passivation curves for a zinc electrode in electrolyte containing borate ions, at 0.25 mA cm^{-2}.

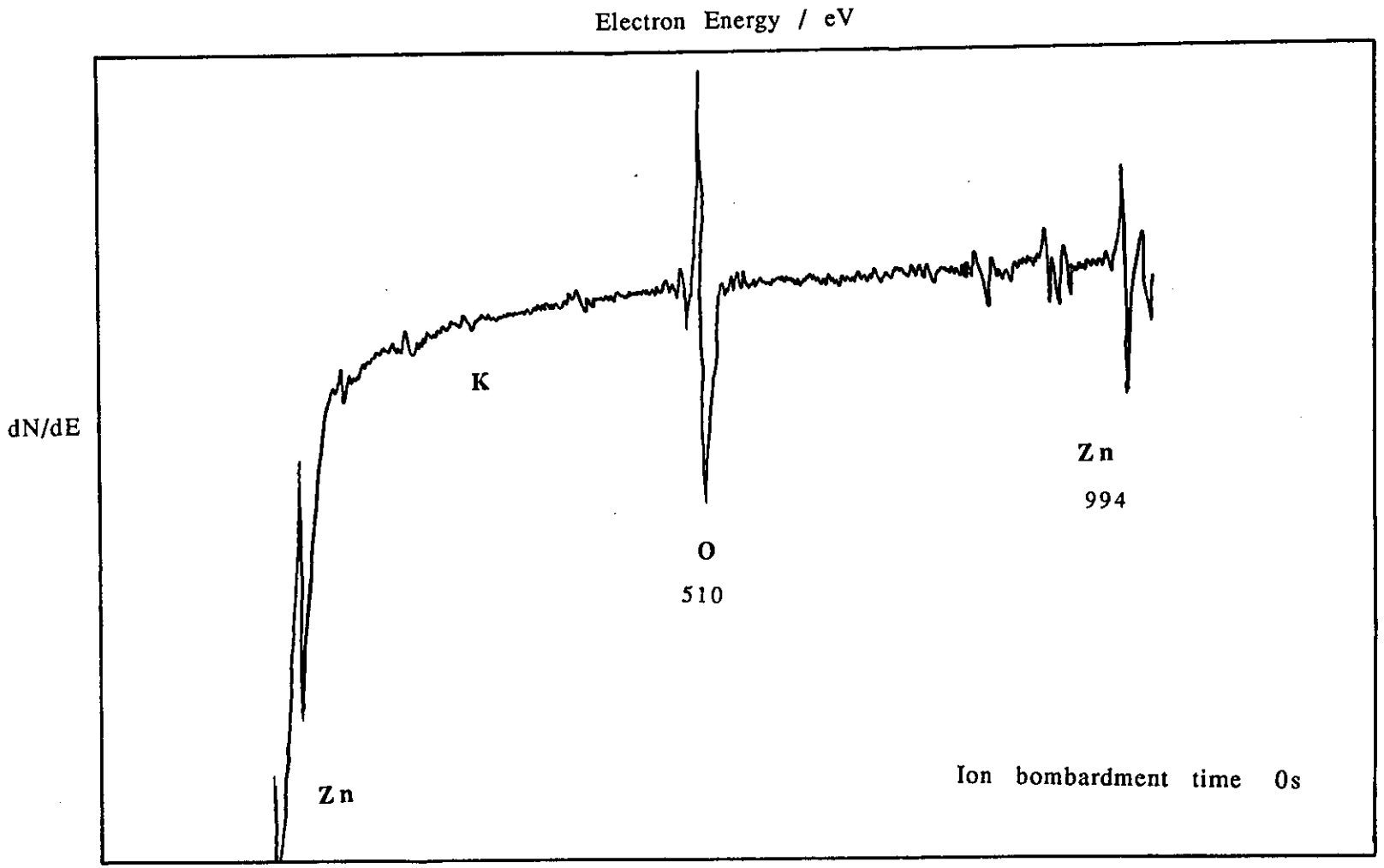

Figure 5.3.9a. Auger analysis of electrode surface after passivation in boric acid solution.

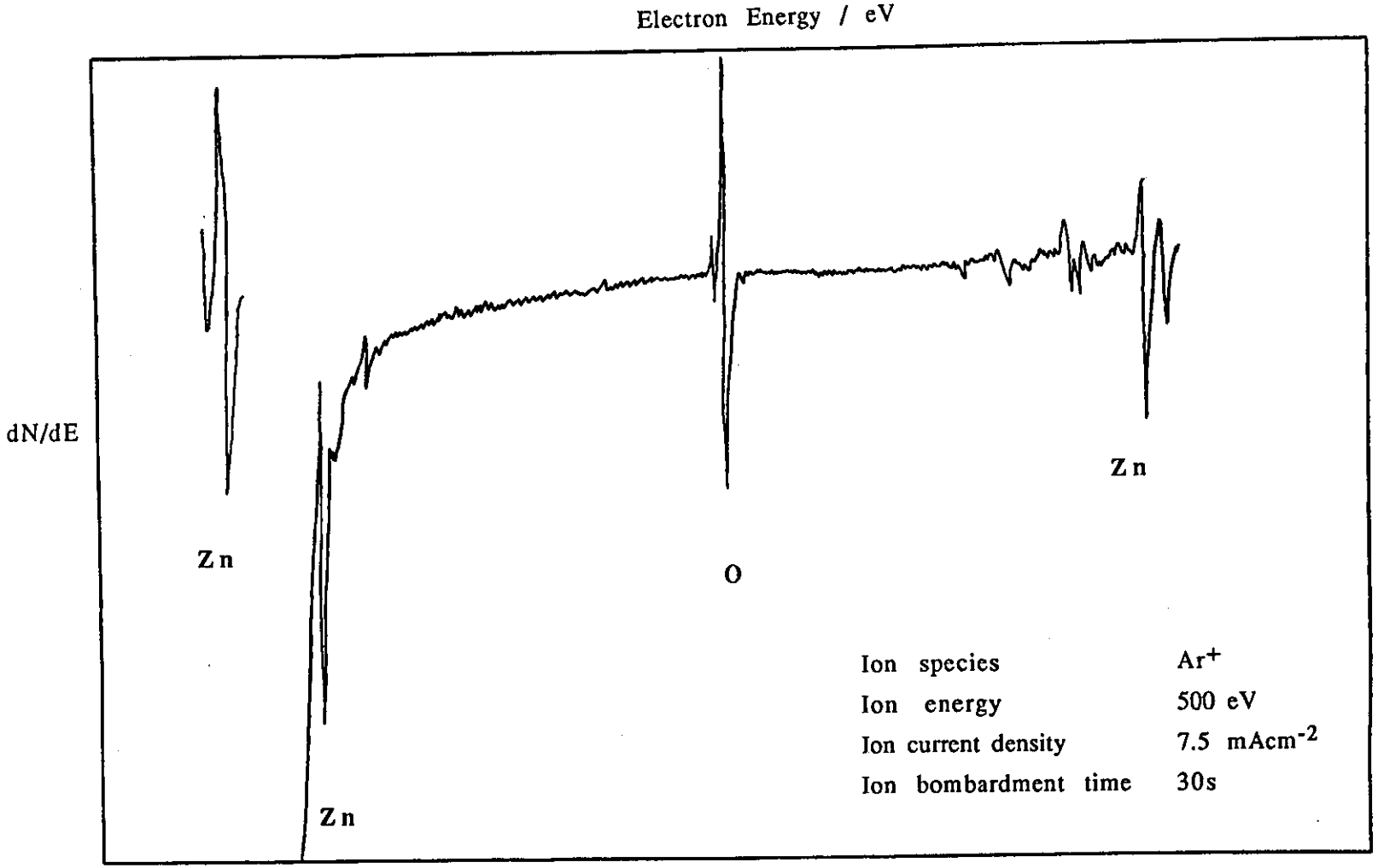

Figure 5.3.9b. Auger analysis of electrode surface after passivation in boric acid solution. After 500 eV Ar ion bombardment for 30s.

Solution	pH
2M KOH alone	14.28
2M + 85 gl^{-1} Boric acid	14.12
90 gl^{-1}	14.05
95 gl^{-1}	13.94
100 gl^{-1}	13.75
2M + 2.5 gl^{-1} chromate	14.30

Table 5.3.1. pH measurements of borate and chromate solutions.

It can be seen that chromate has no significant effect on the pH, whereas increasing the borate concentration decreases the pH. This decrease in pH can thus be linked to the decrease in passivation times.

One final point worth noting, was the decrease in open-circuit potentials for the zinc-anion modified electrolytes. If too much additive was dissolved in the electrolyte, the open-circuit potential suffered a massive drop as the surface passivated - without the need for any external current. This drop was not observed in cationic-zincate electrolytes. Surface film formation of the passivating species can be attributed as the cause of this phenomenon.

In the case of chromate addition this film, of zinc chromate, was very tenacious and was caused by the oxidising nature of the Cr^{6+} ion. The borate ion however, functioned by a different mechanism. The ion caused a reduction in free hydroxyl ions, as indicated by the drop in pH, and therefore caused zinc oxide to precipitate at the electrode surface.

CHAPTER 6

POTENTIOSTATIC POLARISATION STUDIES OF ZINC IN ALKALI

6.1. Introduction

The anodic dissolution, and ultimate passivation, of zinc in alkali under potentiostatic control has been studied previously by numerous workers [41,139-155]. Typically there are four characteristic regions observed on sweeping the potential slowly in the anodic direction.

Initially the current increases exponentially with the applied potential where active dissolution of the zinc occurs. This is followed by a zone of linear variation of current with potential. A prepassive region is next observed where, although a high current level is maintained it is virtually independent of potential. Finally passivation is seen to occur with a rapid decrease in current. On reversal of the potential the current density passes through virtually the same values as the anodic sweep, but in reverse order suggesting the reversible breakdown of the passivation process.

The dissolution process has been described by two differing reaction schemes. Dirkse and Hampson [139,140] proposed a mechanism in which hydrating water molecules are necessary:-

i. $Zn_{kink} + OH^- \rightarrow Zn_{ad}OH^-$ (very slow adatom diffusion with OH^-)

ii. $Zn_{ad}OH^- \rightarrow Zn(OH)_{ad} + e^-$

iii. $Zn(OH)_{ad} + OH^- \rightarrow Zn(OH)_2 + e^-$

iv. $Zn(OH)_2 + 2OH^- + 2H_2O \xrightarrow{fast} [Zn(OH)_4 .2H_2O]^{2-}$

Step ii. is rate determining unless the reaction time is more than 10 μs when surface diffusion or kink site generation i.e. step i., becomes governing [140].

Bockris et al [141] found no evidence in support of an adsorbed species, and therefore proposed an alternative mechanism which involved two consecutive one electron transfers, with the second step rate determining:-

i. $Zn + OH^- \rightarrow ZnOH + e^-$

ii. $ZnOH + OH^- \rightarrow Zn(OH)_2^-$

iii. $Zn(OH)_2^- + OH^- \xrightarrow{r.d.s} Zn(OH)_3^- + e^-$

iv. $Zn(OH)_3^- + OH^- \rightarrow Zn(OH)_4^{2-}$

Whichever mechanism is correct the final product is always the tetrahedral zincate species, $[Zn(OH)_4^{2-}]$ and so the overall reaction can be represented as:

$$Zn + 4OH^- \rightarrow Zn(OH)_4^{2-} + 2e^-$$

Continued anodic dissolution results in a build up of the zincate species at the electrode surface, until passivation can eventually occur. The mechanism of zinc passivation is even less well resolved than that of dissolution, in spite of considerable research effort [41,44,142-155].

Three different models have been proposed to describe the initial film nucleation process, which each account for a large part of the observed experimental results. However, no single mechanism is completely satisfactory.

In the first model, the concentration of the dissolved zincate species at the electrode surface increases until a critical value is reached. At this point of supersaturation an insoluble zinc salt is precipitated onto the electrode. The mechanism can be represented as follows:-

$$Zn(OH)_4^{2-} \rightarrow ZnO + H_2O + 2OH^-$$

This model is known as dissolution - precipitation, and is thought to occur in porous zinc electrodes during their discharge, supersaturation occurring within the matrix. Baugh et al [145 -147] have recently shown that precipitation is not the direct cause of the failure of zinc electrodes, but merely an accelerator of it.

The adsorption model states that the adsorbed intermediate species, $ZnOH_{ad}$, from the Dirske dissolution scheme rejects a proton to form a passive oxide layer [148].

$$ZnOH_{ad} \rightarrow ZnO + H^+ + e^-$$

This process is thought to occur at some critical potential.

In the third model, passivation takes place by the nucleation and growth of a two dimensional layer of the oxide film [149]. Clusters of the film eventually overlap resulting in the formation of a phase monolayer. This simple model assumes a constant number of oxide nuclei during the growth period, and a constant nucleation rate at a given temperature. The rate determining step corresponds to a rearrangement of two OH^- ions into the oxide layers by the rejection of a water molecule. It can simply be represented thus:-

$$Zn + 2OH^- \rightarrow ZnO + H_2O + 2e^-$$

This process is again thought to occur at some critical potential. Distinction between this model and that of the adsorption model is

difficult to make, as it would require the demonstration of the presence of two dimensional nucleation on a polycrystalline solid metal surface.
As well as the confusion over the mechanism of passivation, the exact nature and composition of the passivating film is also not entirely agreed. The film may either be the hydroxide, $Zn(OH)_2$, or the oxide, ZnO, depending on the alkali concentration, discharge conditions and temperature. In addition to this, the film has also been proposed to consist of a dual layer. Again there is disagreement over the composition of these layers. Both Huber [150] and Nikitina [151] have identified the passivating film as the hydroxide, which is then covered with a layer of zinc oxide. However other workers state that two types of zinc oxide bring about passivation [152-153]; the first layer being the result of the precipitation, Type I, and the second due to surface growth, Type II. The choice between these two arguments is also made difficult by the ease of dehydration of zinc hydroxide, limiting the techniques applicable to those involving in-situ examination.

From the above, it is clear that the steps involved in anodic dissolution and passivation of zinc are very complex. Potentiostatic polarisation (or cyclic voltammetry) is an extremely useful technique for following such reactions, since it allows current density measurements to be made at all potentials within a range of interest, and hence identification of any intermediate stages of passivation.

Sanghi and Fleischmann performed a potentiostatic study of solid zinc electrodes in alkaline solutions in 1959 [156]. However, it is probably correct to say that Vozdvizhenskii and Kochmann [157] were the first workers to perform a comprehensive study of the system, with most of their findings being confirmed by subsequent investigations.

Vozdvizhenskii and Kochmann [157] reported the existence of two current peaks before passivation of the electrode. The relative

heights of these peaks depended on the sweep rate employed. Visual examination of the electrode during the sweep revealed that changes in the colour of the electrode surface occurred. This change, from white to black, on passivation was attributed to changes in the composition of the film present at the surface. The dark colouration being due to finely dispersed zinc arising from a disproportionation reaction:

$$Zn + 2OH^- \rightarrow Zn(OH)_2^- + e^-$$

$$2\,Zn(OH)_2^- \rightarrow Zn + Zn(OH)_4^{2-}$$

The following section describes how the technique of cyclic voltammetry was used to monitor the effect of electrolyte additions on the zinc passivation reaction. The effect of rotating the electrode during the potential sweep was also investigated.

6.2. Experimental

Experimental investigations were performed in 7M and 2M KOH electrolytes - the 2M having additions of boric acid and potassium chromate of various concentrations made to it. The electrolyte was purged with oxygen free nitrogen for fifteen minutes prior to, and during, electrochemical investigations. A standard three-limbed electrolytic cell, as described in Chapter 4, was employed for all experiments.

The working electrode throughout was a solid zinc rod set in teflon shroud. Preparation of this electrode was identical to that detailed in the previous chapter's experimental section.

Cyclic voltammograms were obtained for the various electrolyte solutions, the sweep limits being -1450 and -900 mV (vs Hg/HgO). A sweep rate of 1 mV s^{-1} was applied using a ramp generator in conjunction with a potentiostat. The potentials and resultant current profiles were recorded with an X-Y chart recorder.

When rotation of the electrode was required this was performed using a Kemitron RD5 unit.

6.3 Results and Discussion

Figure 6.3.1. shows the current - potential response for a stationary zinc electrode in 7M KOH, with a potential sweep rate of $1 mVs^{-1}$. The response shows many features which are characteristic of the anodic behaviour of zinc in alkali, and have been observed previously by other investigators [143-157]. These features have been described in the introduction of this chapter and will not, therefore, be discussed further here.

The high degree of dissolution observed is problematic with regard to the successful cycling of battery electrodes, as already stated. On the return sweep however there is only a small, virtually non-existent, deposition peak observed due to the zinc species very low concentration in the large volume of electrolyte in the cell (250 ml). Thus the concentration gradient for this process is small, and the mechanism is therefore diffusion limited.

A similar situation is also encountered when the electrolyte concentration is reduced to 2M, Fig. 6.3.2. However, an important difference to note with this solution is the decreased currents obtained. The lowering of the zinc oxide solubility in this solution is the reason for this, as it causes the extent, and rate, of dissolution to be considerably less.

Variation of rotation speed was also investigated at this lower hydroxyl concentration, and revealed an increase in current with rotation speed (Fig. 6.3.2.). This again has previously been observed and is the cause of the easier facilitation of supply of reactant ions to , and the removal of product from the electode , at the faster rotations speeds. Thus the dissolution rate is increased and results in the higher currents observed. Also, on rotating the

Figure 6.3.1. Current-potential response for a stationary zinc electrode in 7M KOH

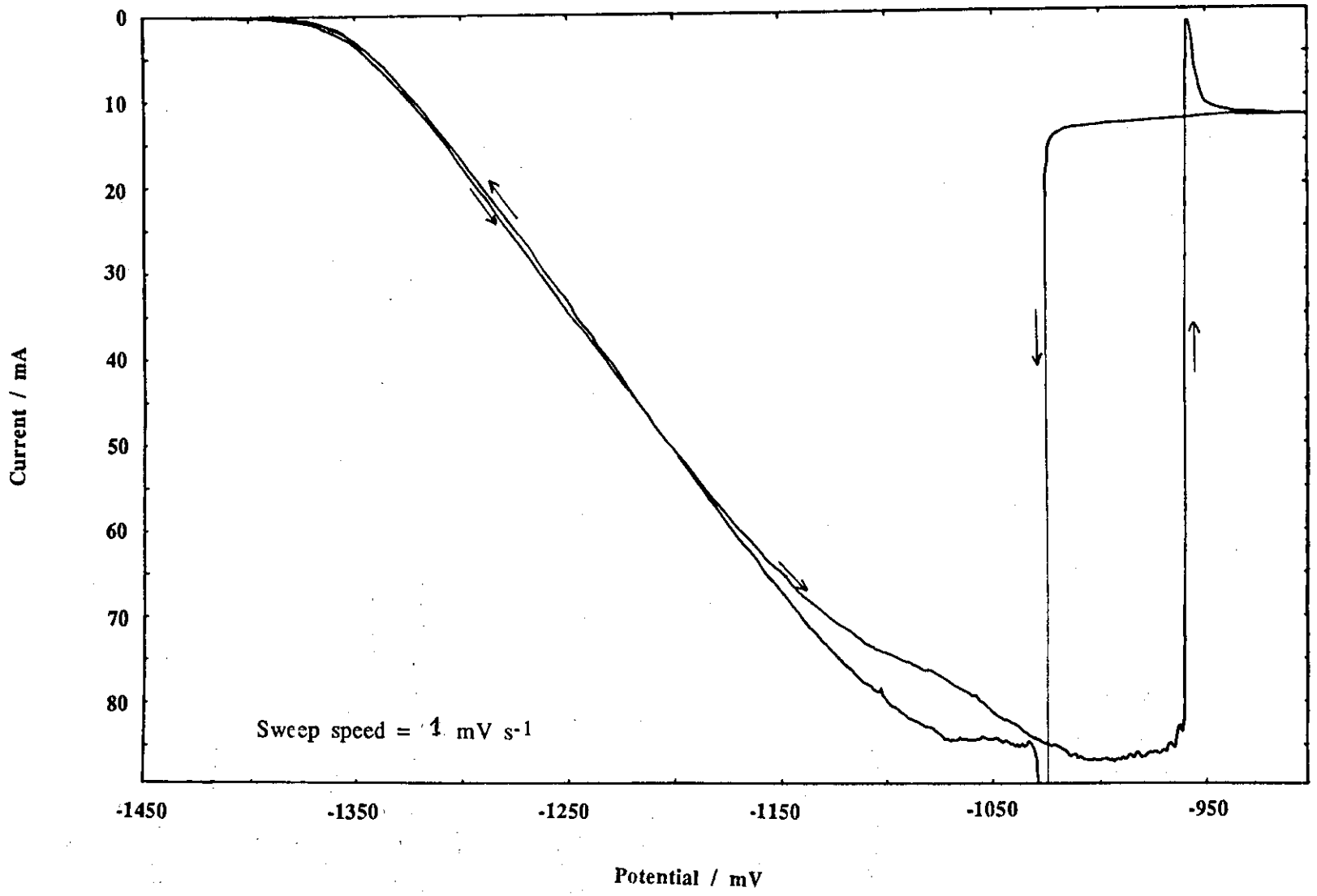

Figure 6.3.2. Current-potential response for a zinc electrode in 2M KOH: — stationary electrode ---- rotation speed 15.9 r.p.s.

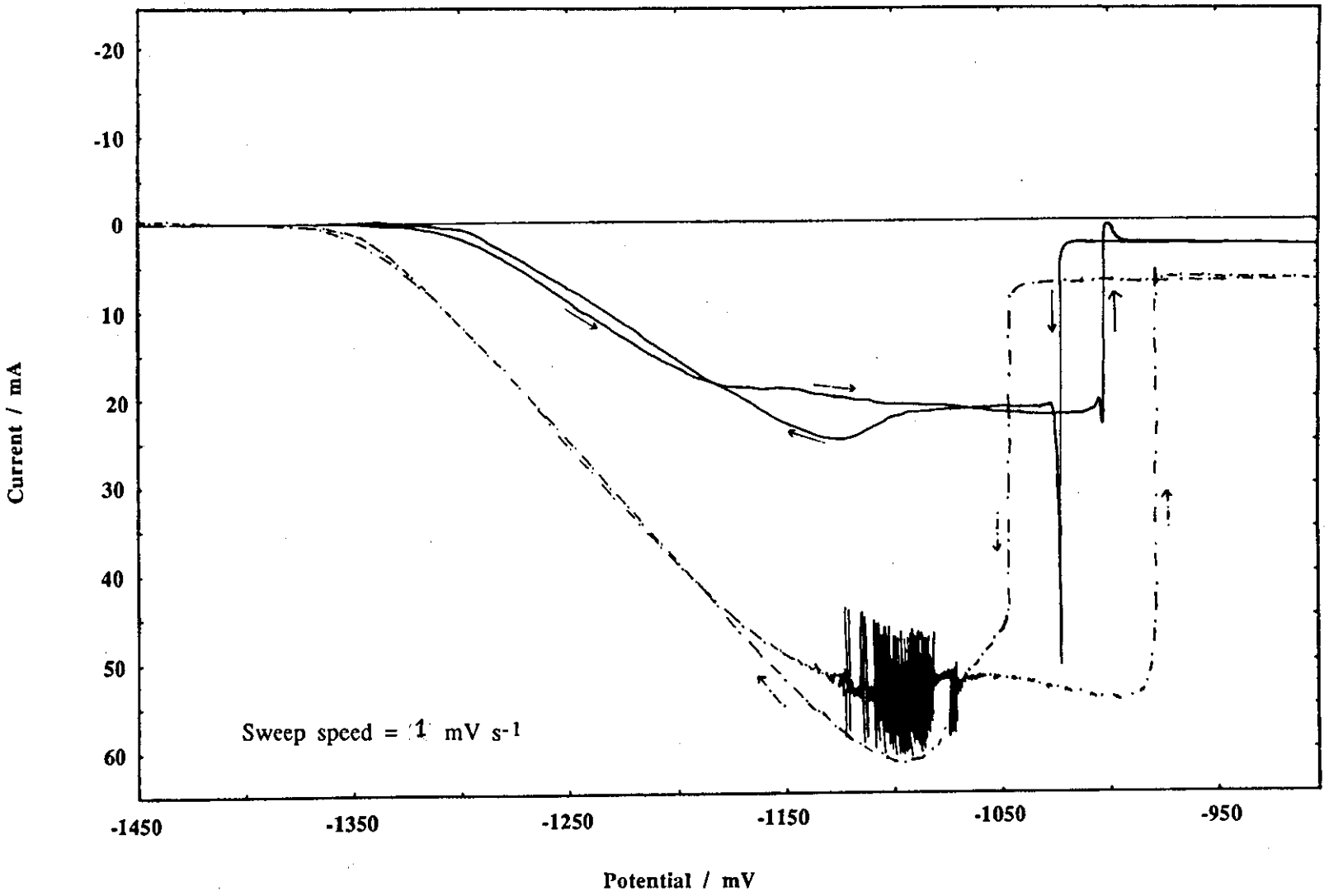

electrode it was noted that current oscillations arose near the point of passivation. These oscillations have previously been assigned to the breakdown and repair of the passivating, Type II, film [143, 152, 153].

In the preceding chapter it was shown that the addition of borate and chromate ions can influence the galvanostatic behaviour of zinc electrodes. The effect of these additives when monitored potentiostatically is given in the following.

The typical behaviour of borate is illustrated by Fig. 6.3.3., which shows the response given by a zinc electrode in 2M / KOH / 85 gl^{-1} boric acid electrolyte when swept at 1 mVs^{-1}. It can be seen that the dissolution peak is much smaller in size than that in 2M KOH alone, due to lower zincate species solubility. In addition a reduction peak is now observed in this solution, which is associated with zinc oxide reduction. The occurrence of this peak suggests that the zinc species is held much closer to the vicinity of the electrode surface, due to the lower solubility in the borate solution.

Another feature noted when borate is added to the electrolyte is that the current associated with the reactivation of the electrode is much less than the anodic sweep current. This is the reverse of the situation observed in borate-free electrolytes, where pitting and surface roughening of the electrode occurs on the anodic scan, consequently causing an increase in the actual surface area. Also, the point of passivation is seen to occur at a less anodic potential in borate solution. Both of these phenomena can be explained in terms of the presence of the film which reduces the tendency for zinc dissolution.

The reduction in reactivation current has important implications with regard to the successful operation of secondary zinc batteries. In lead-acid and nickel-cadmium cells the passivating species is, at most, only sparingly soluble and reduces to the metal, via the

Figure 6.3.3. Current-potential response for a stationary zinc electrode in 2M KOH / 85 gl^{-1} boric acid electrolyte.

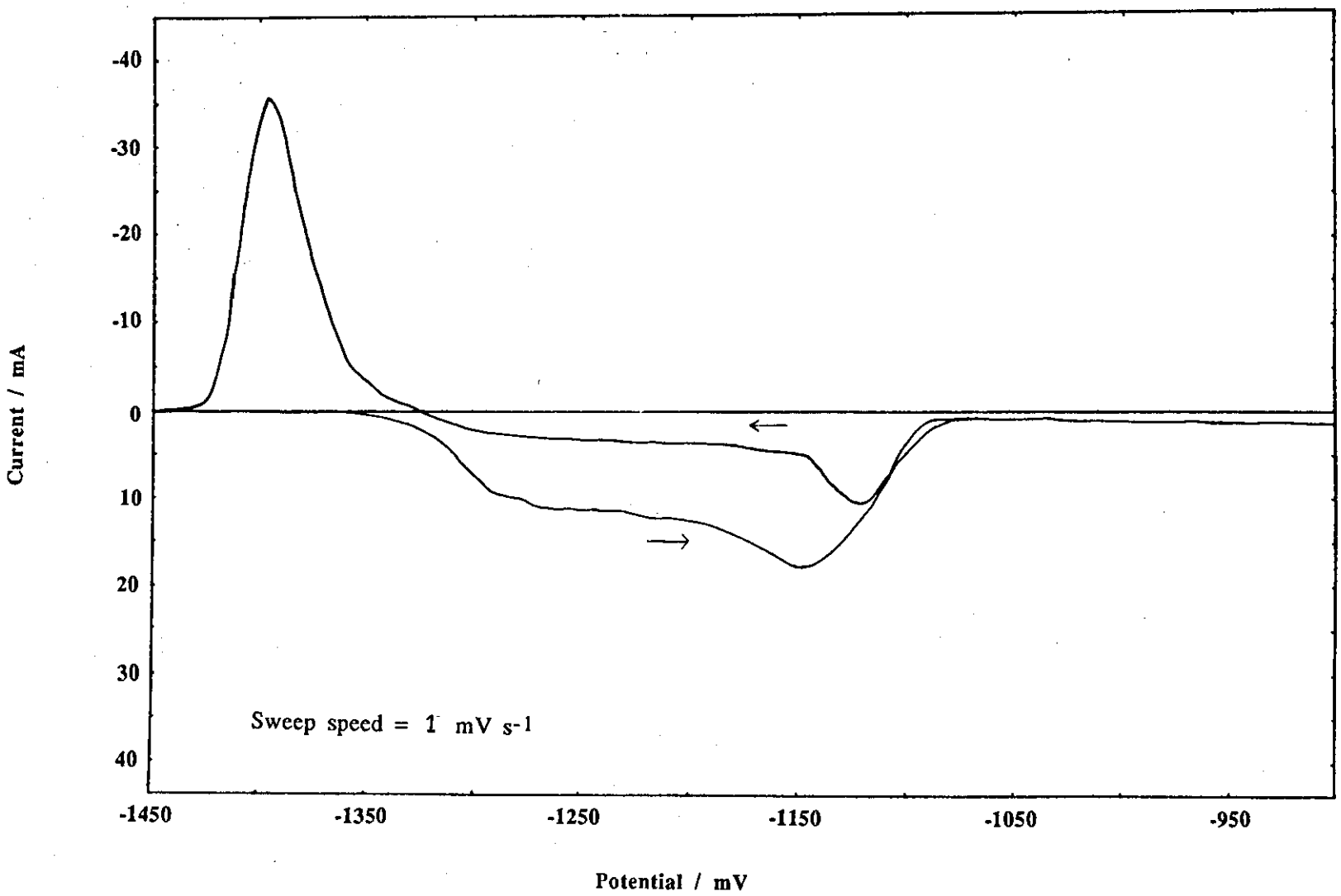

solid-state pathway, at potentials negative of the reversible potential. This is unlike the situation for zinc which undergoes reactivation, and allows a large amount of zinc to enter solution from this 'extra' dissolution. On subsequent recharge this causes dendritic growth and shape change of the electrode. Therefore, if the dissolution via reactivation can be reduced, then this will help to alleviate the problems normally associated with rechargeable zinc cells.

Figures 6.3.4 - 6.3.8 show the effect of rotating the electrode in this solution. The dissolution current is seen to increase with the rotation speed, the reactivation current is also larger due to the passivating film breaking down more easily. However the reduction peak is seen to decrease in size, since there is less zinc species retained at the surface, relative to that going into solution i.e. rotating the electrode causes a return to the situation seen in 2M KOH alone.

Figures 6.3.9. - 6.3.12 show the effect of increasing the borate concentration in the electrolyte. At the higher concentrations, the tendency to passivate is much greater, giving rise to the smaller currents observed. This is as expected, since zinc oxide is more easily formed as the borate concentration increases thus shutting off the electrode reaction. Another feature noted with increasing borate concentration, was the rest potential of zinc shifting to more anodic potentials with increasing concentration (also noted in previous chapter: Table 5.2.1.) - caused by the reduction in pH, as the borate ions reduced the amount of free hydroxyl ions in solution.

The effect of rotation at these higher concentrations was also investigated and gave similar trends as those obtained using 2M / 85 gl^{-1} electrolyte.

Figure 6.3.4. Current-potential response for a zinc electrode in 2M KOH / 85 gl^{-1} boric acid electrolyte when rotated at 3.29 r.p.s.

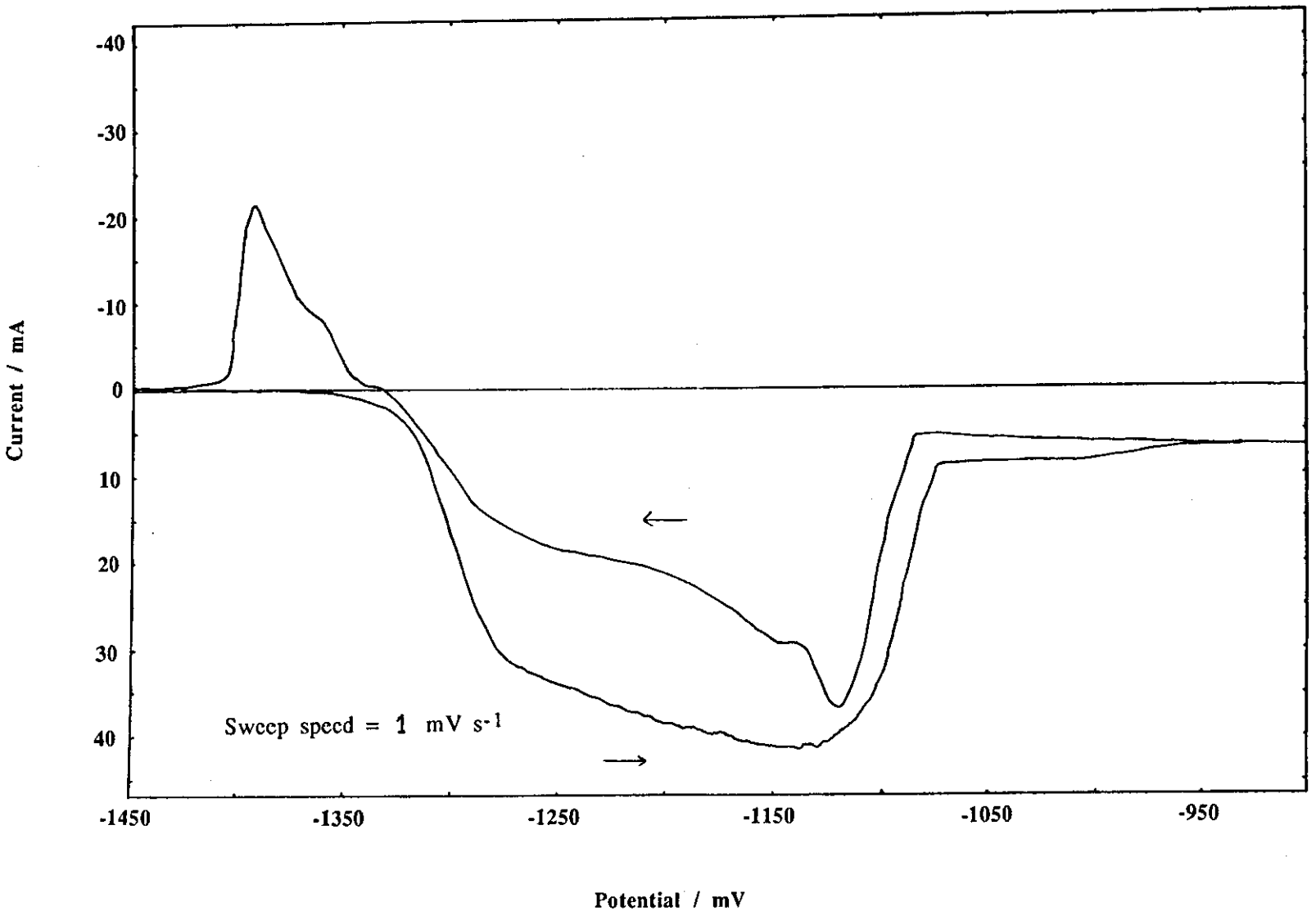

Figure 6.3.5. Current-potential response for a zinc electrode in 2M KOH / 85 gl^{-1} boric acid electrolyte when rotated at 4.91 r.p.s.

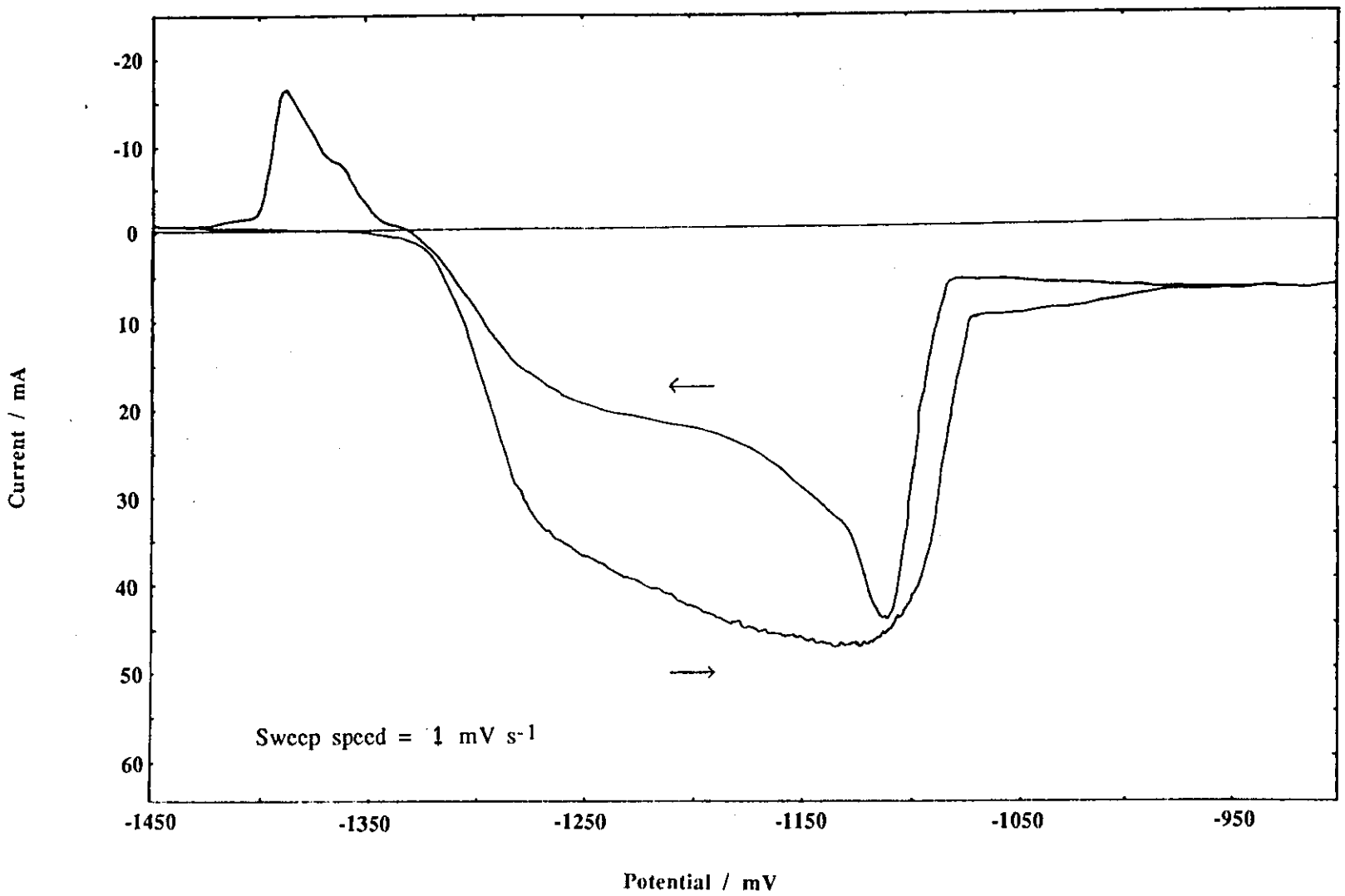

Figure 6.3.6. Current-potential response for a zinc electrode in 2M KOH / 85 gl^{-1} boric acid electrolyte when rotated at 8.12 r.p.s.

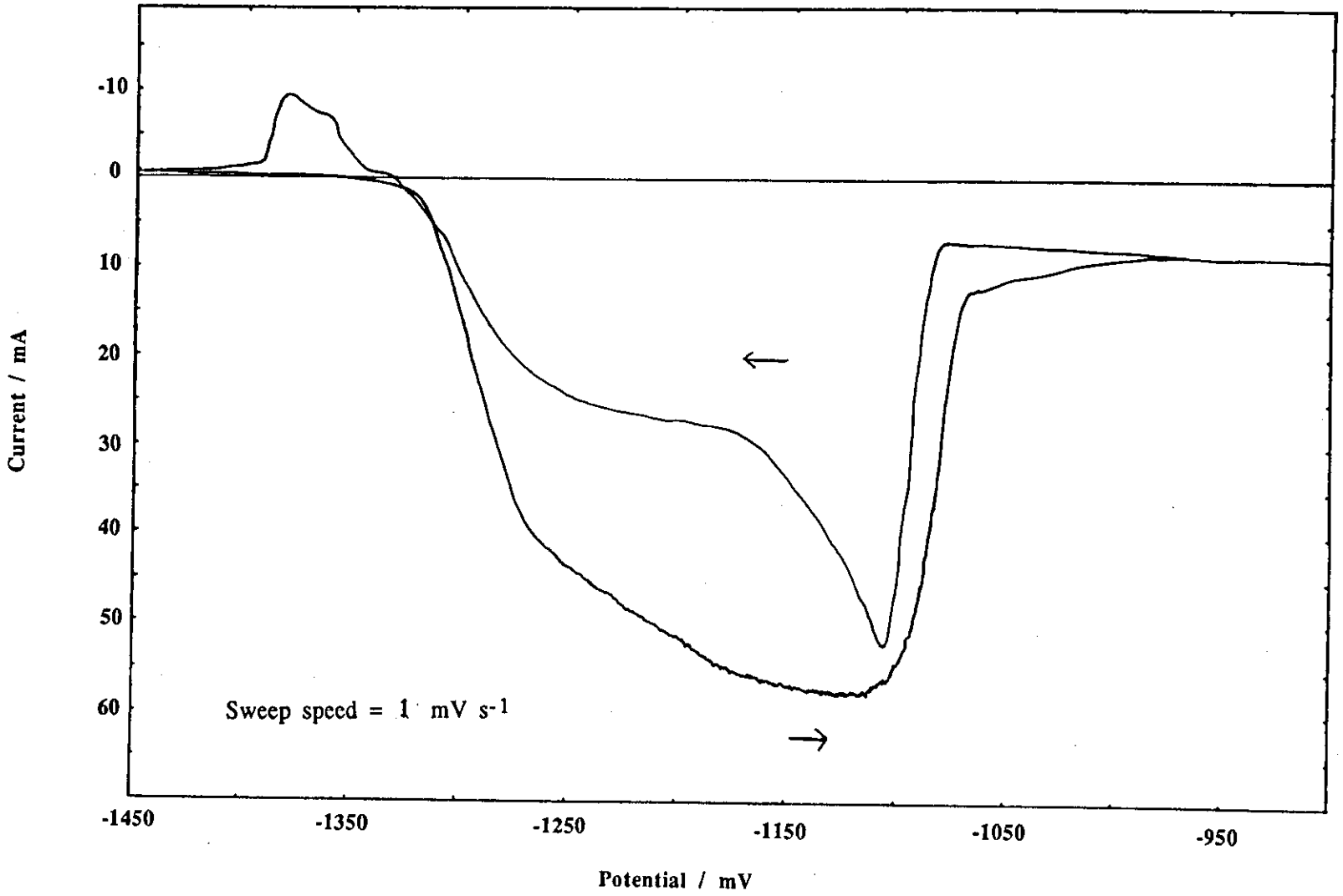

Figure 6.3.7. Current-potential response for a zinc electrode in 2M KOH / 85 gl^{-1} boric acid electrolyte when rotated at 15.9 r.p.s.

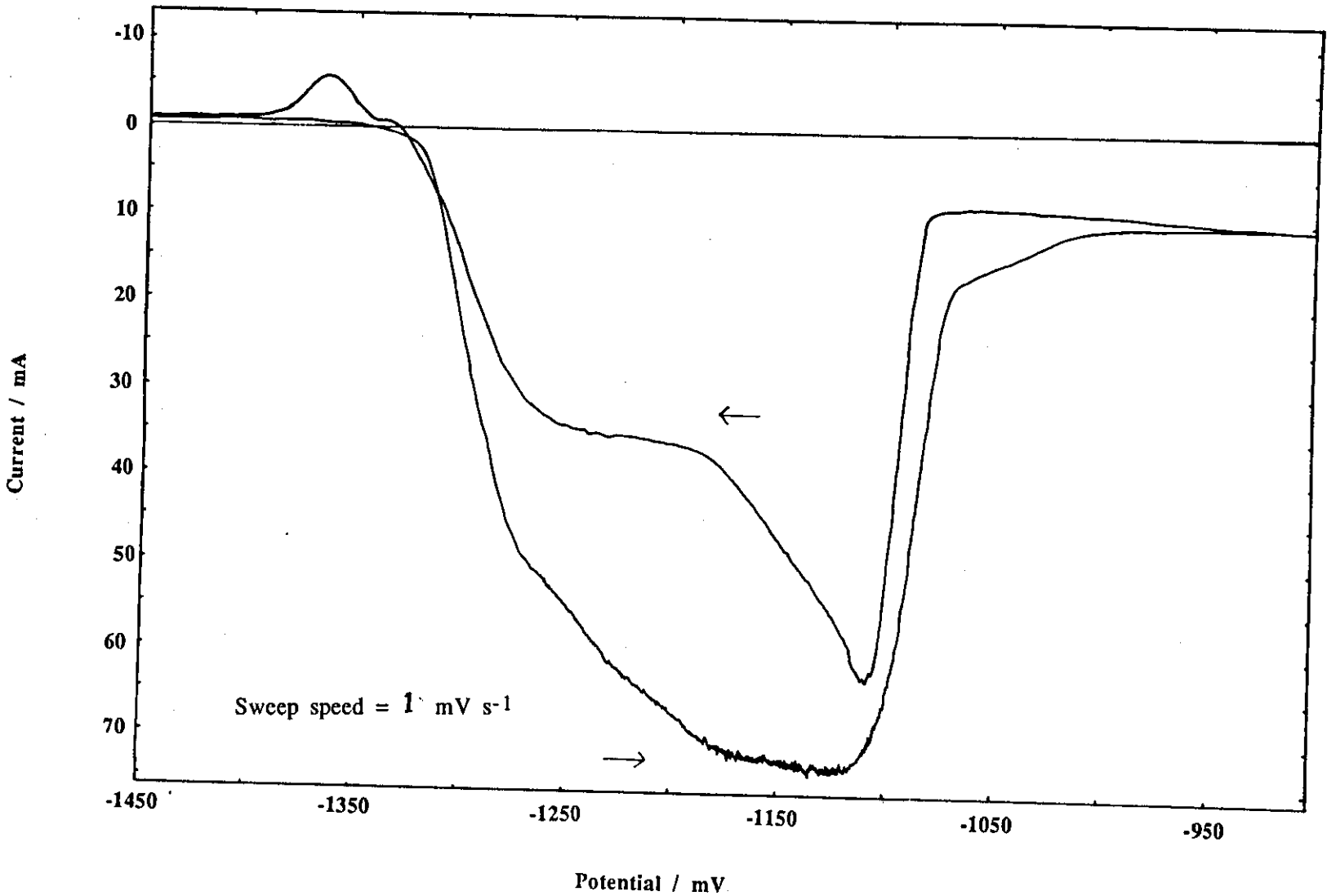

Figure 6.3.8. Current-potential response for a zinc electrode in 2M KOH / 85 gl^{-1} boric acid electrolyte when rotated at 44.2 r.p.s.

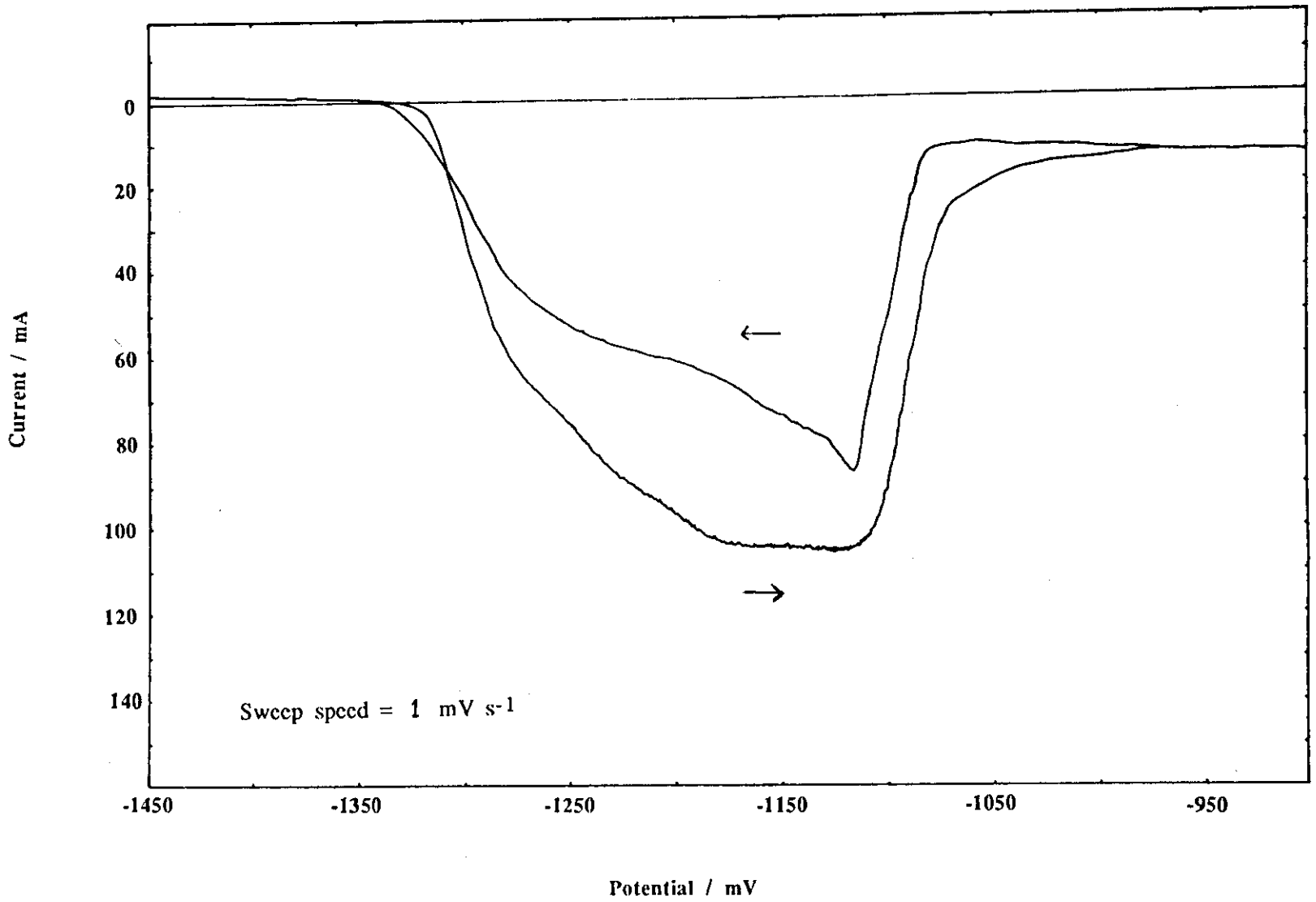

Figure 6.3.9. Current-potential response for a [illegible] zinc electrode in 2M KOH / 90 gl^{-1} boric acid electrolyte:
____ stationary electrode ---- rotation speed 15.9 r.p.s.

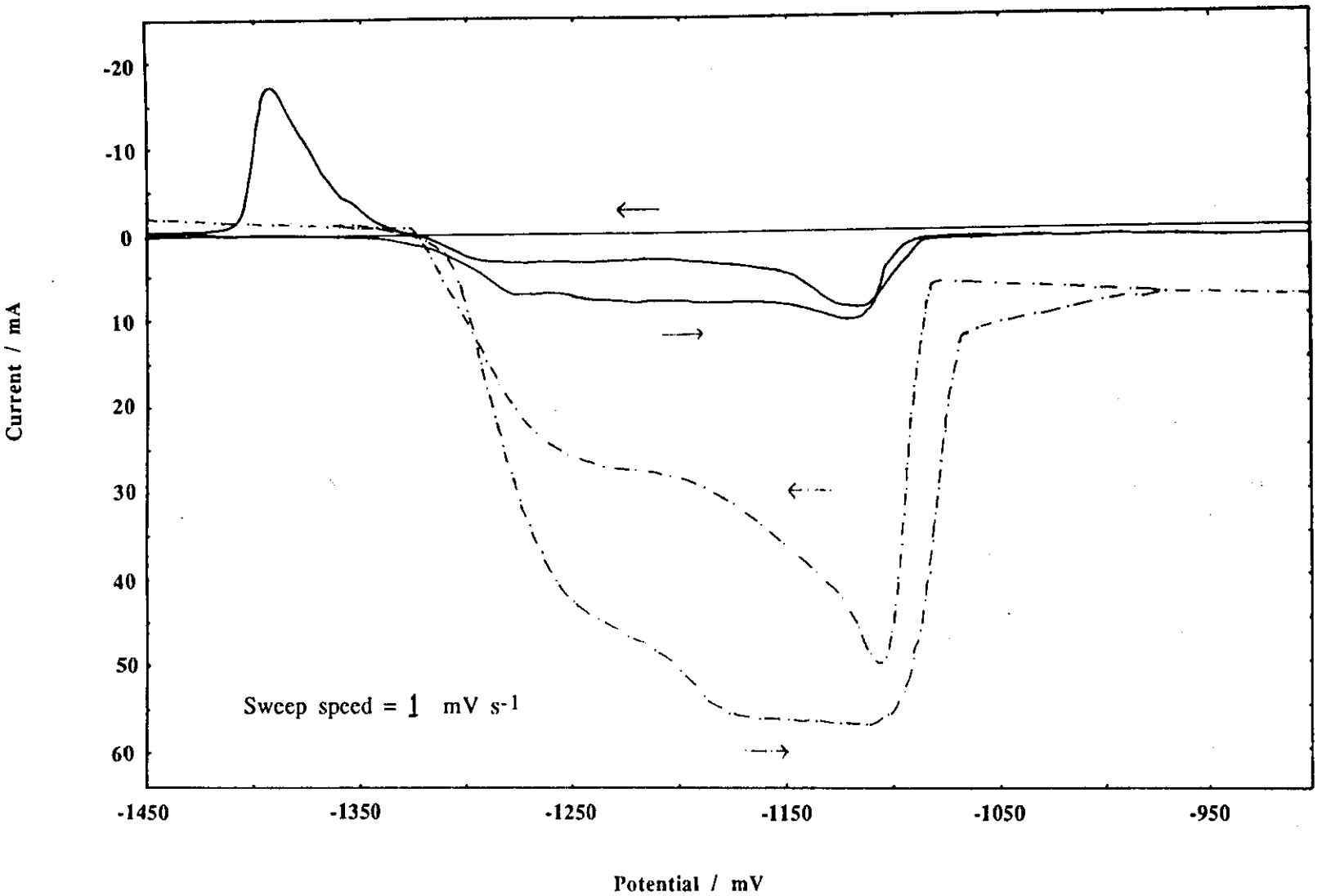

Figure 6.3.10. Current-potential response for a [illegible] zinc electrode in 2M KOH / 95 gl^{-1} boric acid electrolyte:

____ stationary electrode ---- rotation speed 15.9 r.p.s.

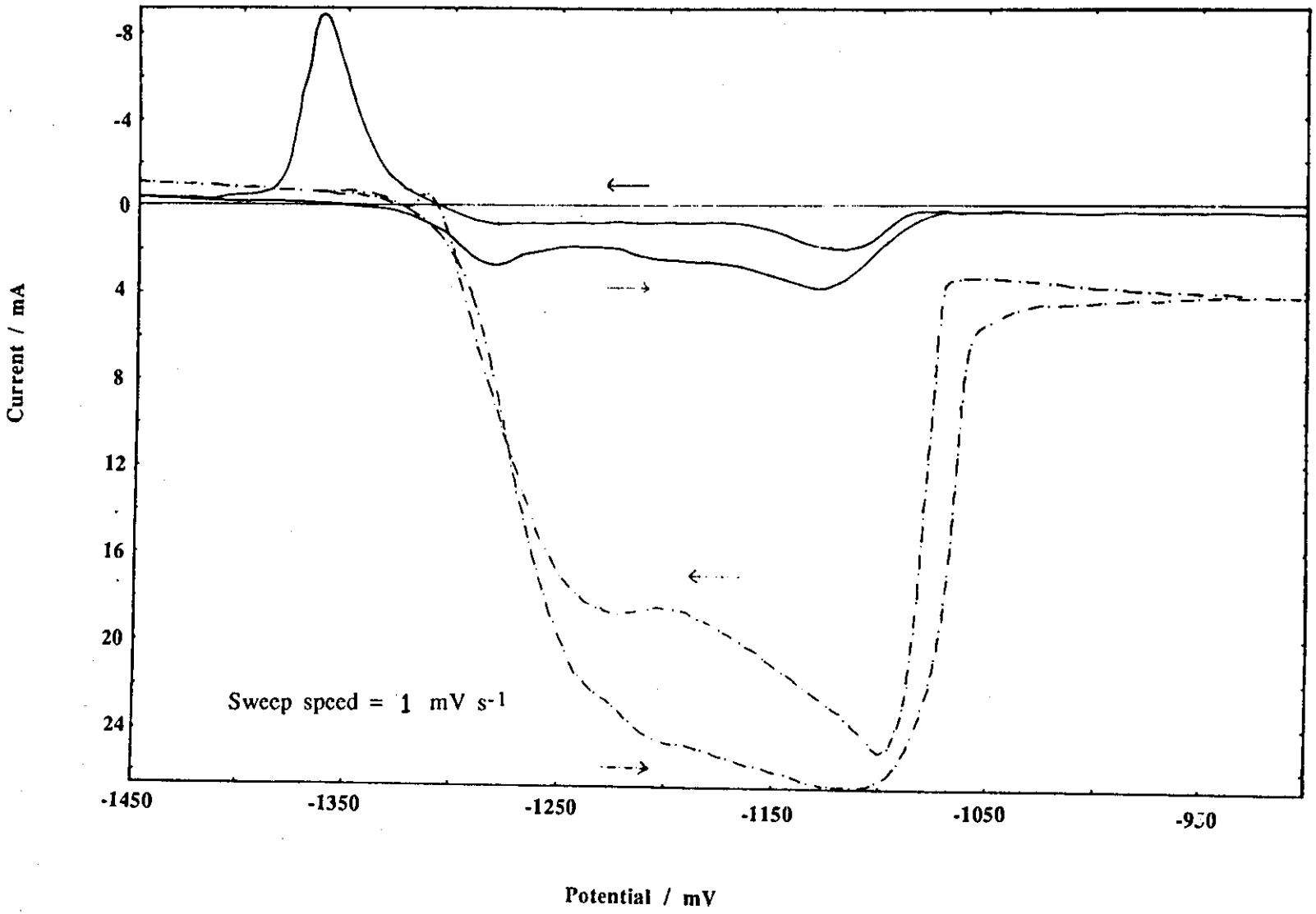

Figure 6.3.11. Current-potential response for a zinc electrode in 2M KOH / 100 gl^{-1} boric acid electrolyte:
____ stationary electrode ---- rotation speed 15.9 r.p.s.

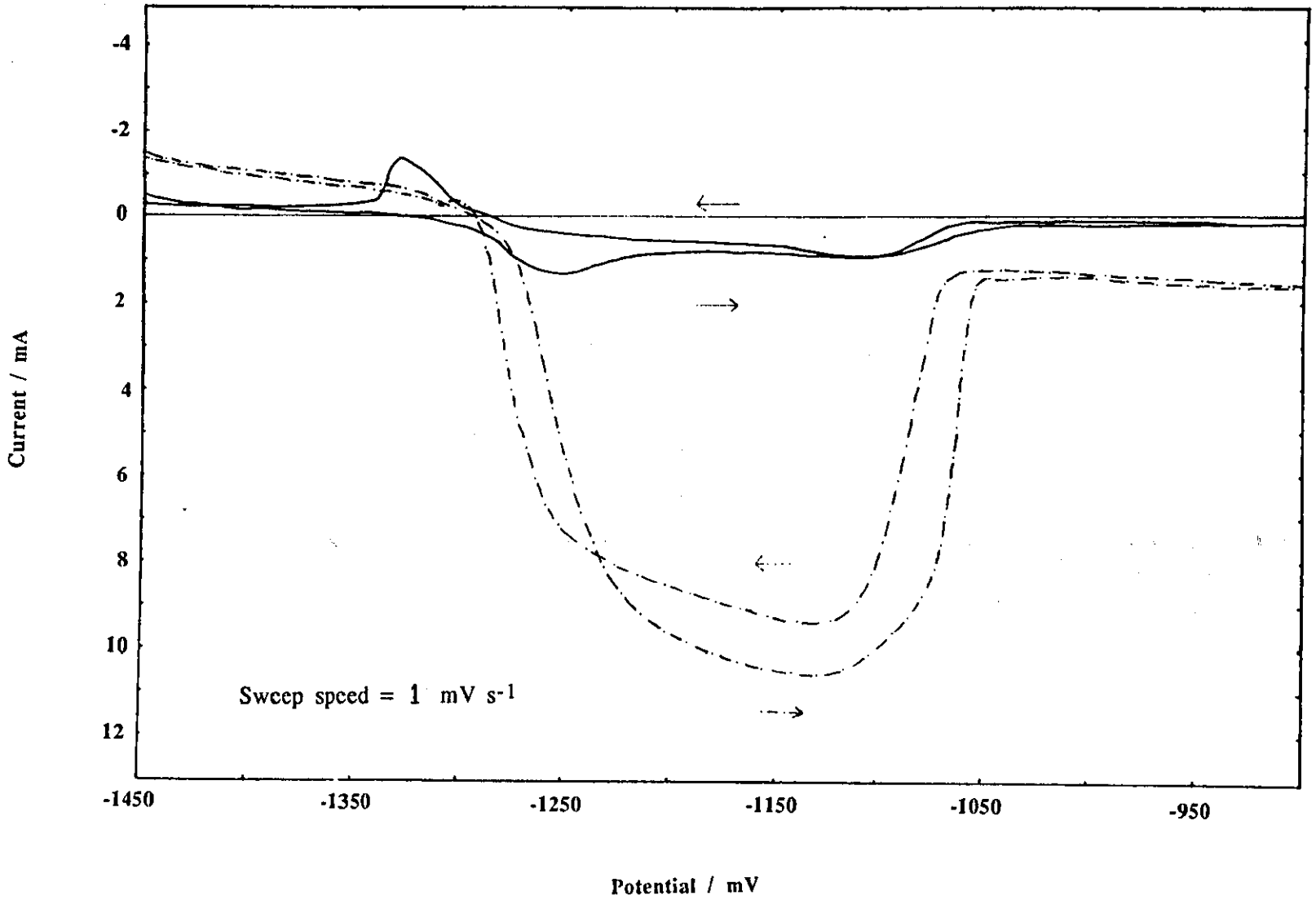

Figure 6.3.12. Current-potential response for a [illegible] zinc electrode in 2M KOH / 105 gl^{-1} boric acid electrolyte:

____ stationary electrode ---- rotation speed 15.9 r.p.s.

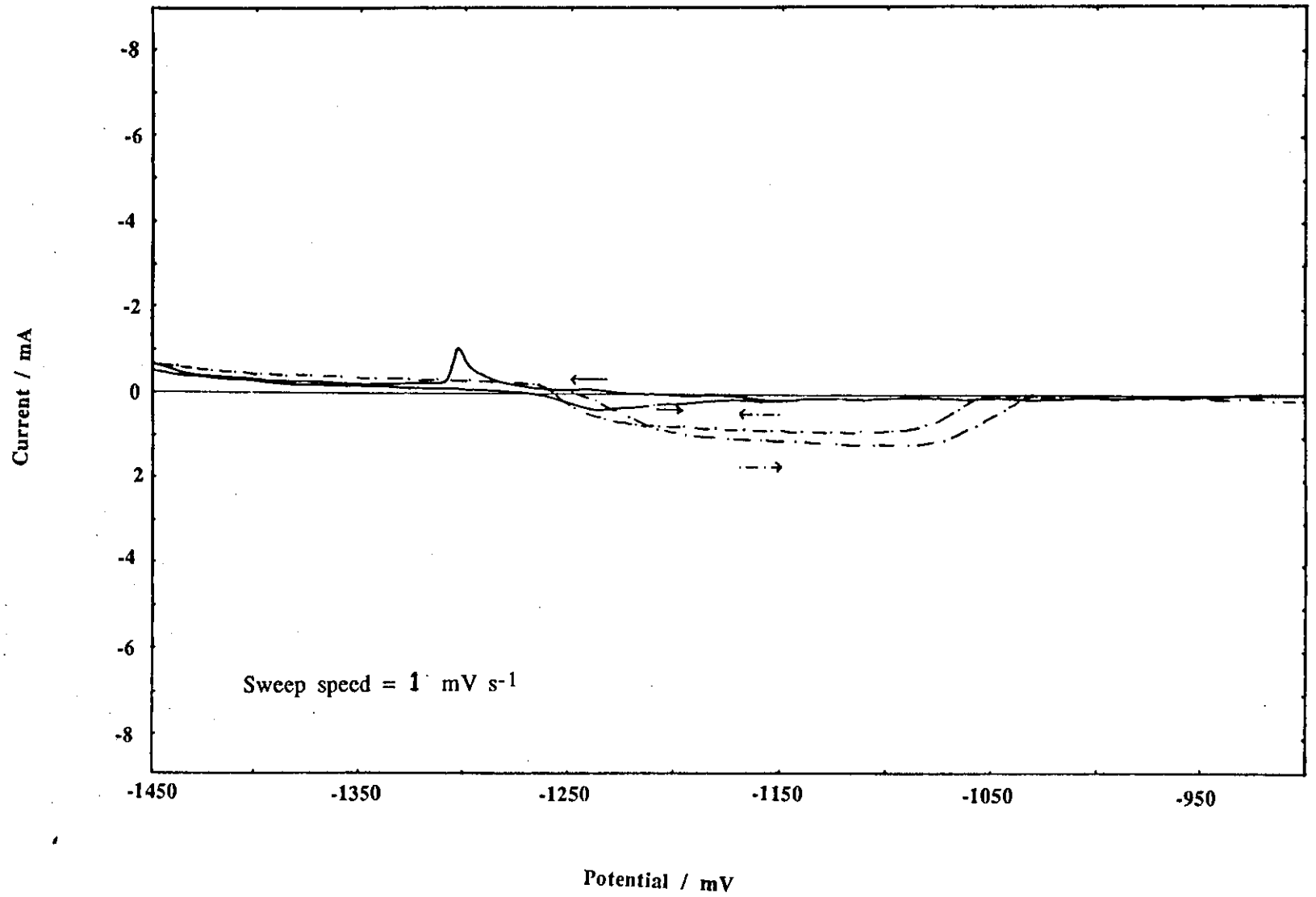

Multicycle sweep experiments were also performed in 2M / 95 gl^{-1} electrolyte, Figure 6.3.13. These showed an initial increase in current for both anodic and cathodic processes, due to the development of a porous structure. This process is analogous to a porous matrix which is undergoing a solid-state transition. After approximately 30 cycles a decrease in capacity was seen due to constriction of the front face of the electrode, restricting access of the electrolyte - this phenomenon is also observed in porous electrodes, as described by Harman and Mitchell (158).

A similar series of experiments were performed with electrolytes containing chromate additions. Figure 6.3.14. shows the results obtained for a solution containing 1 gl^{-1} chromate / 2M KOH in an unstirred solution. At this chromate concentration, it appears that the characteristic dissolution-passivation-reactivation processes typical of zinc are occurring. However the boundaries of each of these stages are ill-defined due to the oxidative and passivating properties of the chromate ion. as described previously. Also illustrated in this figure, is the effect of increasing the rotation speed of the electrode. It can be seen that when stationary the dissolution peak is smaller than the reactivation peak, whereas when the rotation speed is increased the situation is gradually reversed. This phenomenon is due to the film which is ultimately formed, being substantially more resilient, and resistant, to reactivation when the electrode is rotated. The higher the rotation speed, the more resilient the film.

On increasing the chromate concentration even further, the tendency to reactivate is minimal. In the anodic process the dissolution/passivation currents are very small due to the formation of the chromate film. A reduction peak is also observed at potentials more negative than the equilibrium potentials, Figure 6.3.15a. These features can also be attributed to the direct formation of zinc chromate at the electrode surface, as previously described. The nature of this film is likely to be

Figure 6.3.13. Multi-cycle results for a zinc electrode in 2M KOH / 95 gl^{-1} boric acid electrolyte.

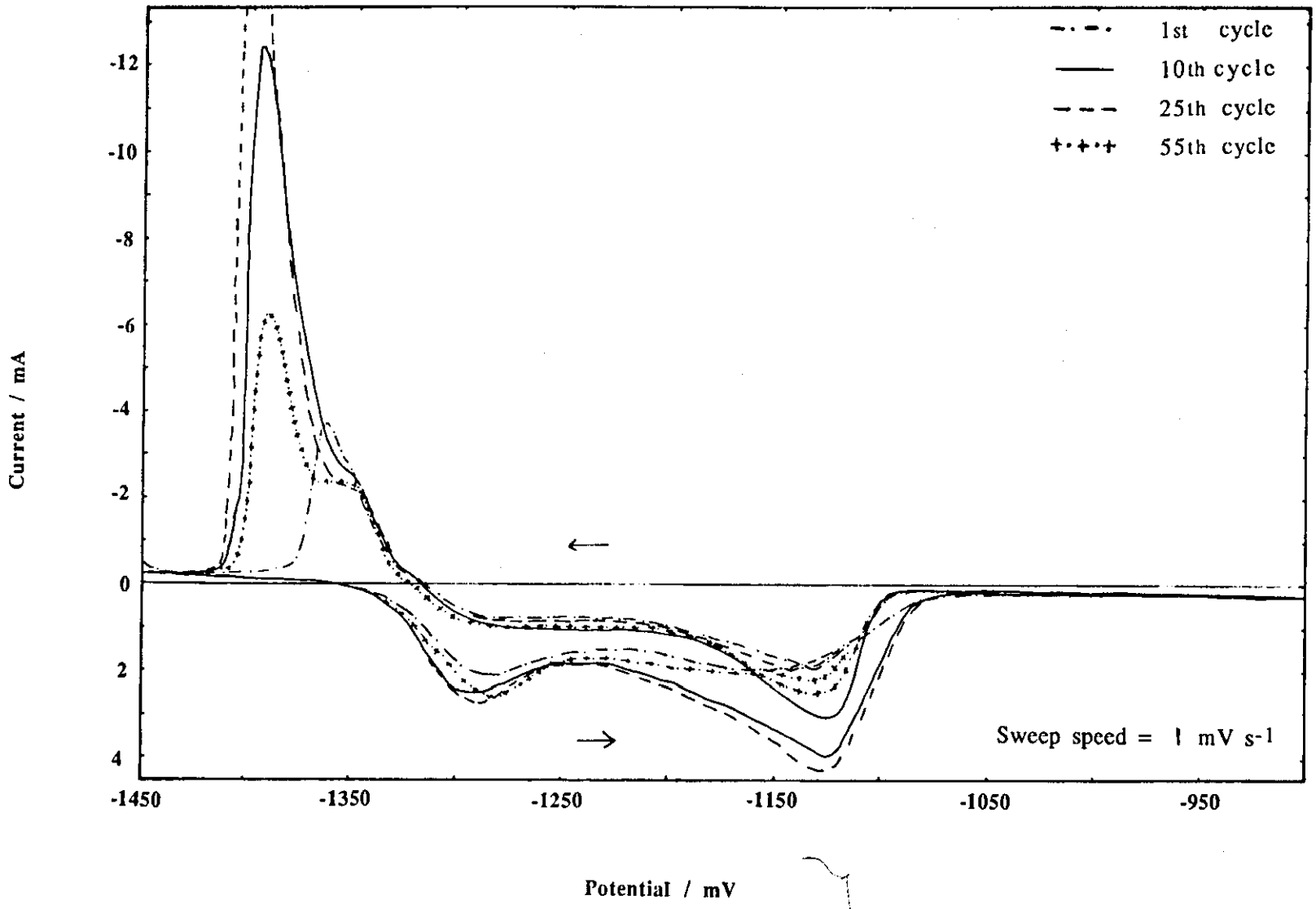

Figure 6.3.14. Current-potential response for a zinc electrode in 2M KOH / 1 gl^{-1} potassium chromate electrolyte:
—— stationary electrode ---- rotation speed 15.9 r.p.s.

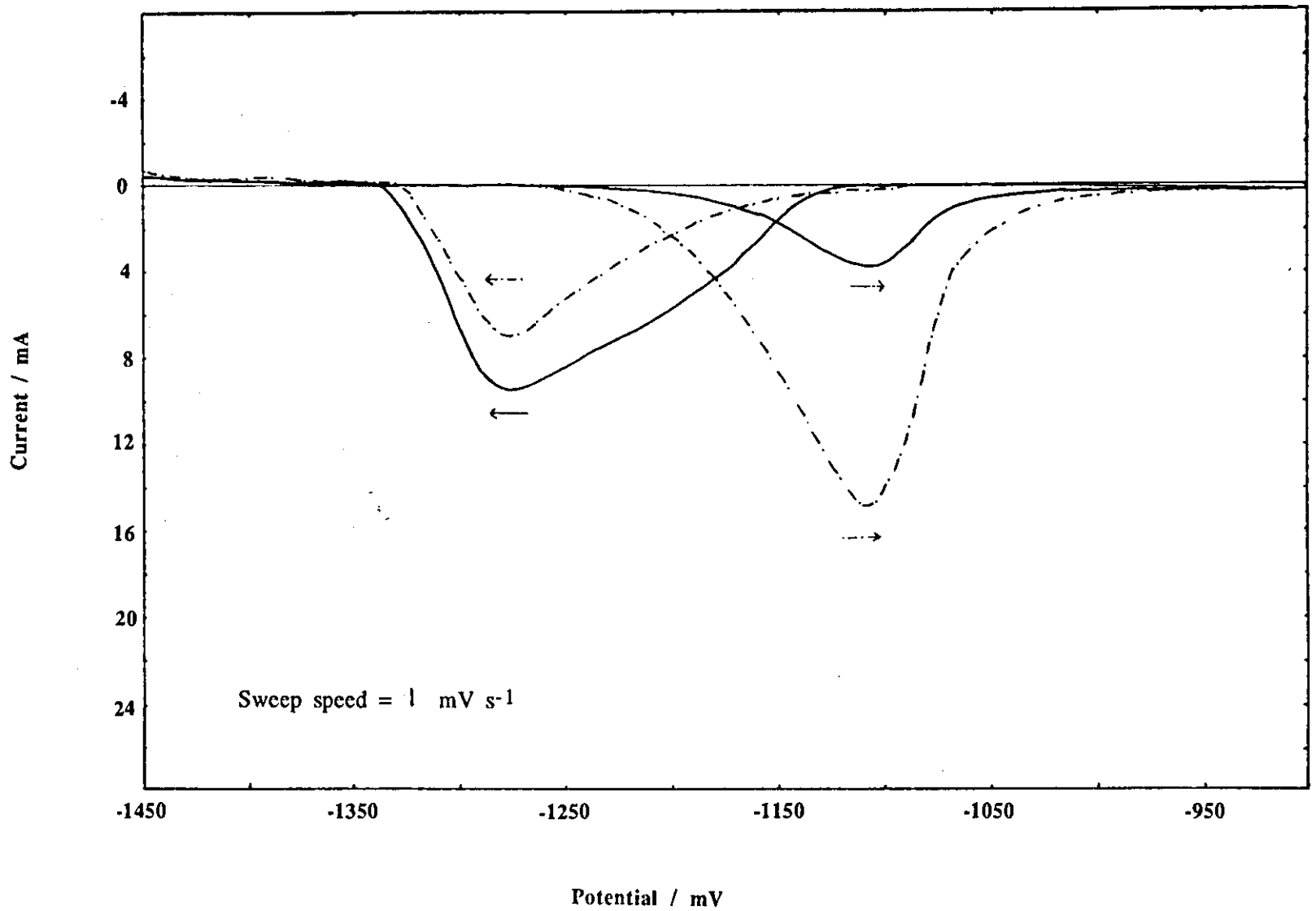

Figure 6.3.15a. Current-potential response for a stationary zinc electrode in 2M KOH / 2.5 gl^{-1} potassium chromate electrolyte.

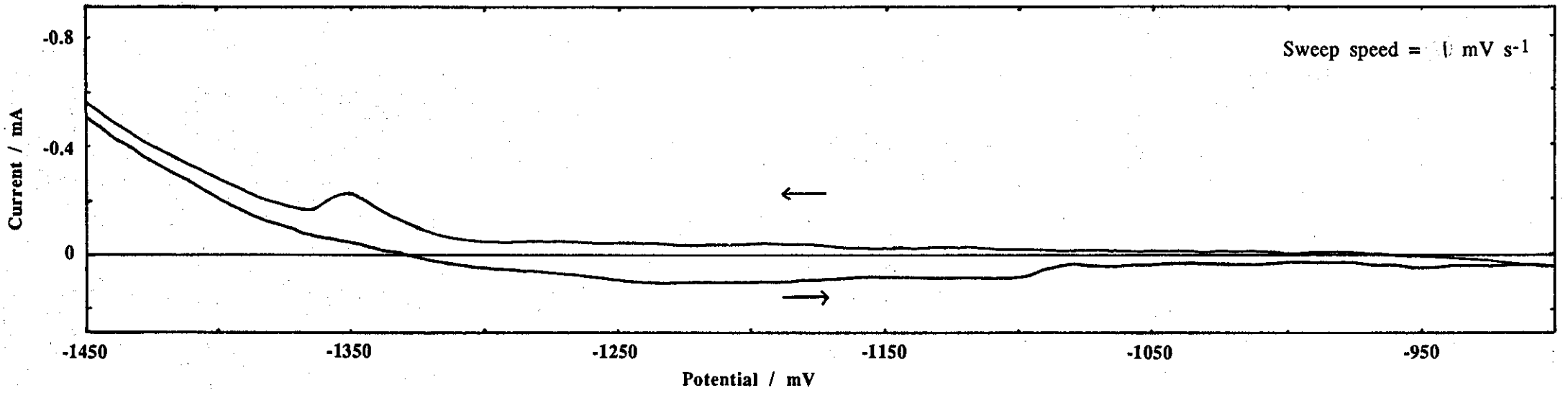

Figure 6.3.15b. Current-potential response for zinc electrode in 2M KOH / 2.5 gl^{-1} potassium chromate electrolyte when rotated at 15.9 r.p.s.

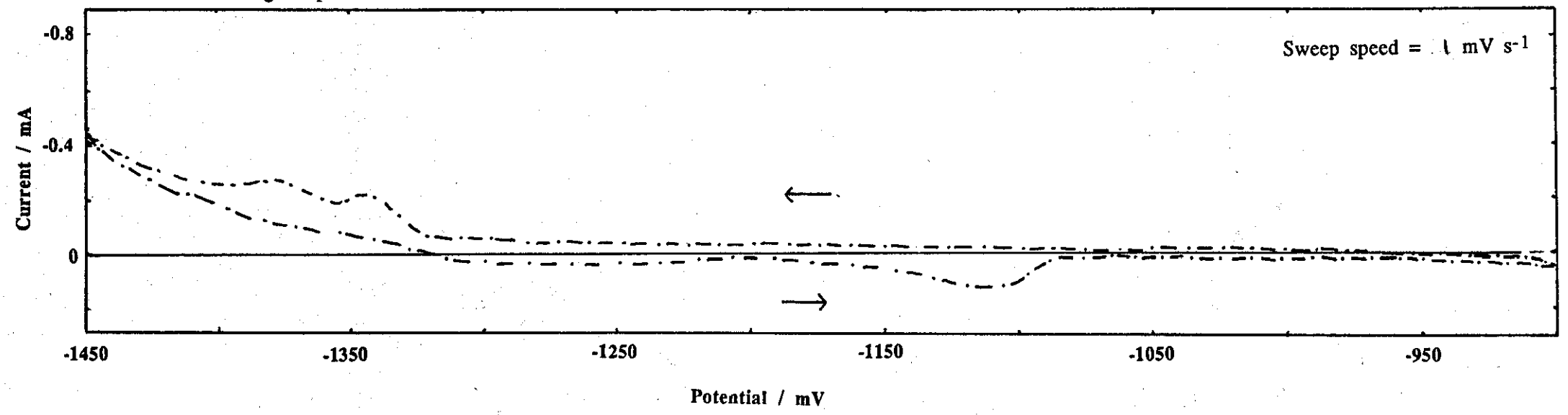

highly passivating and hence considerably minimises zinc dissolution.

Comparison with Figure 6.3.15b shows that the mechanism at these chromate concentrations (2.5 gl^{-1} and above) is virtually rotation speed independent. In addition the currents obtained are exceedingly small.

These results can be explained by the initial anodic plateau being due to the chemically formed film through which dissolution can occur at a constant rate, and is therefore potential independent. At a critical potential this film breaks down, suddenly releasing a large number of zinc ions into the solution, which ultimately get repassivated. This passive film is very resilient and, therefore, does not reactivate on the return sweep until it is reduced at potentials more negative than the equilibrium potential. The hydrogen evolution current on the reduced film is less than that of the original surface, as a result of the incomplete reduction of the zinc chromate layer.

These results indicate that both, chromate and borate could prove useful in practical rechargeable battery systems, since they can reduce the amount of zinc entering solution. However, in the chromate system continual passivation of the electrode occurred, even at open circuit. In actual systems this wold prove to be extremely detrimental. In addition to this drawback the currents obtained using chromate were extremely small, also the use of chromate is presently environmentally unacceptable. Consequently only borate containing electrolytes were further investigated.

CHAPTER 7

DISCHARGE AND CYCLING BEHAVIOUR OF PASTED ZINC ELECTRODES

7.1. Introduction

The principal objective of this research was to produce a rechargeable zinc battery system which would give satisfactory cycle-life performance, but without the need for expensive separators. The techniques described in the preceding chapters, can give a good indication of which additives could prove to be useful in practical battery systems.

Such fundamental investigations are important, since not only do they help explain some of the underlying electrochemistry of the system, but they can also reduce the number of time-consuming, and costly, cycling tests required. However, the ultimate test of an additive is how it effects the cell's performance during actual cycling. It was, therefore, necessary to perform cycle-life tests on small scale cells, to confirm if the results obtained in the previous chapters are in good correlation with the actual cell performance obtained.

Comparison of the cycle-life results obtained by other workers can be both difficult and confusing, due to the vast range of experimental variables concerned. For that reason it is better to consider the general trends that each individual experiment reveals, rather than compare all results with each other.

The system employed in these experiments was similar to that of Duffield et al [72-74], i.e. zinc/p.t.f.e. pasted sheets, pressed onto a copper current collector. However, even using the same paste formulation did not allow direct comparison of Duffield's results with those in the present investigation. Differences arose because

the former investigator tried to obtain high zinc performance and utilisation by using highly alkaline electrolytes, whilst controlling shape change and dendritic growth with three layers of microporous separator (Celgard). The elimination of this expensive separator was a prime aim in this work, and was combatted by solubility considerations. As a consequence, this called for the use of a different cycling regime. This will be described in the following sections.

7.2 Experimental

Fabrication of porous zinc electrodes was made by mixing the following constituents in the method detailed in section 4.3:

Zinc Oxide (F.S.A. 99.999%)
5% PTFE (ICI 'Fluon' 60% w/w suspension)

plus additives of one of the following, at the indicated amount:

10% Carboxyl Methyl Cellulose (C.M.C.), or
10% Poly Vinyl Alcohol (P.V.A.), or
32% Graphite (Lonza K.S. 2.5)

The resultant mixture was treated in a similar manner to the electrodes used by Duffield.

Capacities of the electrodes were calculated from the formula:

$$\text{Capacity, C/Ahr} = 0.66 \text{ Ahr g}^{-1} \times \text{mass paste} \times \text{fraction of ZnO in the paste}$$

Sheets of the paste were rolled to the required thickness and then cuts into rectangular pieces (3 x 2.5 cm). One piece was placed either side of a copper foil current collector wrapped in a layer of non-woven polypropylene absorber material and heat sealed at the edges. The tab section of the current collector had previously

been nickel plated to prevent corrosion at the air/electrolyte interface. Each electrode was fabricated to have a capacity of 1Ahr.

The whole electrode was then pressed at 2 tonnes $inch^{-2}$ (5 tonnes $inch^{-2}$ for the graphite electrodes).

Rigid porous polypropylene spacers were inserted between the zinc electrode and nickel gauze counter electrodes, placed either side. The whole assembly being clamped between two perspex plates (finger tight) before immersion in 1M KOH electrolyte. Formation of the zinc electrodes was then performed at C/10 (100 mA) for 15 hours i.e. 50% overcharge. The electrode was taken in this fully charged state, and soaked for 2 hrs in any different electrolyte prior to experimentation.

For discharge experiments the formed electrodes were freely suspended in a beaker with a nickel gauze counter electrode encircling the inner wall of the beaker.

For cycling experiments the zinc electrode was again freely suspended, but the counter electrode was changed to two nickel oxyhydroxide electrodes placed equal distance either side of the zinc. The combined capacity of the counter electrodes was ~ 10 Ahr, so that any failure of electrodes seen was due to the zinc.

The electrodes were subjected to a cycling regime of 60 mA (C/5, rate from discharge experiments) charge for 6 hrs; 60 mA discharge for 5 hrs (or until a cut-off voltage of -800 mV vs Hg/HgO was reached). Each cell was individually monitored, i.e. all cells were independent of each other.
Cycling experiments were monitored in a similar manner to that outlined by Hampson and McNeil [70], except that a cut-off unit was also utilised.

7.3. Results

The discharge profiles for a pasted zinc electrode in pure potassium hydroxide solution, both 7M and 2M, when discharged at 200 mA (theoretical C/5), are shown in Fig. 7.3.1. The profiles show that approximately 100% utilisation is obtained from these electrodes which compares with only ~20% for an identical electrode when discharged at the same current density, but in 2M KOH / 95 gl^{-1} boric acid electrolyte. Fig. 7.3.1. also shows the discharge profile for this solution. The reduction in utilisation in borate electrolyte is due to the free-hydroxyl concentration being decreased, and hence lowering of zinc species solubility.

In order to obtain meaningful results a re-rating of the electrode in borate electrolytes was therefore necessary. Fig. 7.3.2. illustrates the profiles obtained at 200mA discharge rates for electrolytes containing borate, at three different concentrations. The results reveal that increasing the borate ion concentration decreases the discharge capacity of the electrode. Once again this can be attributed to the reduction in the free hydroxyl ion concentration and hence zinc species solubility - this result is in complete agreement with those of preceding chapters.

The electrolyte composition which was selected for subsequent investigations was 2M / 95 gl^{-1} boric acid, as this gave reasonable utilisation and discharge performance. From Fig. 7.3.3. it can be concluded that when the electrode was discharged at 60 mA the life-time was approximately 5 hrs, giving a nominal capacity of 300 mA hr . This represents a total zinc utilisation of 30%. When compared to other anode systems such as cadmium (~80%) and lead (~40%), this figure does seem to be rather low. However, the cost and weight of zinc are important, and favourable, considerations which must be taken into account when assessing the viability of a battery system. Also the gravimetic capacity

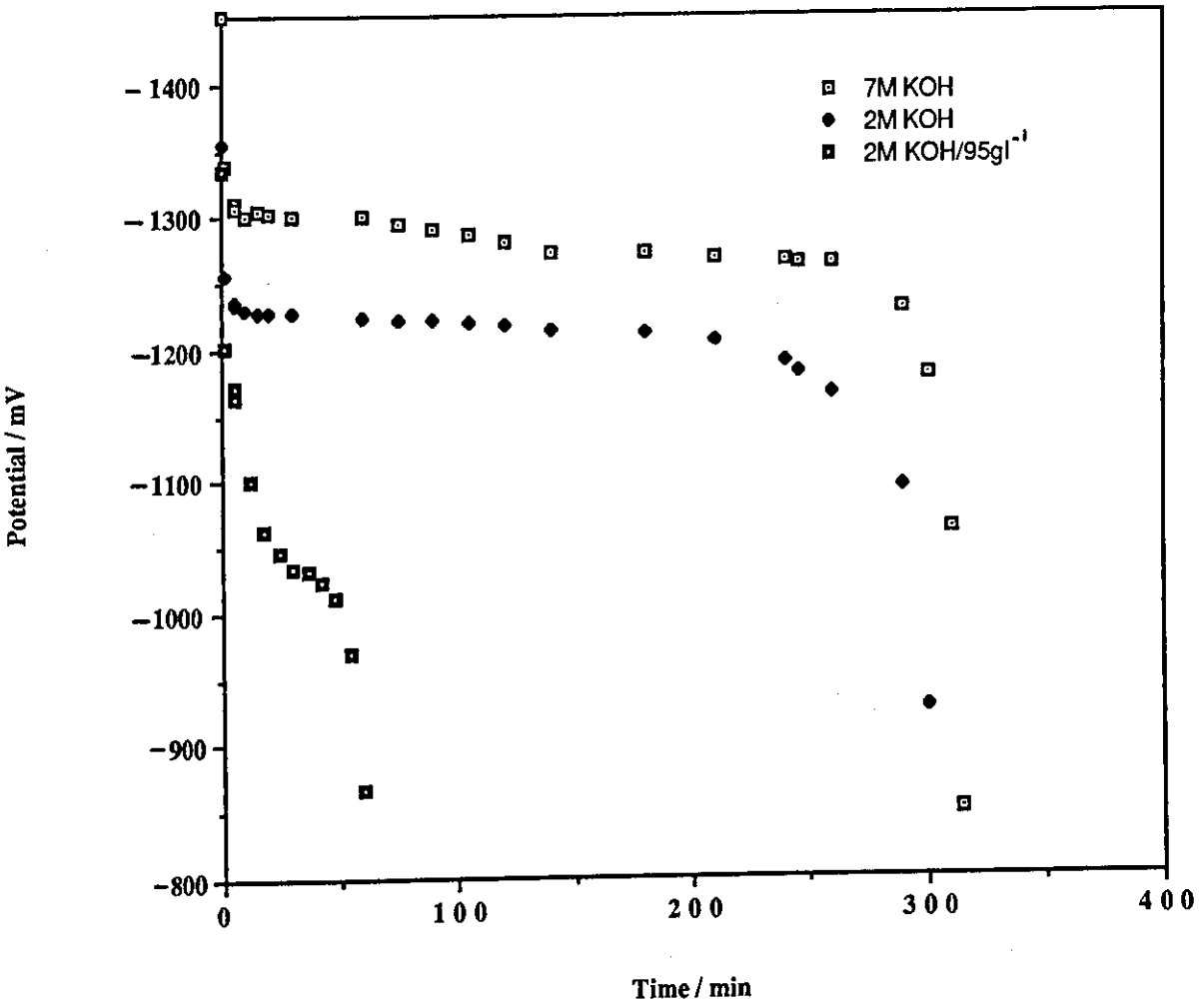

Figure 7.3.1. Discharge profiles for zinc electrode in 7M, 2M and 2M / 95 gl^{-1} electrolytes, discharged at 200 mA . .

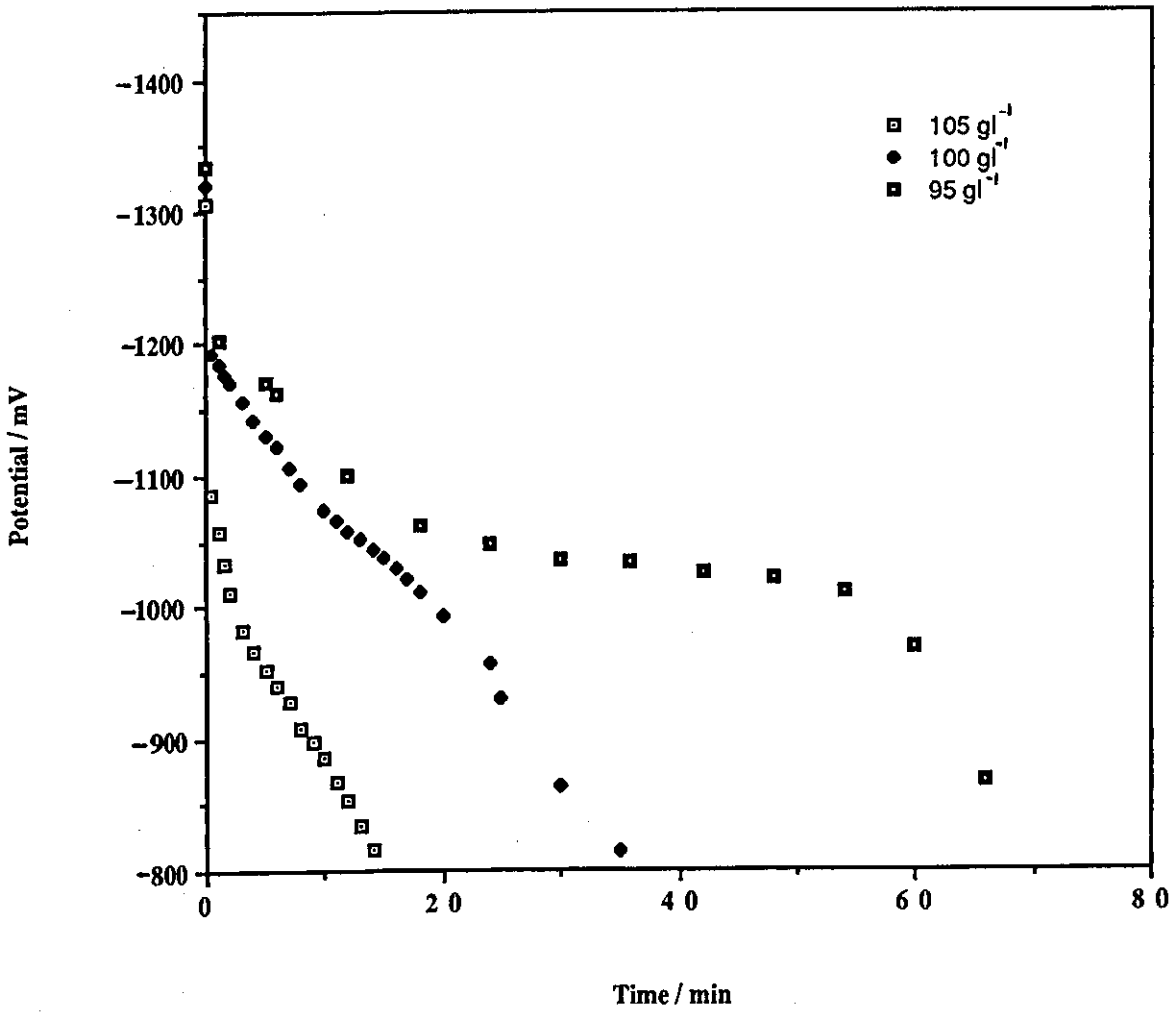

Figure 7.3.2. Discharge profiles for zinc electrode in 2M / borate electrolyte at various concentratons, at 200 mA .

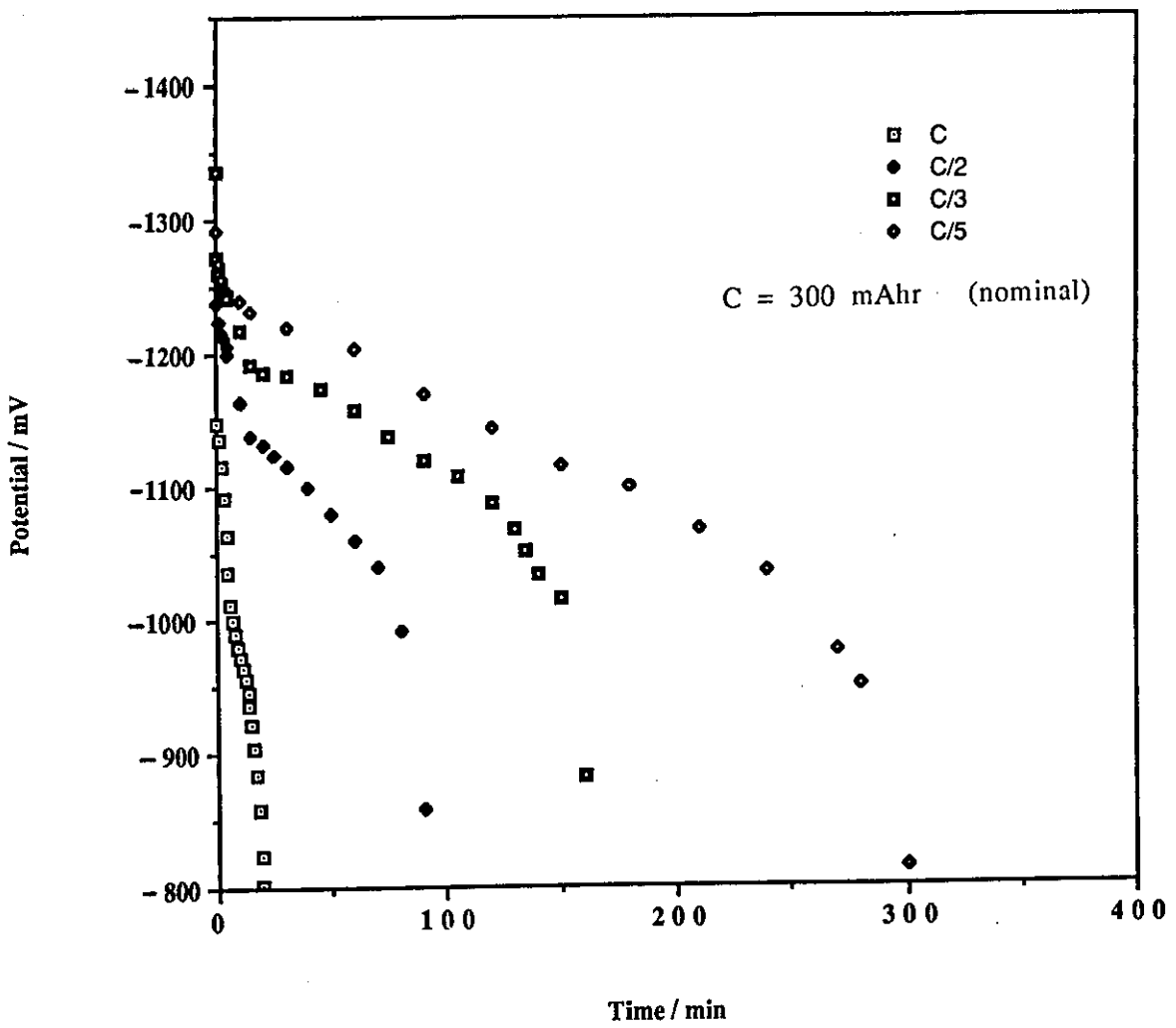

Figure 7.3.3. Discharge profiles for zinc electrode in 2M KOH / 95 gl^{-1} electrolyte at various discharge rates.

density is close to that of cadmium (240 mA hr g^{-1}) even at 30% zinc utilisation. Also zinc has higher operating voltages.

The cycle-life behaviour of a zinc electrode in 2M / 95 gl^{-1} boric acid solution is shown in Fig. 7.3.4. An important feature to note is that the capacity of the electrode remains above the 800 mV cut-off level for the first 20 cycles. Thus the electrodes were slightly under-rated from the discharge profiles.

After these initial cycles, the capacity is seen to gradually decline with each cycle, until after 50 cycles it has decreased to 25% of its initial rated value. This reduction is due to the pores within the electrode becoming blocked by zinc oxide, which was precipitated at these sites on previous discharges and not re-reduced. Although the capacity had dropped it was noted that there were no dendrites penetrating the polyamide separator (shown in Fig. 7.3.5.). This is in complete contrast to an electrode cycled at an identical rate (60 mA . ·), but in 2M KOH alone (Fig. 7.3.6.), where after only two cycles there is a profusion of dendrites covering the electrode surface and protruding through the separator. It was noted that the potential in 2M KOH electrolyte was much higher than in 2M / 95 gl^{-1} boric acid solution, thus indicating the need of a trade off in operating potential and cycle-life performance for this zinc electrode system.

Duffield [72-74] reported that the addition of graphite, of the correct particle size, could greatly improve the cycle-life performance of his electrodes. He postulated that the effect of graphite was to provide a bulky, open, porous conductive matrix within the electrode, which retained any oxidised zinc species within the vicinity of the electrode during discharge. On subsequent recharge, the reduction of any zinc oxide is more easily facilitated by its close proximity of the conductive graphite.

In an attempt to improve the performance of the electrodes in the present investigation a similar addition of graphite was tested.

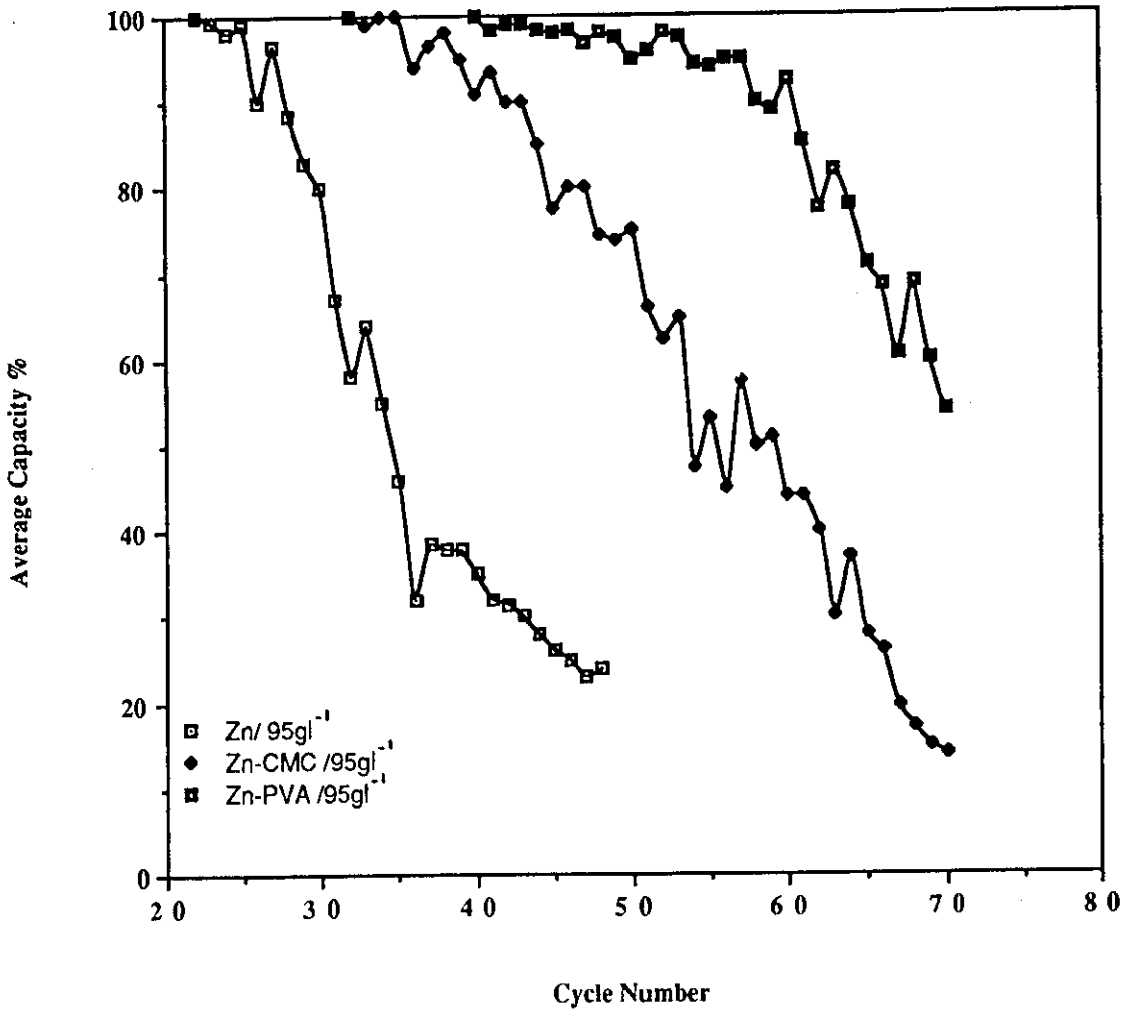

Figure 7.3.4. Cycle-life behaviour for zinc electrode, zinc/C.M.C electrode, and zinc/P.V.A electrode in 2M KOH / 95 gl^{-1} boric acid electrolyte.

Figure 7.3.5. Photograph of zinc electrode after cycling in 2M KOH / 95 gl^{-1} boric acid electrolyte for 50 cycles.

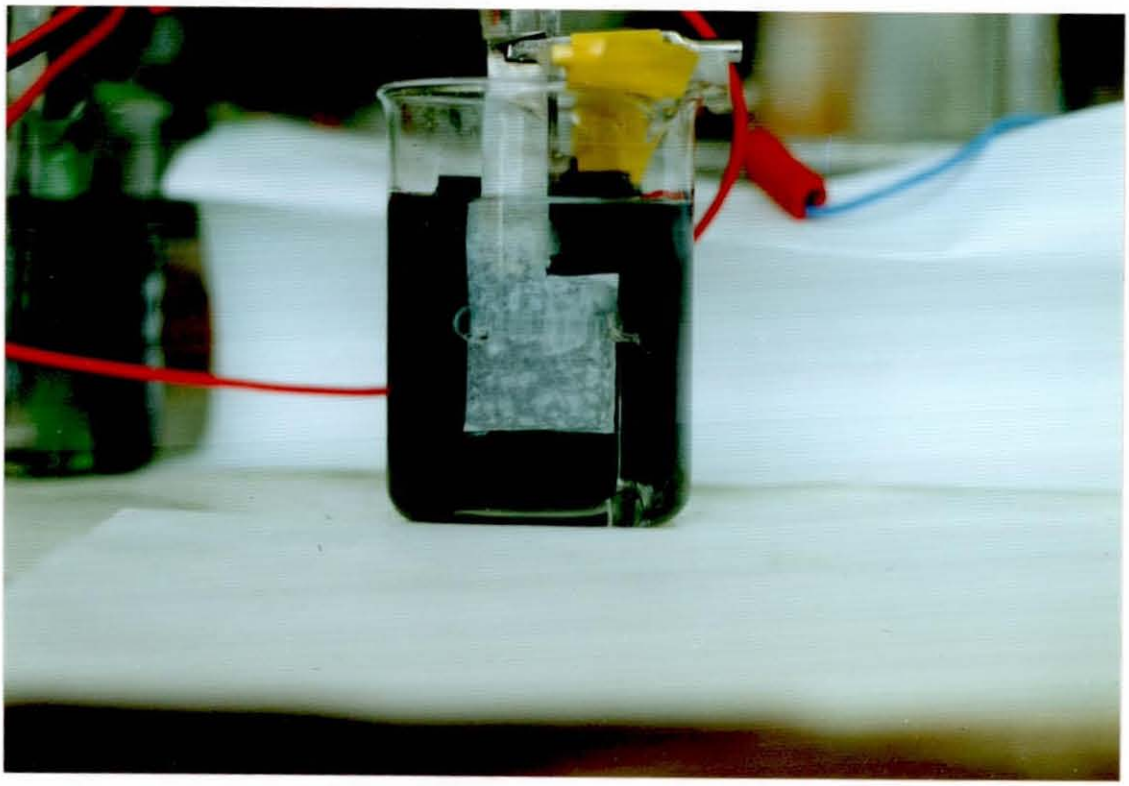

a. Face view. Magnification x 0.70

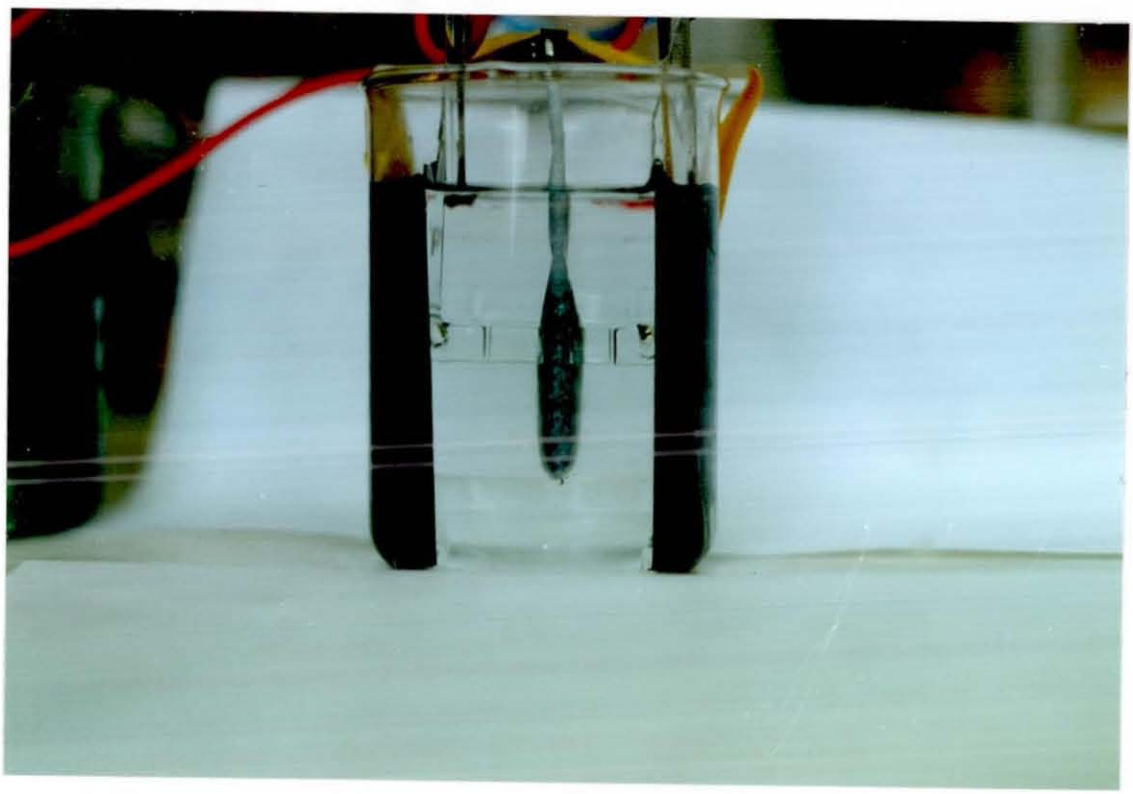

b. Edge view. Magnification x 0.80

Figure 7.3.6. Photograph of zinc electrode after cycling in 2M KOH for 2 cycles.

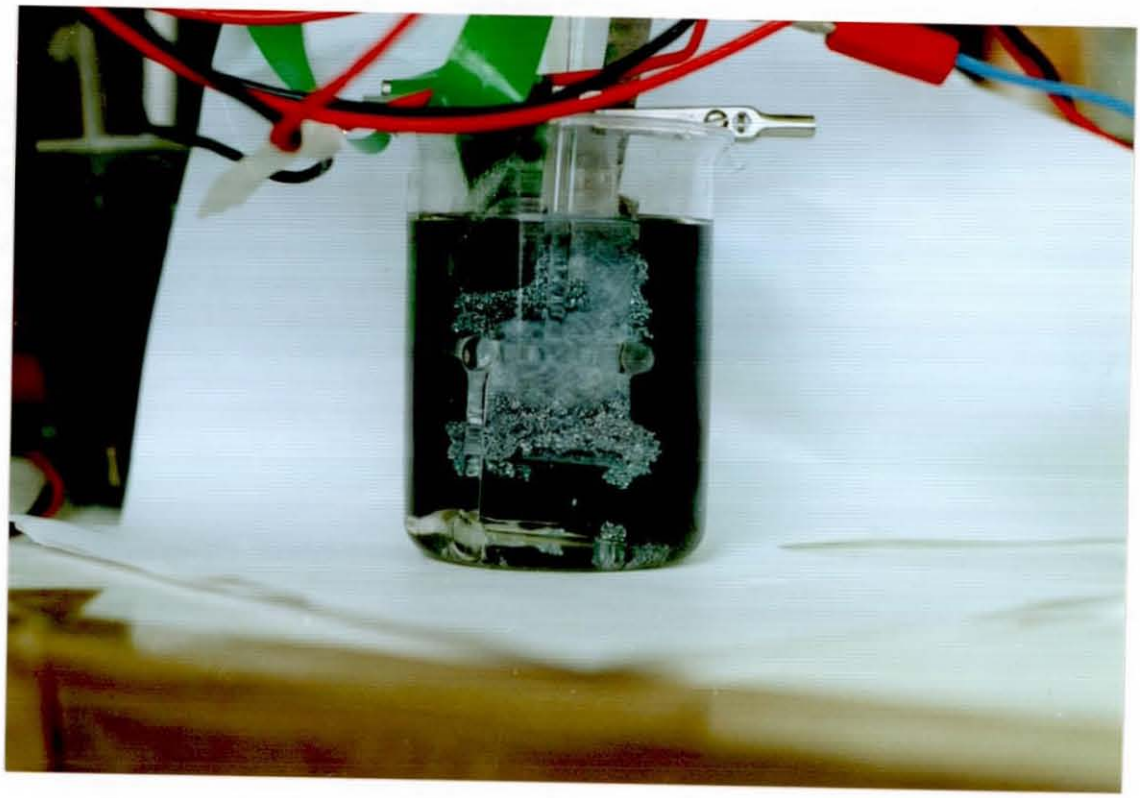

a. Face view. Magnification x 0.77

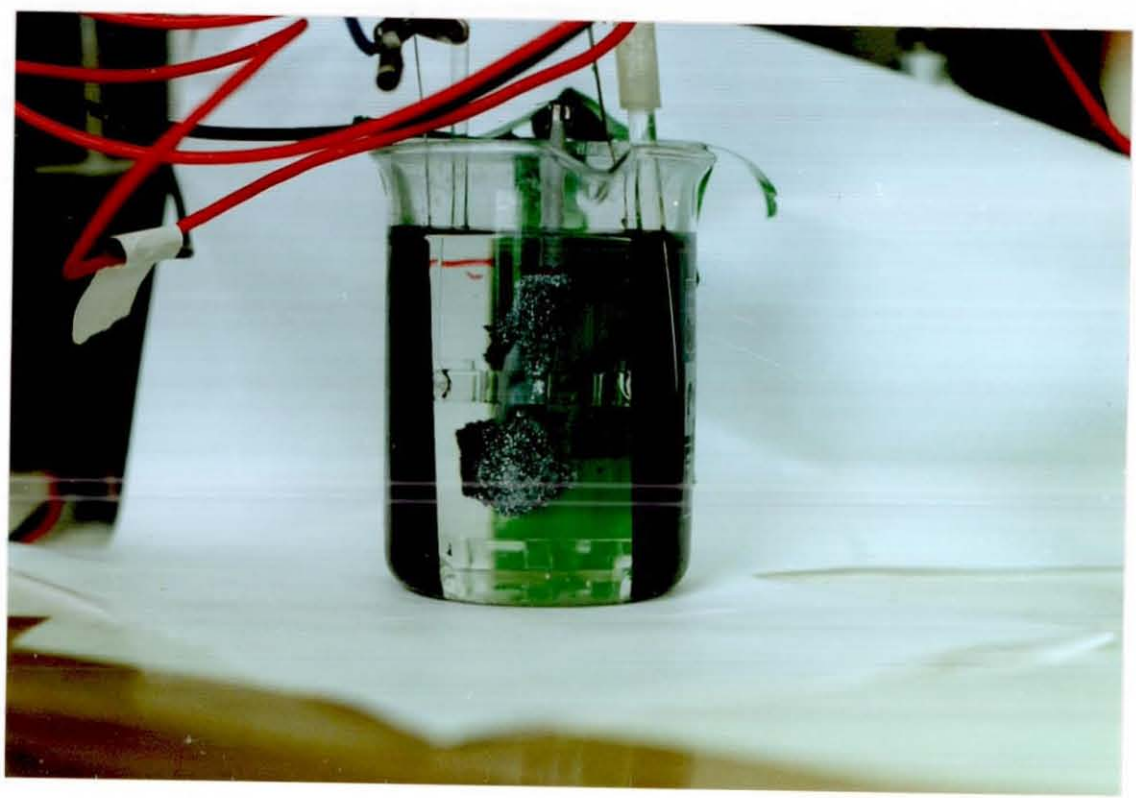

b. Edge view. Magnification x 0.83

However, comparison of the discharge profiles of a 32% graphite electrode with a plain zinc electrode, at identical discharge rates, showed that the graphite addition caused a reduction of the useful capacity of the electrode, Fig. 7.3.7. Therefore it must be concluded that graphite is not a porosity enhancer, it merely improves the conductivity. In fact in these experiments it acts more as a diluent, since the addition of 32% graphite caused a reduction in the discharge capability of a similar magnitude. A large expansion of the electrode was also observed during the cycling experiments performed on the electrode. This may in part be attributable to excess hydrogen evolution given off the graphite during recharge, consequently reducing efficiency, and hence cyclable capacity - shown in Fig. 7.3.8. This gassing problem was investigated further and will be discussed in the following chapter.

The search for other electrode additives which could be used to increase the active surface area, led to two which have previously found use in other alkaline battery systems.

Carboxymethyl cellulose (C.M.C.) is used extensively in primary zinc-manganese dioxide batteries as a gelling agent [99], which immobilises the electrolyte. Polyvinyl alcohol (P.V.A.) is used in a large number of cadmium systems as a binding agent in the electrode, replacing p.t.f.e. [67]. It is known to exhibit swelling properties in caustic solutions. Paste mixtures containing a 10% wt/wt addition of one, or other, of the additives were fabricated into electrodes and assessed.

Figures 7.3.9 and 7.3.10. show the resultant discharge profiles for electrodes, at various discharge rates. It can be seen that the P.V.A. electrode gives a slightly better performance than the C.M.C. electrode. Both are better than an unmodified zinc electrode. However, the high rate discharges are still not as good as would be hoped, and unless this situation can be further improved the system may be limited to low and medium rate applications

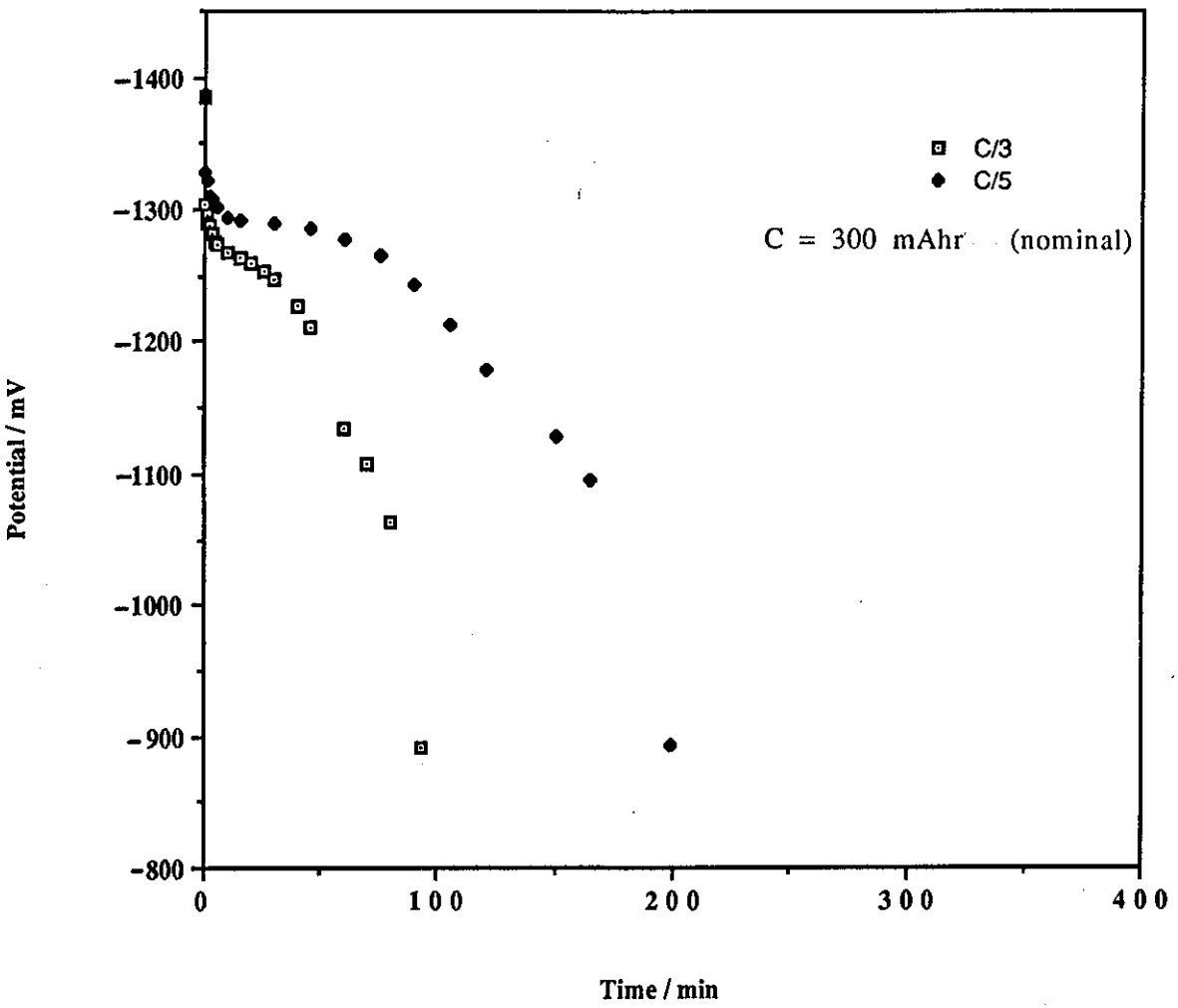

Figure 7.3.7. Discharge profiles of zinc/graphite electrode in 2M KOH / 95 gl^{-1} boric acid electrolyte.

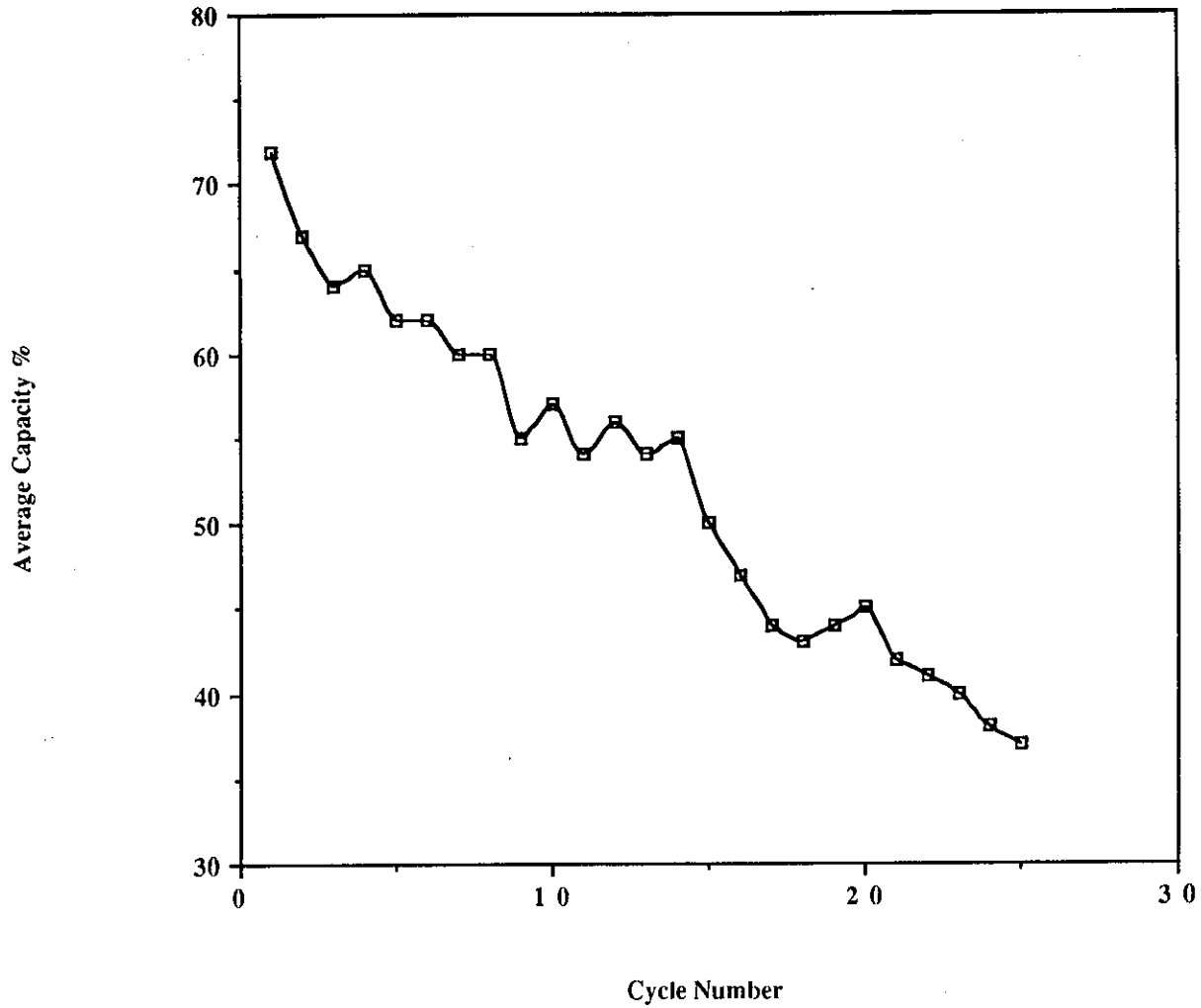

Figure 7.3.8. Cycle-life behaviour for zinc/graphite electrode in 2M KOH / 95 gl^{-1} boric acid electrolyte.

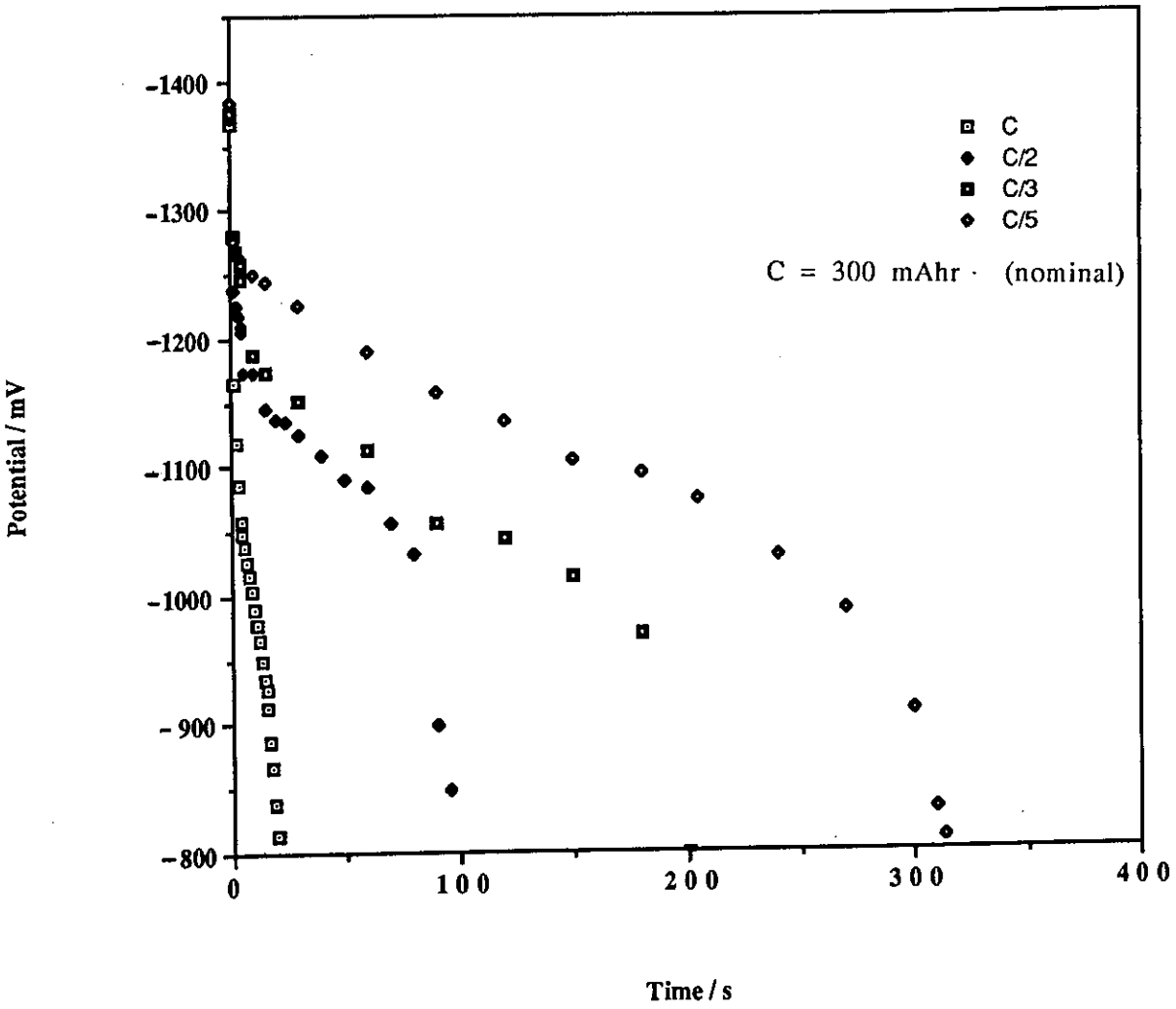

Figure 7.3.9. Discharge profiles of zinc/C.M.C. electrode in 2M KOH / 95 gl^{-1} boric acid electrolyte.

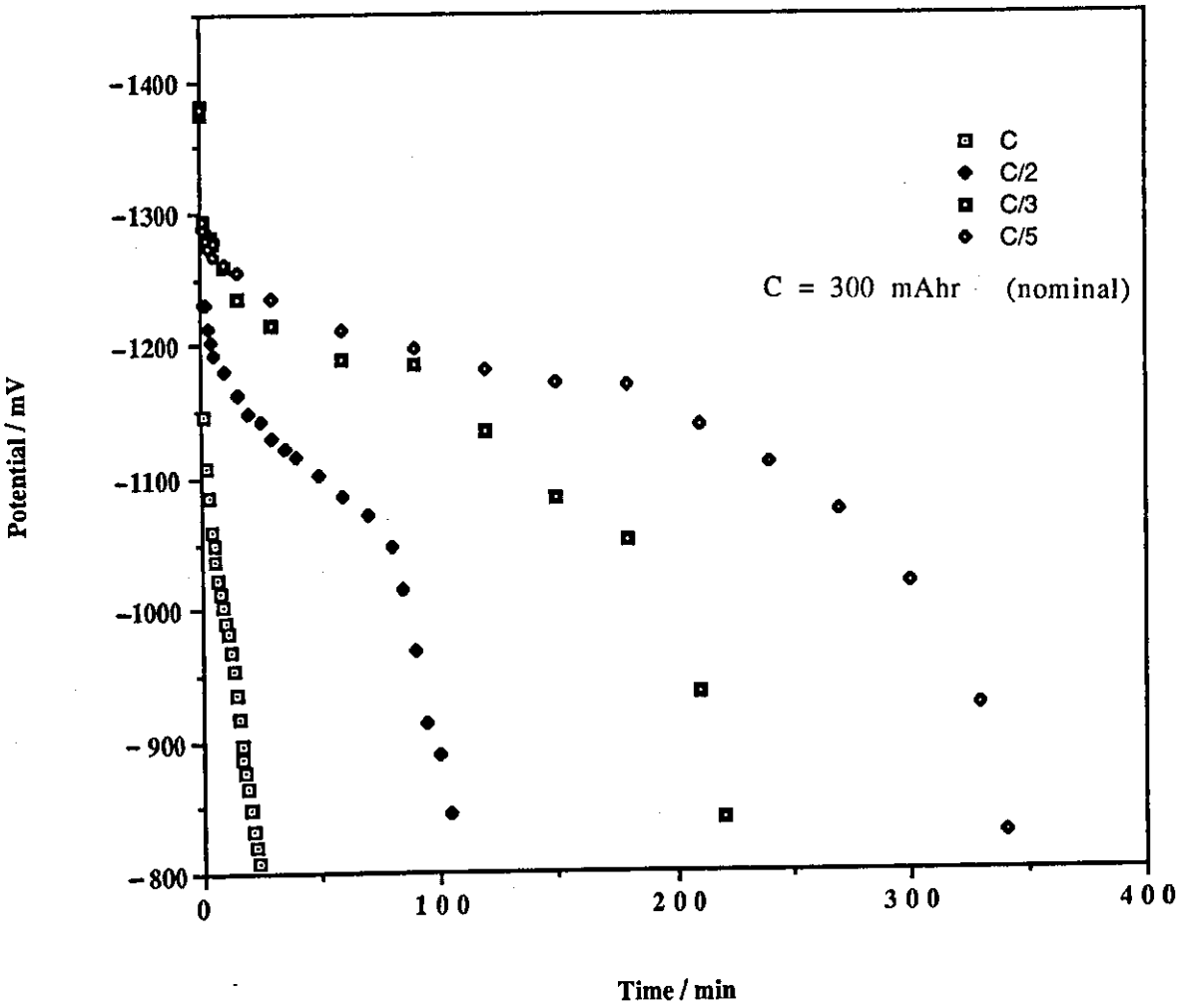

Figure 7.3.10. Discharge profile of zinc/P.V.A. electrode in 2M KOH / 95 gl^{-1} boric acid electrolyte.

e.g. for low drain consumer products.

Cycle-life performance of these electrodes, in 2M / 95 gl^{-1} boric acid solution, are given in Fig. 7.3.4. Again it is seen that the capacity of the initial cycles was more than their initial rating suggested. Also P.V.A. gave better cycle-life performance than C.M.C. both were better than unmodified electrodes, as in the discharge profiles. In fact the P.V.A. electrode still retained over 50% of its capacity after 70 cycles.

Morphological examination (scanning electron microscopy - S.E.M.) was performed on the P.V.A. and C.M.C. electrodes at the end of cycling. This revealed that the C.M.C. had a tight film-like surface covering it, whereas the P.V.A. had a much more open structure, with cracks and craters. This may help explain why the P.V.A. electrode gave a better performance, since the active surface area was considerably greater (Figs. 7.3.11 to 7.3.16.).

A separate cycling experiment was performed using 2M / 85 gl^{-1} boric acid electrolyte, with an electrode containing 10% P.V.A. It was found that for the first 30 cycles the potential was higher than that of an electrode in 2M / 95 gl^{-1} solution. At this point, however, dendrites were seen to penetrate the polyamide separator. Continuation of the cycling led to these dendrites growing, and eventually breaking off. The capacity was then seen to decline rapidly due to this shedding action. Again this proves the need for a trade-off with capacity and cycle-life performance.

Thus the best system was found to be 2M KOH / 95 gl^{-1} boric acid electrolyte, with a p.t.f.e. bound zinc electrode with an addition of 10% P.V.A. This gave over 70 charge-discharge cycles whilst still retaining over 50% of its original capacity without the use of costly separators.

Figure 7.3.11. S.E.M. photograph of zinc/C.M.C. electrode after 70 cycles.

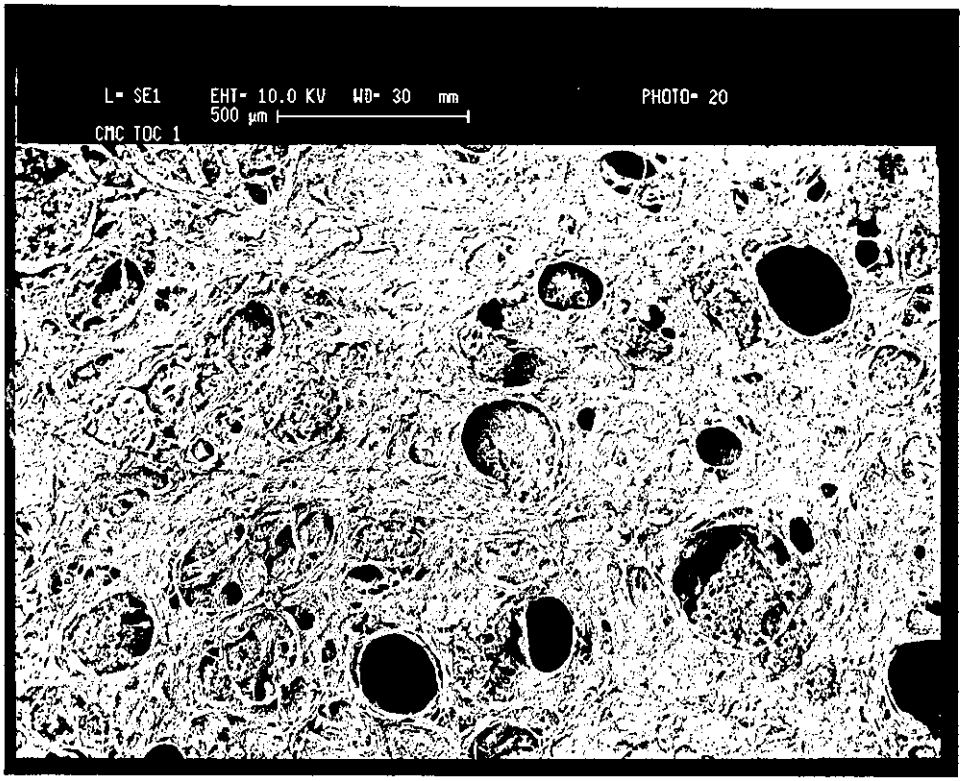

a. At top of charge. Magnification x 50.

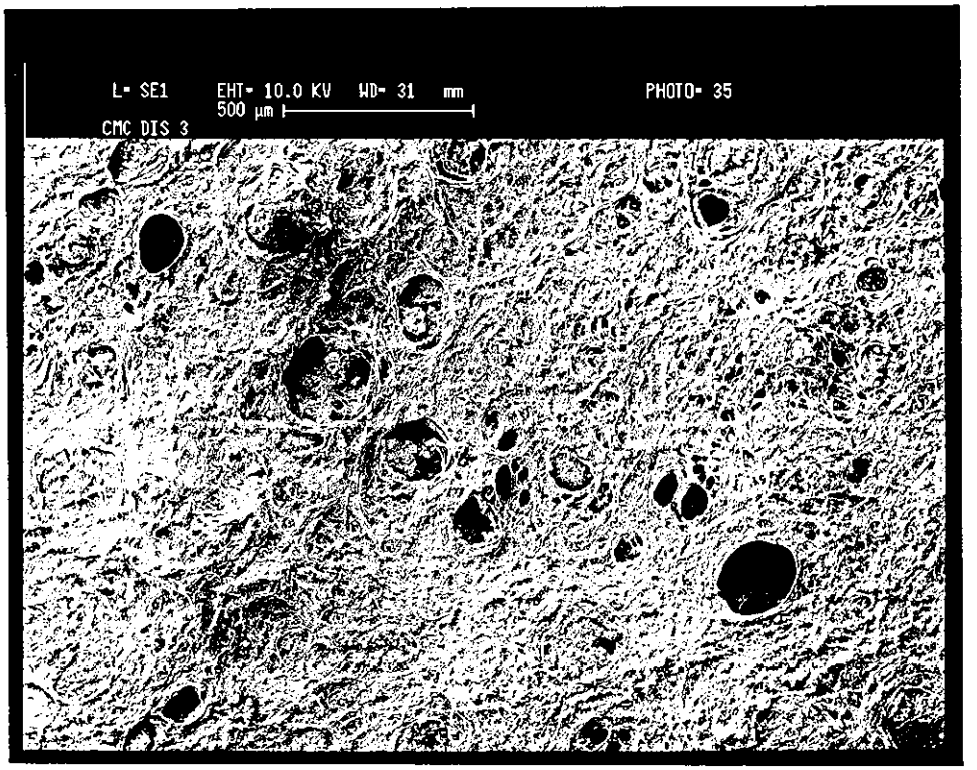

b. At end of discharge. Magnification x 50.

Figure 7.3.12. S.E.M. photograph of zinc/C.M.C. electrode after 70 cycles.

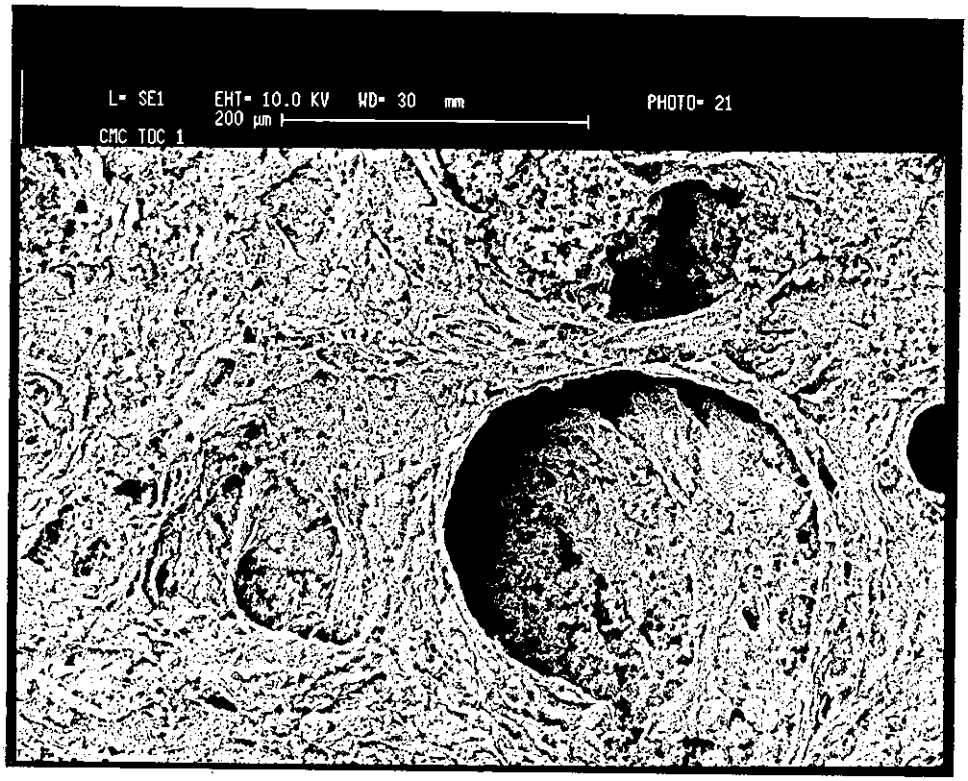

a. At top of charge. Magnification x 200.

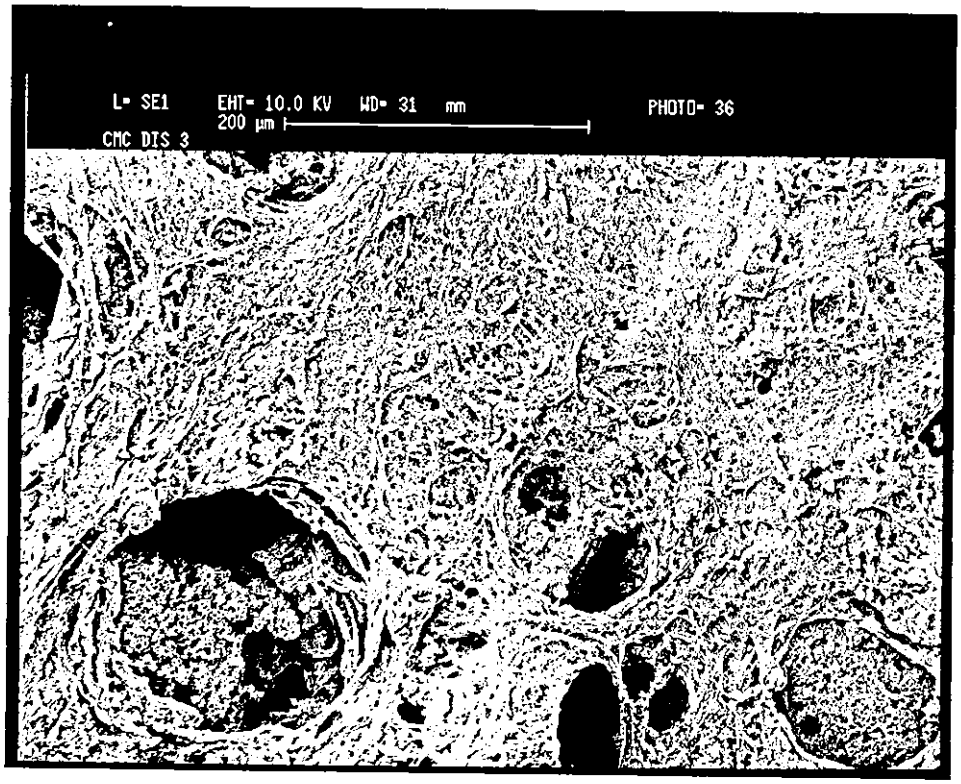

b. At end of discharge. Magnification x 200.

Figure 7.3.13. S.E.M. photograph of zinc/C.M.C. electrode after 70 cycles.

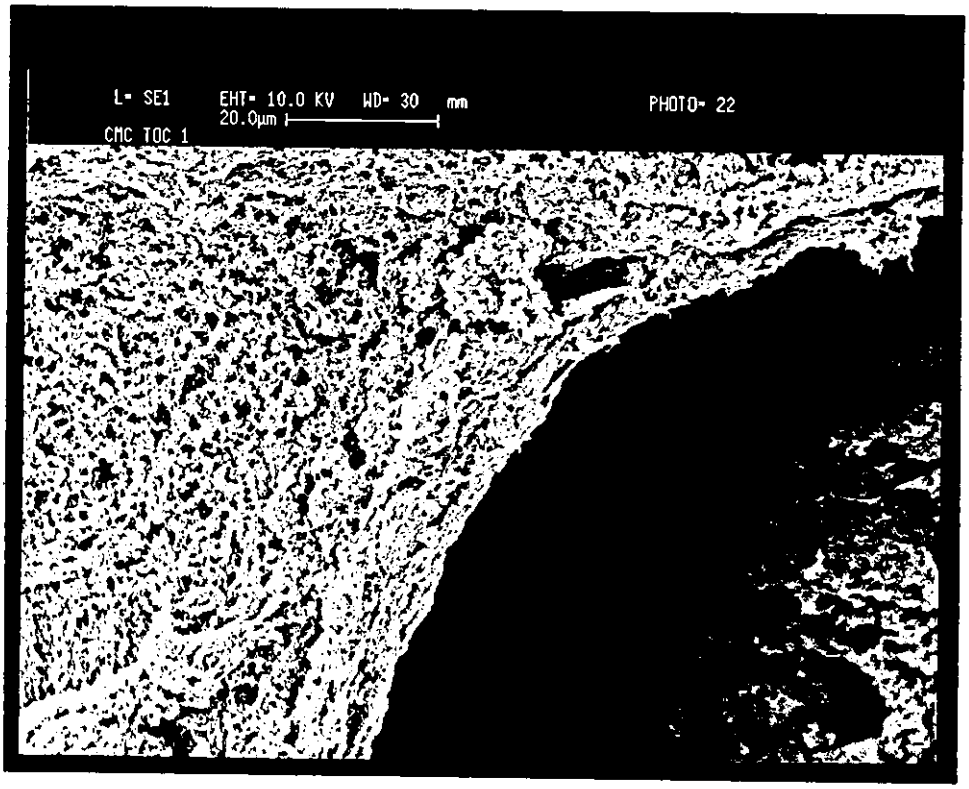

a. At top of charge. Magnification x 1000.

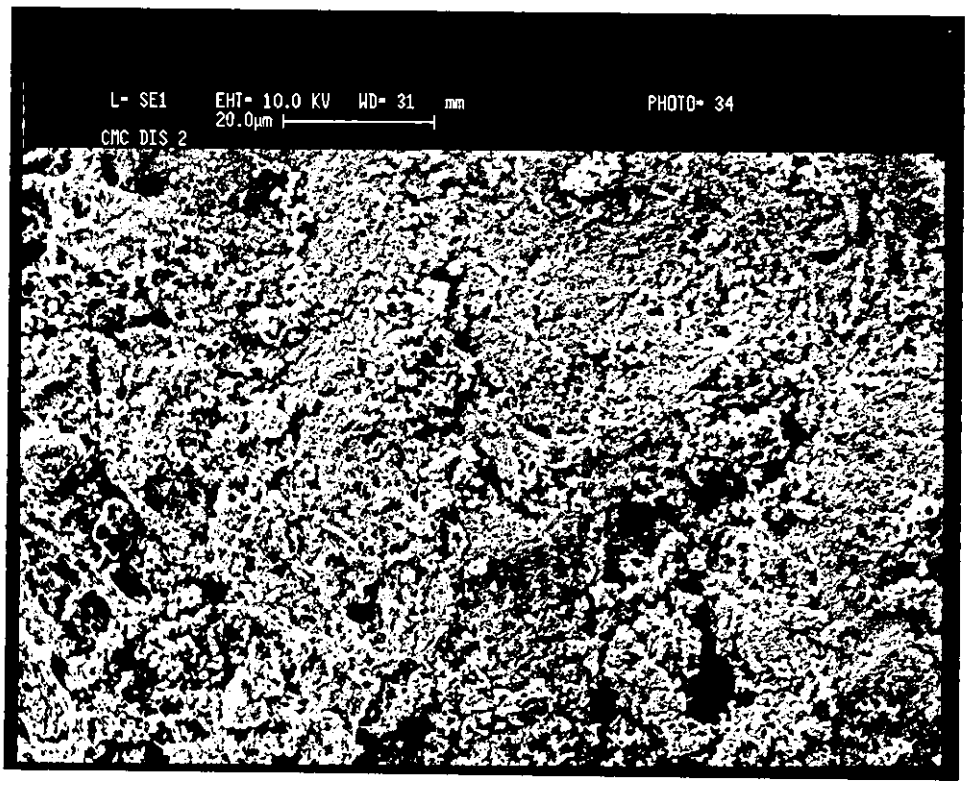

b. At end of discharge. Magnification x 1000.

Figure 7.3.14. S.E.M. photograph of zinc/P.V.A. electrode after 70 cycles.

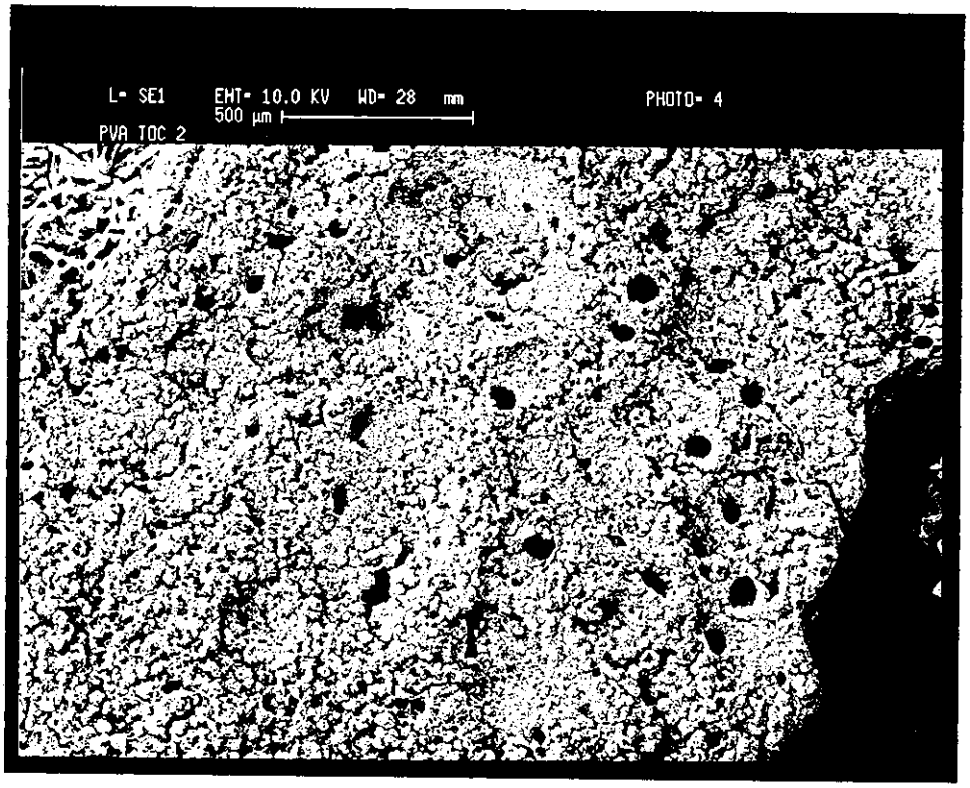

a. At top of charge. Magnification x 50.

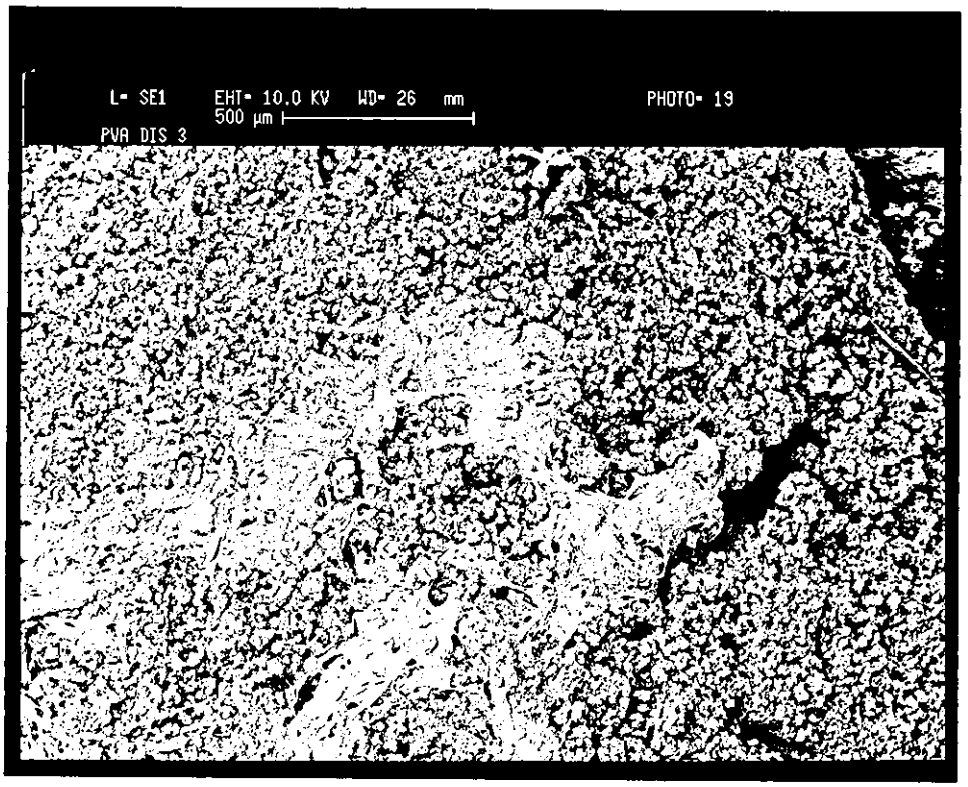

b. At end of discharge. Magnification x 50.

Figure 7.3.15. S.E.M. photograph of zinc/P.V.A. electrode after 70 cycles.

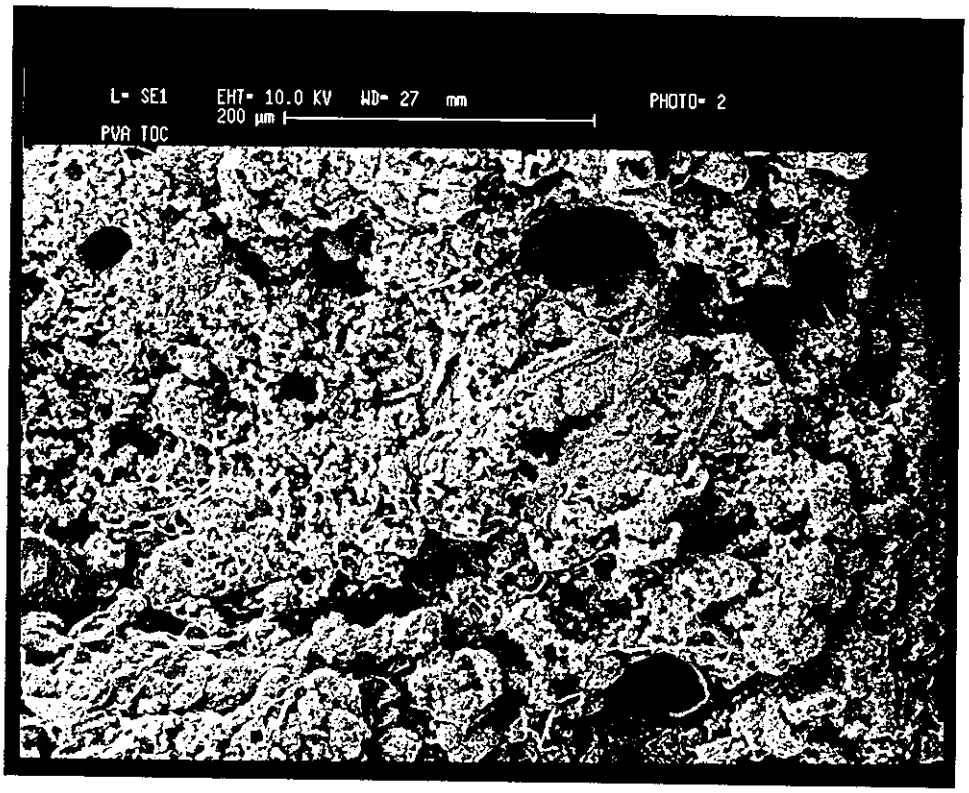

a. At top of charge. Magnification x 200.

b. At end of discharge. Magnification x 200.

Figure 7.3.16. S.E.M. photograph of zinc/P.V.A. electrode after 70 cycles.

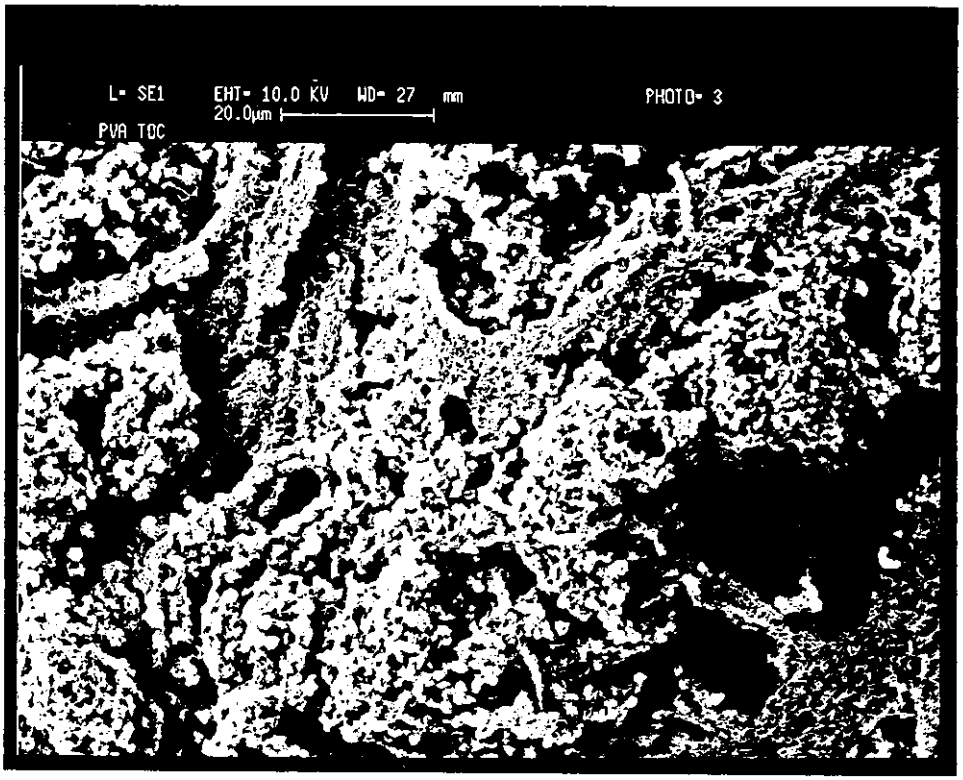

a. At top of charge. Magnification x 1000.

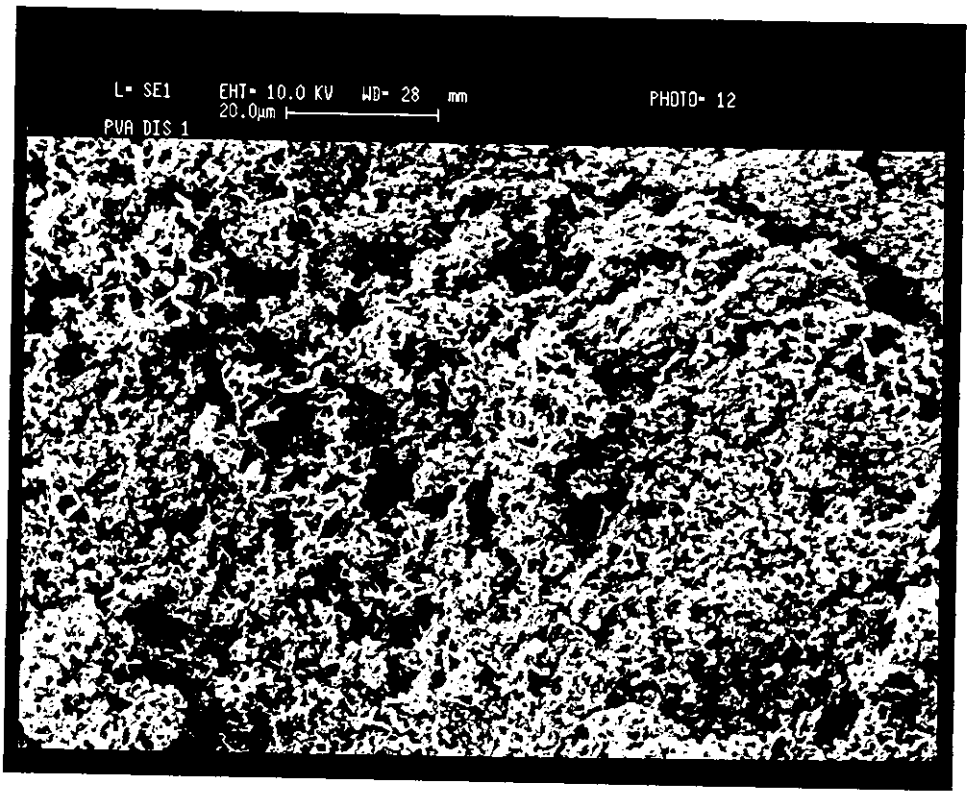

b. At end of discharge. Magnification x 1000.

CHAPTER 8

ELECTRODEPOSITION OF ZINC ONTO GRAPHITIC CARBON SUBSTRATES

8.1. Introduction

The incorporation of graphite in secondary zinc electrodes has previously been reported to greatly enhance cycle-life. During the present investigation, however, the capacity and cycle-life behaviour of the electrodes was actually found to decrease with the addition of graphite, as outlined in the preceding chapter. The electrodes also suffered a large expansion thought to be caused by hydrogen evolution off the graphite surface during recharge. The low hydrogen overpotential of graphite (lower than that of zinc) could account for the high level of gassing observed.

By studying the electrodeposition, and dissolution, of zinc on graphite substrates, it was hoped that differences in the results described above could be accounted for.

The electrodeposition of zinc onto various substrates has been reported [159-161]. In particular McBreen et al [159, 160] found evidence of underpotential deposition (to a monolayer thickness) prior to bulk deposition. This was only applicable to metals whose work function was higher than that of zinc.

The electrodeposition of zinc onto graphitic substrates is, however, not widely reported. Despic [162] has performed such investigations, but these were in a buffered, acidic zinc sulphate solution. Viswanathan et al [163] did examine a zinc-potassium hydroxide system, with graphite electrodes, but these workers

were interested primarily in the commercial production of electrodeposited zinc powder.
It was therefore considered pertinent to study the electro-deposition, and dissolution, of zinc on planar and pasted graphitic substrates in a series of potassium hydroxide electrolytes containing zincate. In order to magnify any changes in the resultant current profiles 7M potassium hydroxide was utilised. This choice also facilitated comparison with the results reported by Duffield [72-74].

8.2. Experimental

Experimental investigations were carried out in a 7M KOH electrolyte containing varying amounts of dissolved zinc oxide (0 ---> 40 gl^{-1}).

Three types of working electrode were employed: solid zinc, solid graphite and pasted graphite. Their construction has been shown in section 4.3.

The surface preparation of the zinc electrode was identical to that detailed in section 6.2. The solid graphite electrode had a similar pre-treatment to the zinc, consisting of polishing on 600 and 1200 grade SiC paper. Vigourous rubbing on tissue paper followed, to remove any SiC from the surface. Immersion in 10% v/v HNO_3 (S.G. 1.42) was then performed before a final rinse in triple-distilled water. Preparation of the porous graphite electrode has already been discussed, in section 4.3.

Cyclic voltammograms were obtained for the various electrode and electrolyte compositions. The sweep limits for the two forms of graphite were 0 and -2000 mV (a less negative cathodic limit was utilised when only the initial zinc deposition reaction was of interest). A sweep rate of 20 mV s^{-1} was applied using a ramp generator in conjunction with a potentiostat. Current and potentials were again recorded with an X-Y chart recorder.

8.3. Results and Discussion

Figure 8.3.1. illustrates the cyclic voltammogram for a solid graphite electrode in a 7M KOH / 5 gl^{-1} ZnO electrolyte, with a potential window set between 0 and -2000 mV. Initially, on sweeping in the cathodic direction zinc deposition commences at -1430 mV, with a current maximum at -1500 mV. The current then diminishes due to the mass transport limitation of zincate species (as discussed in section 2.5) until the ultimate onset of hydrogen evolution. No evidence was found for underpotential deposition on this substrate. This fact cannot be used to refute or support the empirical relationship between work function and underpotential deposition proposed by McBreen et al [159, 160]. This is because the reported values for the work functions of graphite and zinc overlap - falling within the ranges 4.34 eV to 5.0 eV respectively[130,164,165]. On sweep reversal, zinc stripping commences at -1440 mV, this process exhibiting 100% coulombic efficiency with respect to deposition.

This behaviour can be compared with that shown in Fig. 8.3.2., for a solid graphite electrode in 7M KOH without the addition of zinc oxide. The only significant feature of this voltammogram is the evolution of hydrogen, which is seen to commence at -1400 mV with the resultant current continuing to rise until sweep reversal at -2000 mV. The superposition of the two responses (i.e. Figs. 8.3.1. and 8.3.2.) indicates that in the presence of zincate species, at potentials more cathodic than -1430 mV, both zinc metal deposition and hydrogen evolution from the graphite surface are thermodynamically feasible. The low residual current observed at potentials around -1400 mV in Fig. 8.3.2. suggests that both processes occur concurrently. The subsequent rapid rise in current due to zinc deposition seen in Fig. 8.3.1., shows that it is this reaction which is kinetically more favourable at these potentials. It is evident that the subsequent hydrogen evolution

profile in Fig. 8.3.1. i.e. off electrodeposited zinc, exhibits marked differences from that of the uncovered graphite. The latter exhibiting behaviour indicative of a lower hydrogen overvoltage than that of zinc. This is illustrated by comparison with Fig. 8.3.3. where the hydrogen evolution current from a planar zinc electrode is recorded, in the absence of zincate species. It can be seen that the evolution of hydrogen from zinc occurs at a potential some 250 mV more cathodic than it occurs from graphite. This observation is important with regard to zinc-anoded secondary cells containing graphite as a conductor modifier. When the cell is charged its acceptance efficiency will be determined by the hydrogen evolution potential. Thus it will be beneficial if the graphite in the electrode is overplated with zinc before such potentials are reached.

A series of voltammetric experiments were conducted with varying concentrations (5, 10, 20 and 40 gl^{-1}) of zinc oxide dissolved in 7M KOH. The resultant voltammograms are shown in Figs. 8.3.4. to 8.3.8. These show that the ease with which zinc deposits onto graphite is dependent on the concentration of the electroactive zincate species in solution. With increasing zinc oxide concentration the potential for metallic deposition becomes less negative. Since the substrate surface is consistent, this is likely to be a Nernstian phenomenon. Increasing zinc oxide concentration also leads to the peak sizes and overall charges increasing (due to the relationship between exchange current and zincate concentration). The salient results of the series of experiments are summarised in Table 8.3.1.

Another series of experiments were performed with pasted electrodes, using the same electrolyte concentrations as with the solid graphite. The resultant voltammograms are shown in Figs. 8.3.9. to 8.3.13. Similar behaviour was observed for these porous electrodes as for solid graphite. In general, both the deposition and dissolution peaks obtained with pasted electrodes are much broader than their planar equivalents. This is due to surface

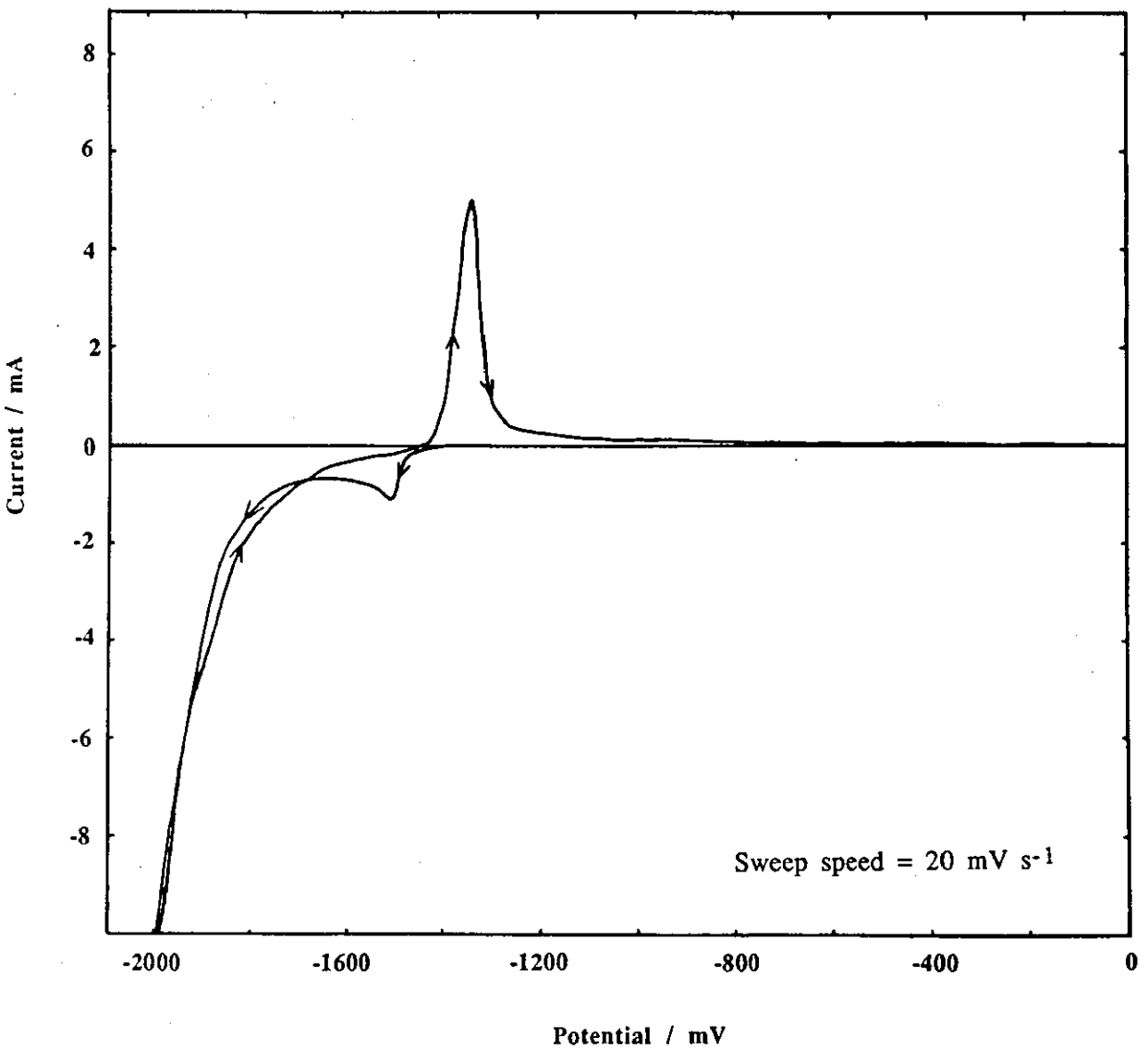

Figure 8.3.1. Cyclic voltammogram for solid graphite electrode in 7M KOH electrolyte with addition of 5 gl^{-1} ZnO

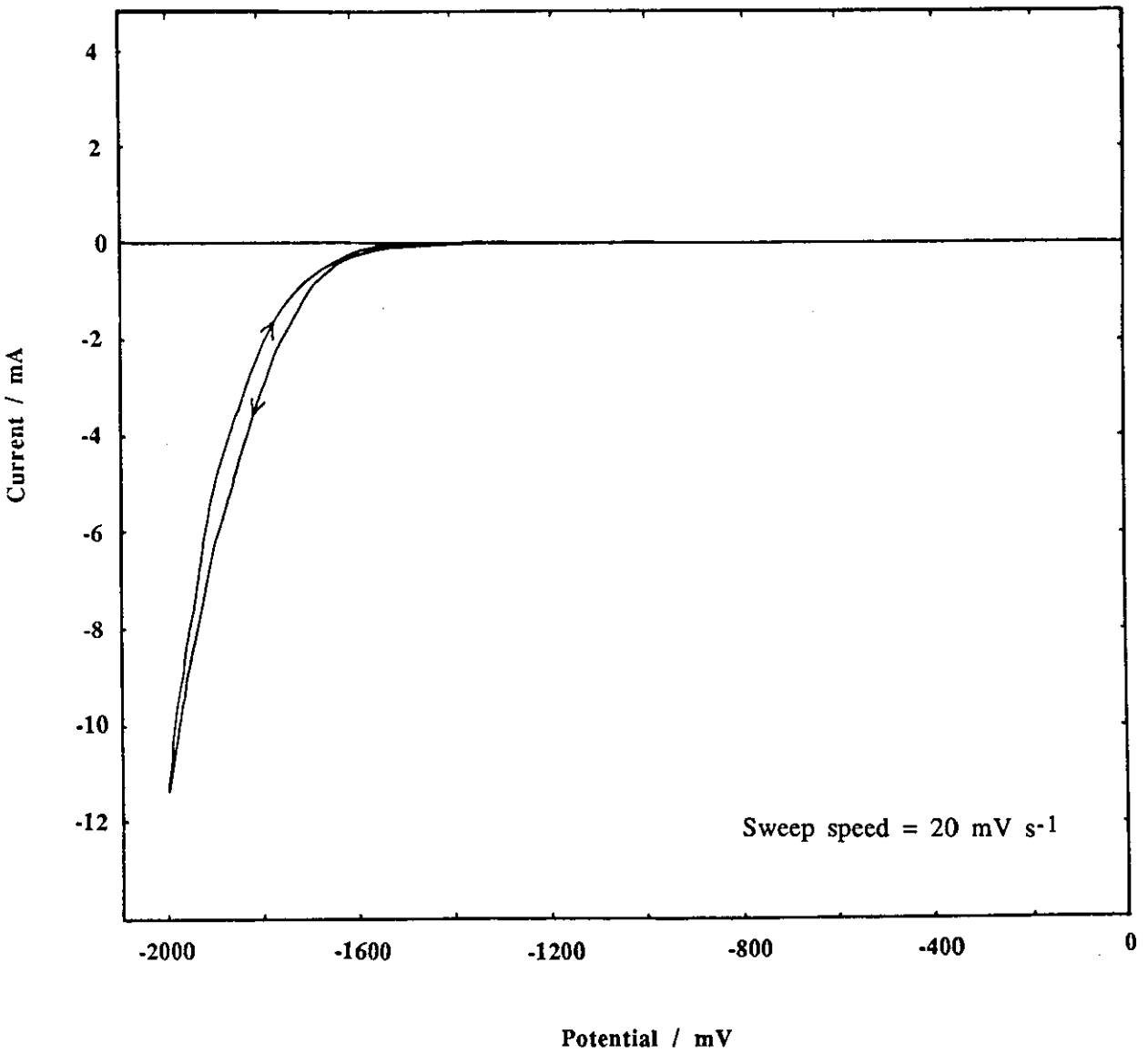

Figure 8.3.2. Cyclic voltammogram for solid graphite electrode in 7M KOH electrolyte with no addition.

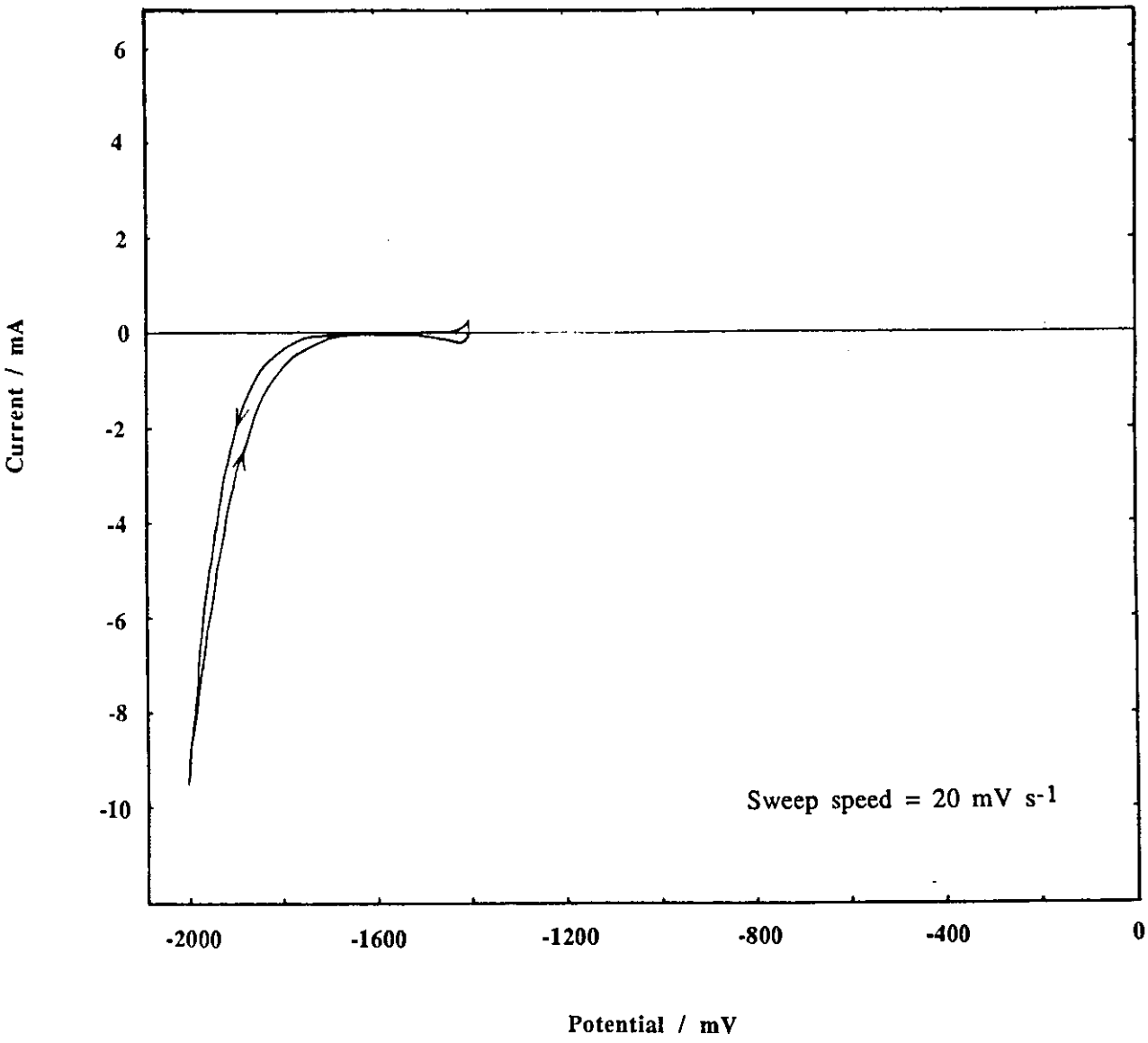

Figure 8.3.3. Cyclic voltammogram for solid zinc electrode in 7M KOH electrolyte.

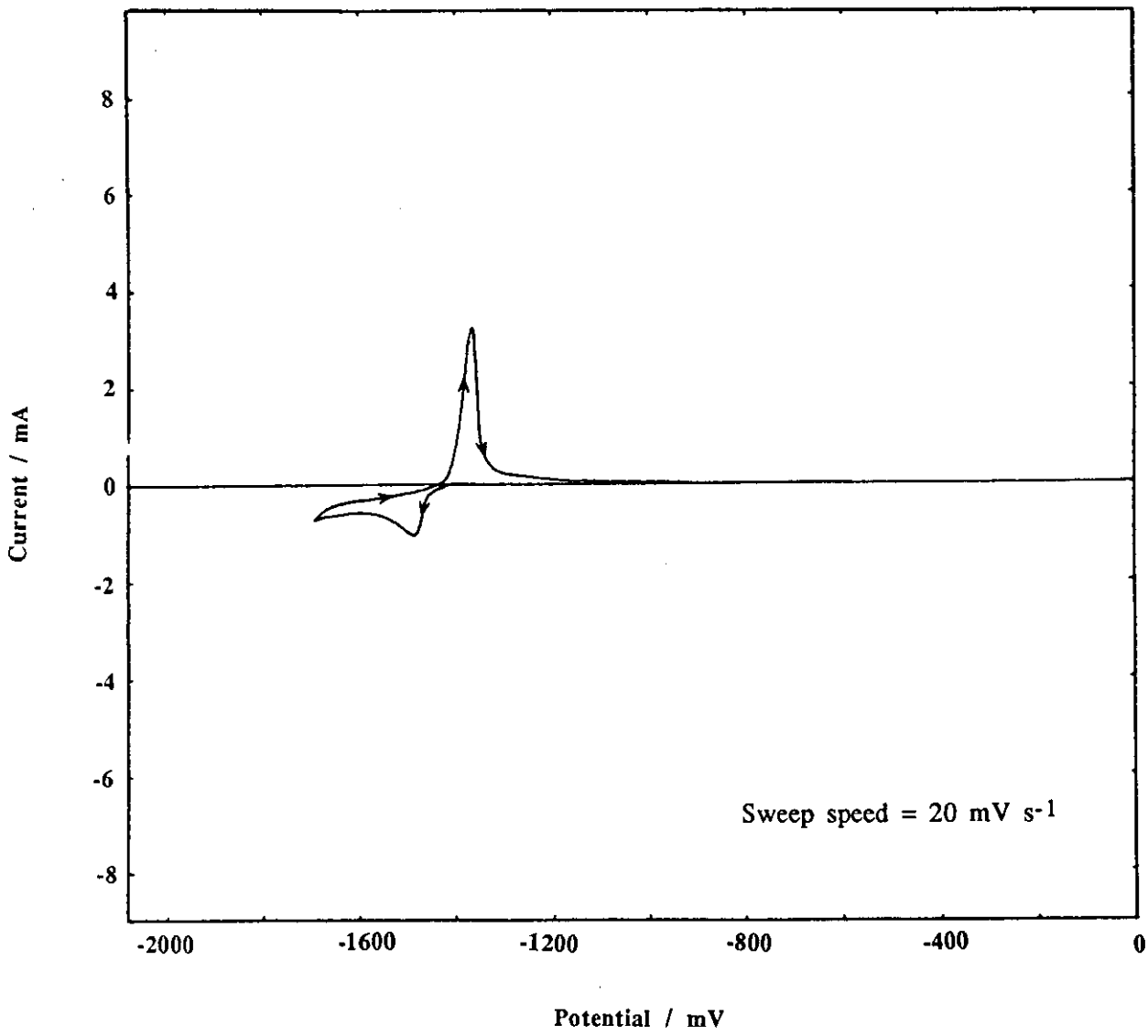

Figure 8.3.4. Cyclic voltammogram for solid graphite electrode in 7M KOH electrolyte with addition of 5 gl^{-1} ZnO.

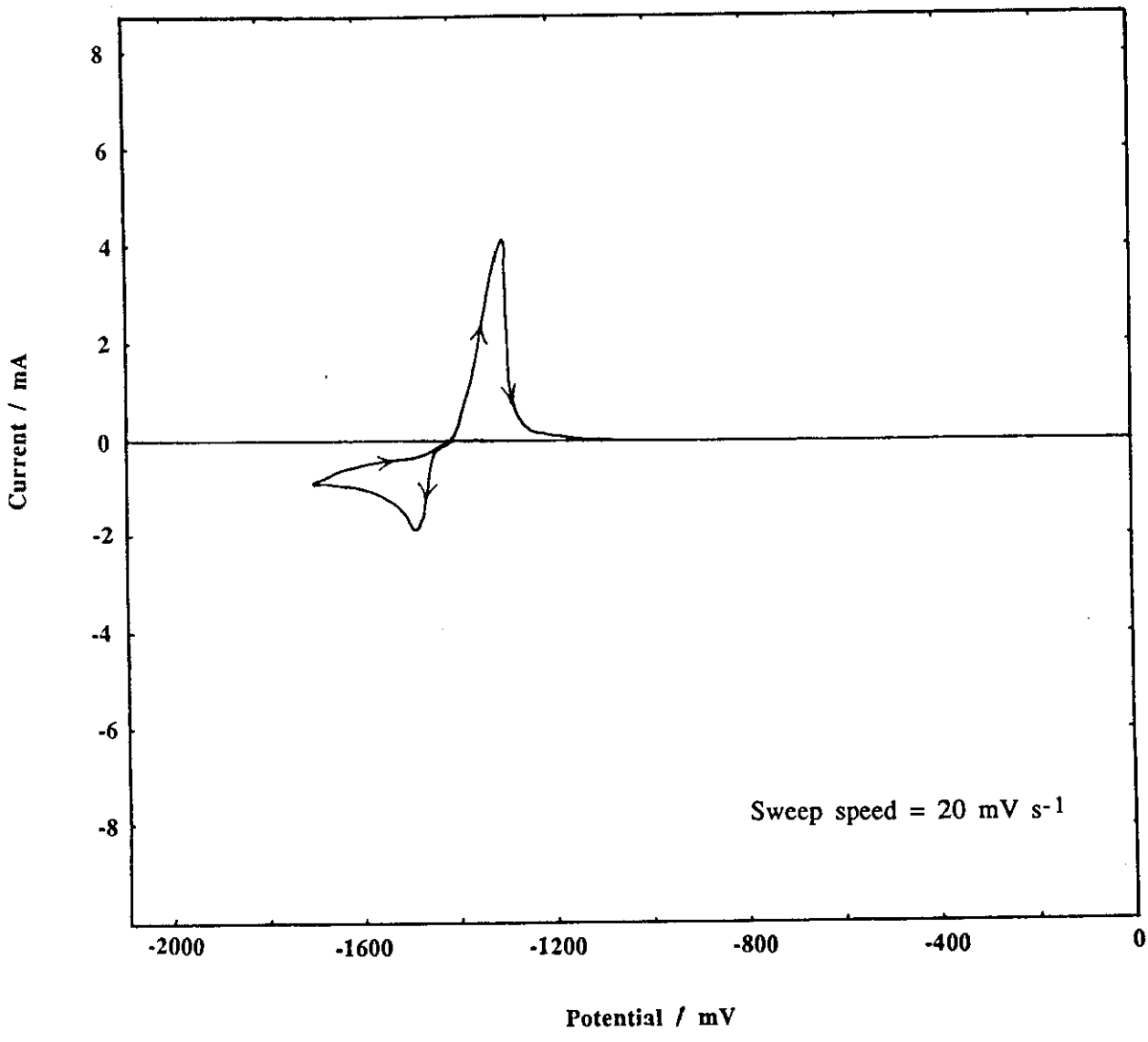

Figure 8.3.5. Cyclic voltammogram for solid graphite electrode in 7M KOH electrolyte with addition of 10 gl^{-1} ZnO.

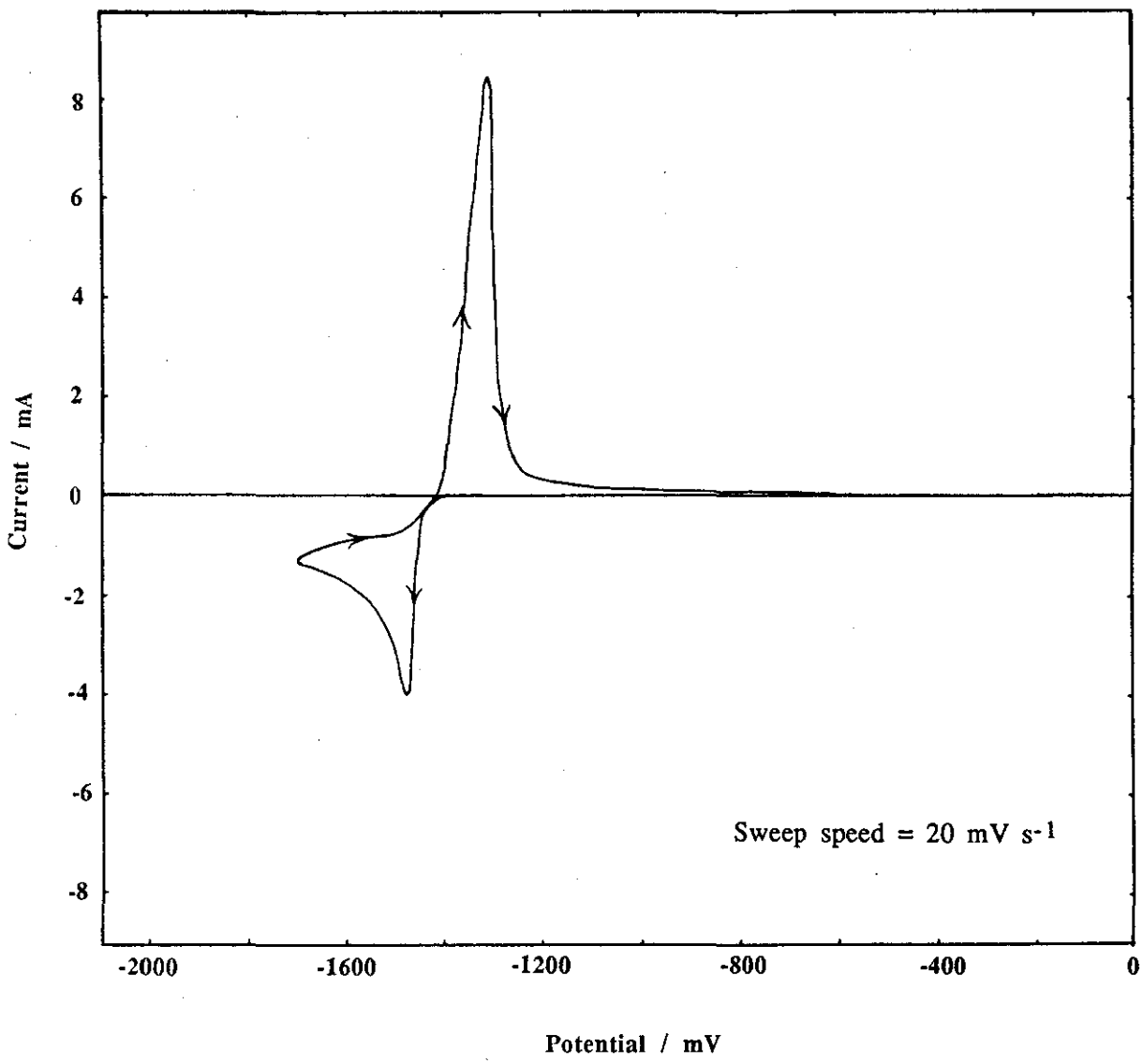

Figure 8.3.6. Cyclic voltammogram for solid graphite electrode in 7M KOH electrolyte with addition of 20 gl^{-1} ZnO.

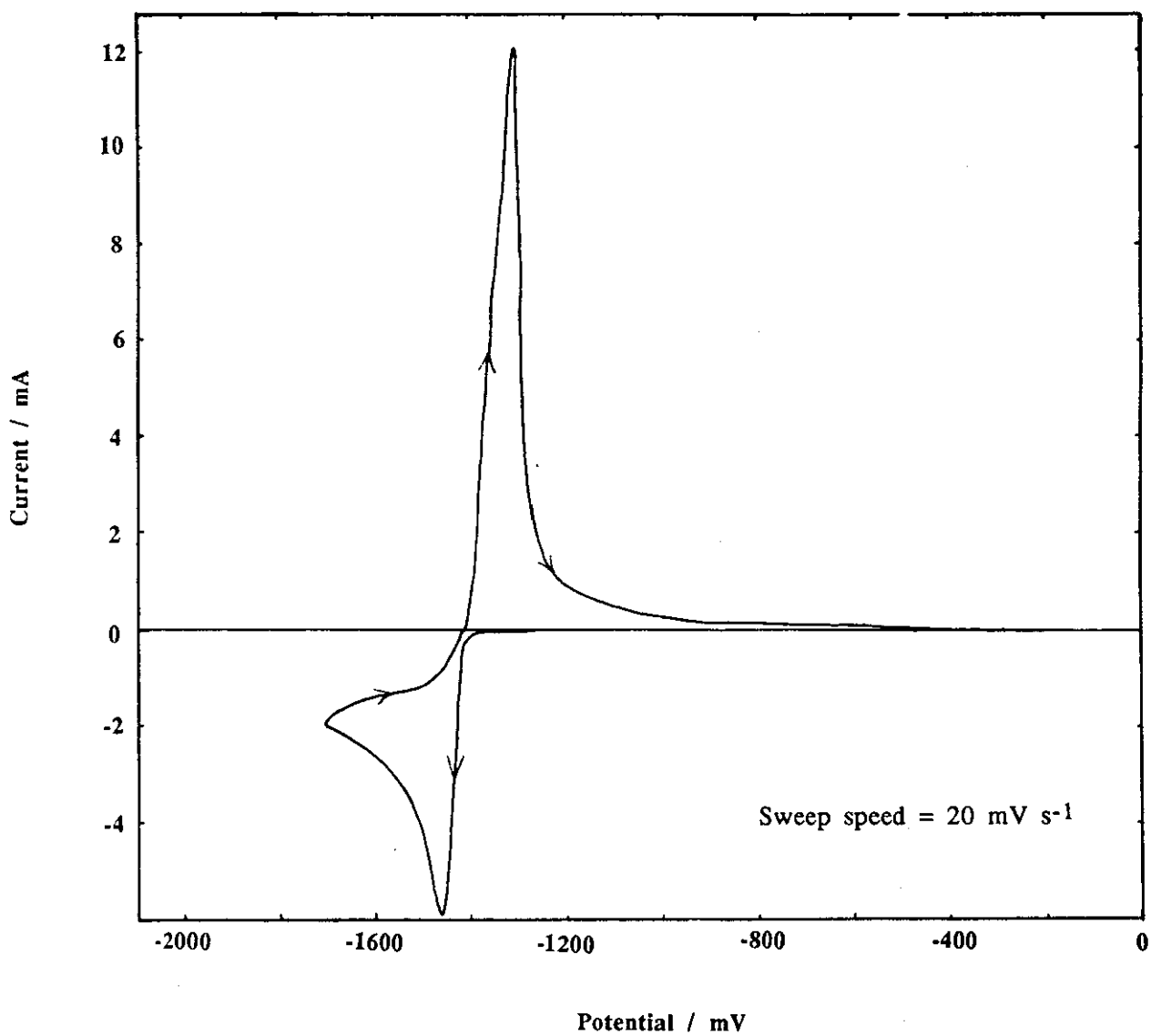

Figure 8.3.7. Cyclic voltammogram for solid graphite electrode in 7M KOH electrolyte with addition of 40 gl^{-1} ZnO.

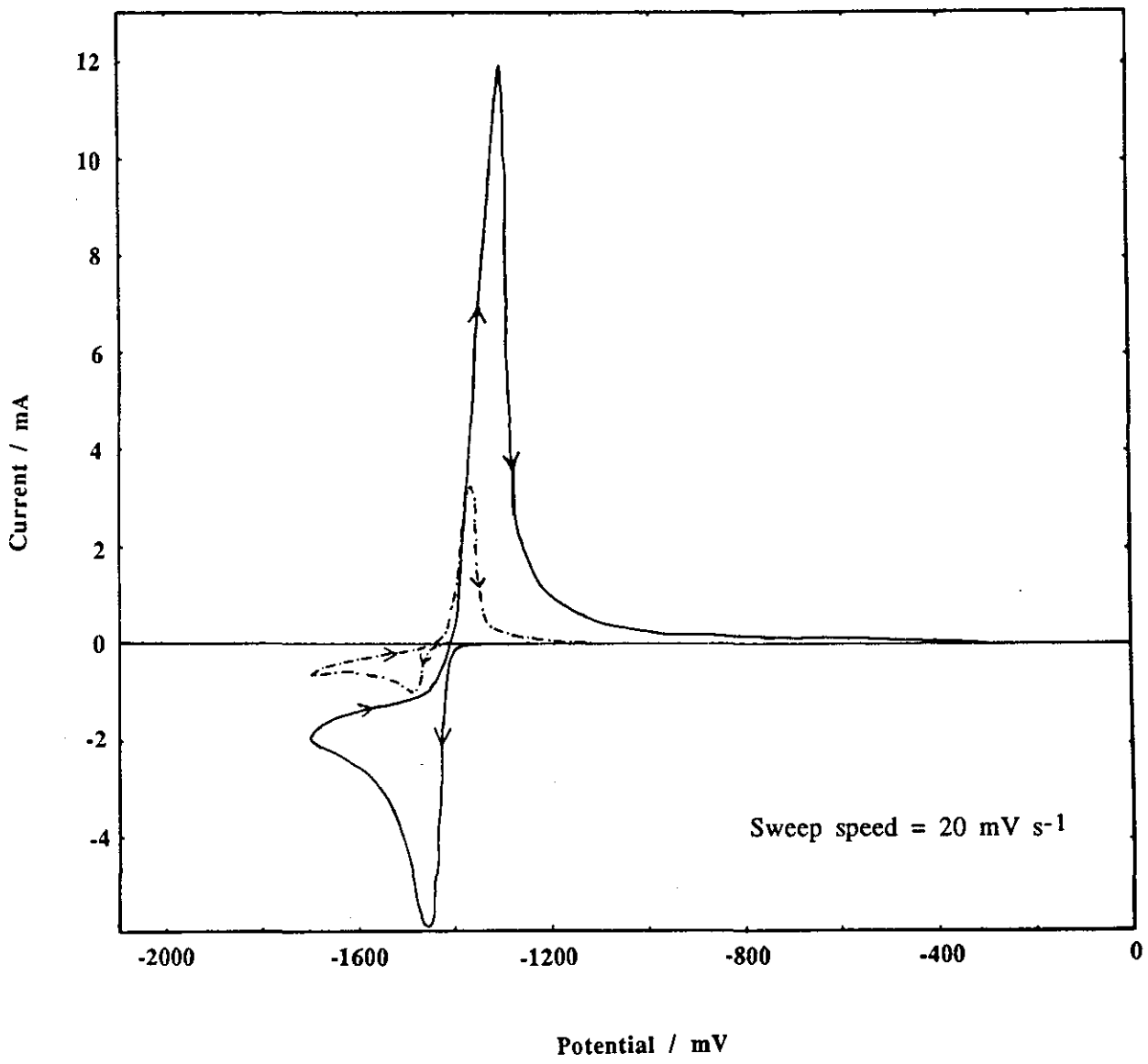

Figure 8.3.8. Comparison of cyclic voltammograms of solid graphite electrode in 7M KOH electrolyte with additions of 5 and 40 gl^{-1} ZnO.

Concentration of ZnO (gl^{-1})	Onset of deposition (mV)	Potential at current maximum (mV)	Charge in deposition peak (mC)	Onset of dissolution (mV)
5	-1430	-1500	11.3	-1440
10	-1415	-1490	21.4	-1420
20	-1405	-1470	37.3	-1415
40	-1395	-1460	64.1	-1410

Table 8.3.1. Results obtained from various concentrations of zinc oxide with planar graphite electrodes.

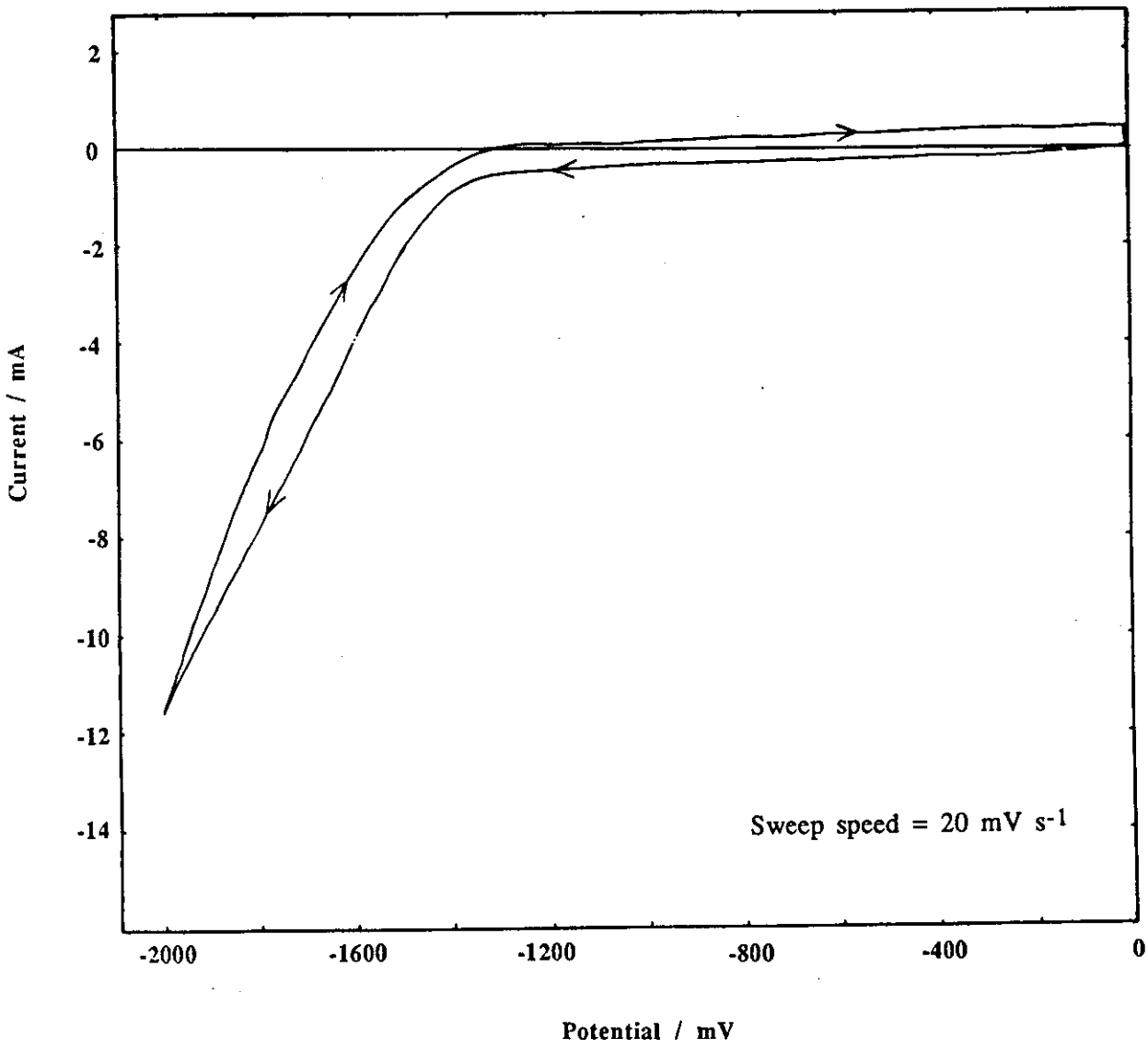

Figure 8.3.9. Cyclic voltammogram for pasted graphite electrode in 7M KOH electrolyte with no addition.

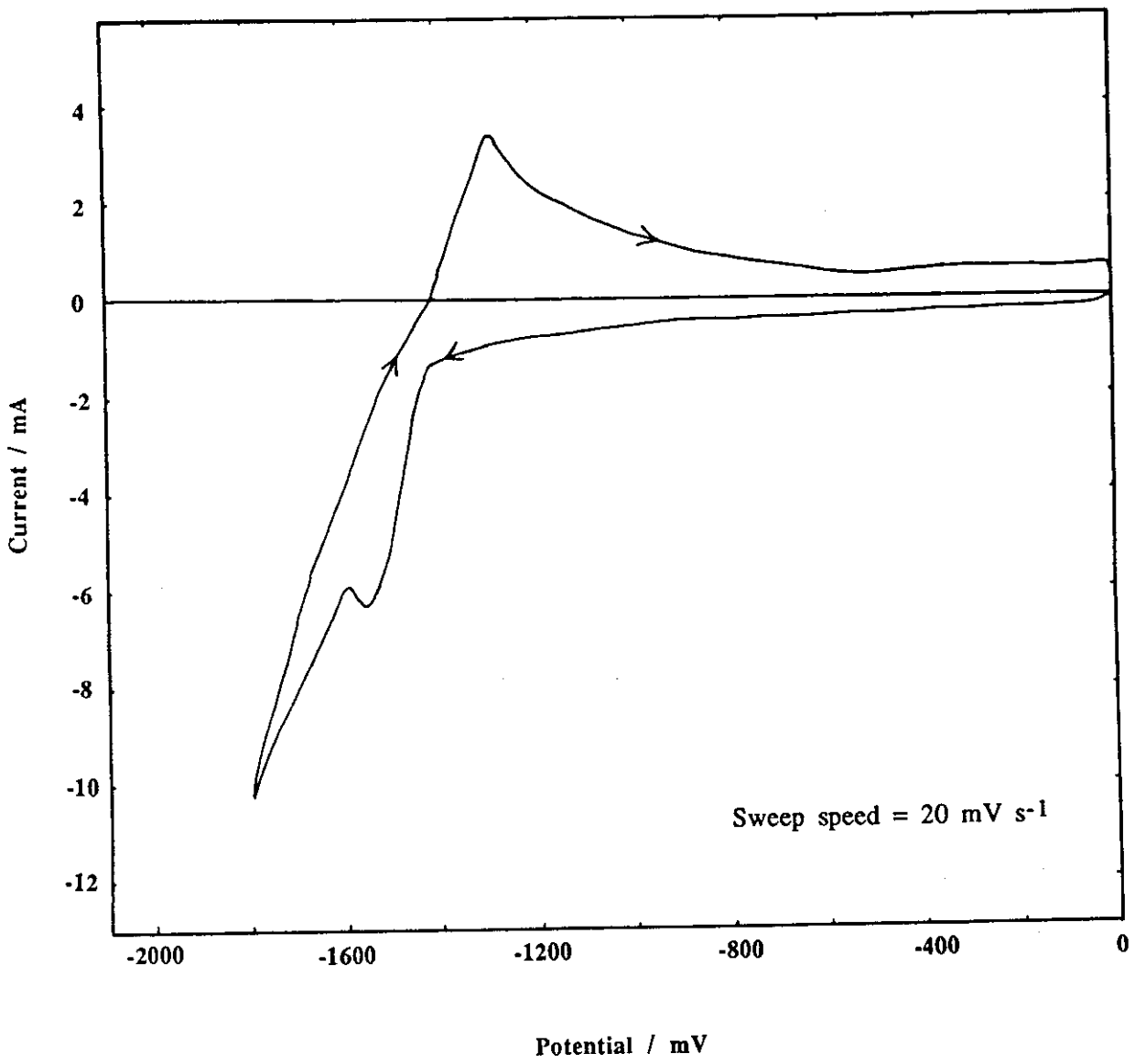

Figure 8.3.10. Cyclic voltammogram for pasted graphite electrode in 7M KOH electrolyte with addition of 5 gl^{-1} ZnO.

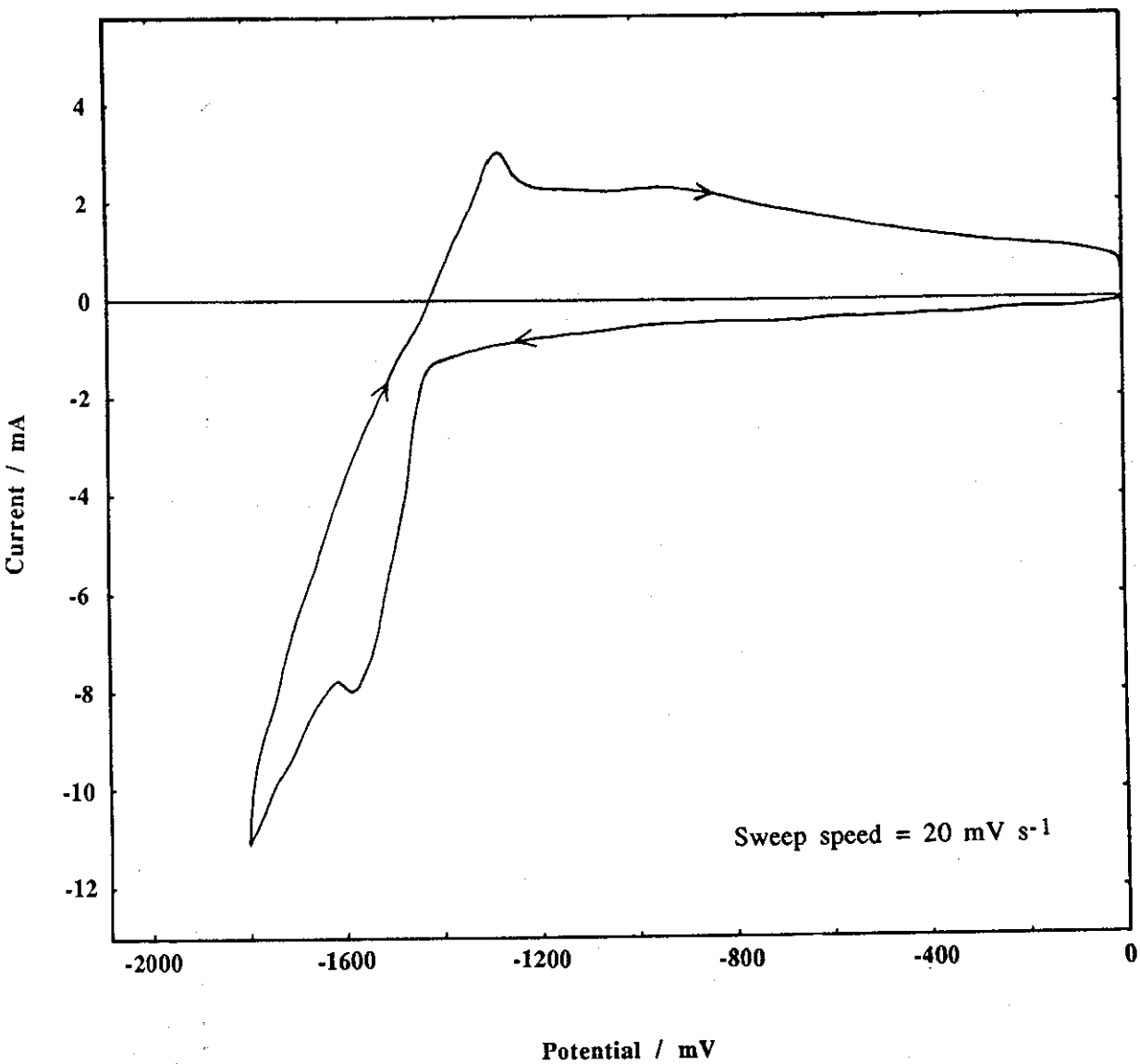

Figure 8.3.11. Cyclic voltammogram for pasted graphite electrode in 7M KOH electrolyte with addition of 10 gl^{-1} ZnO.

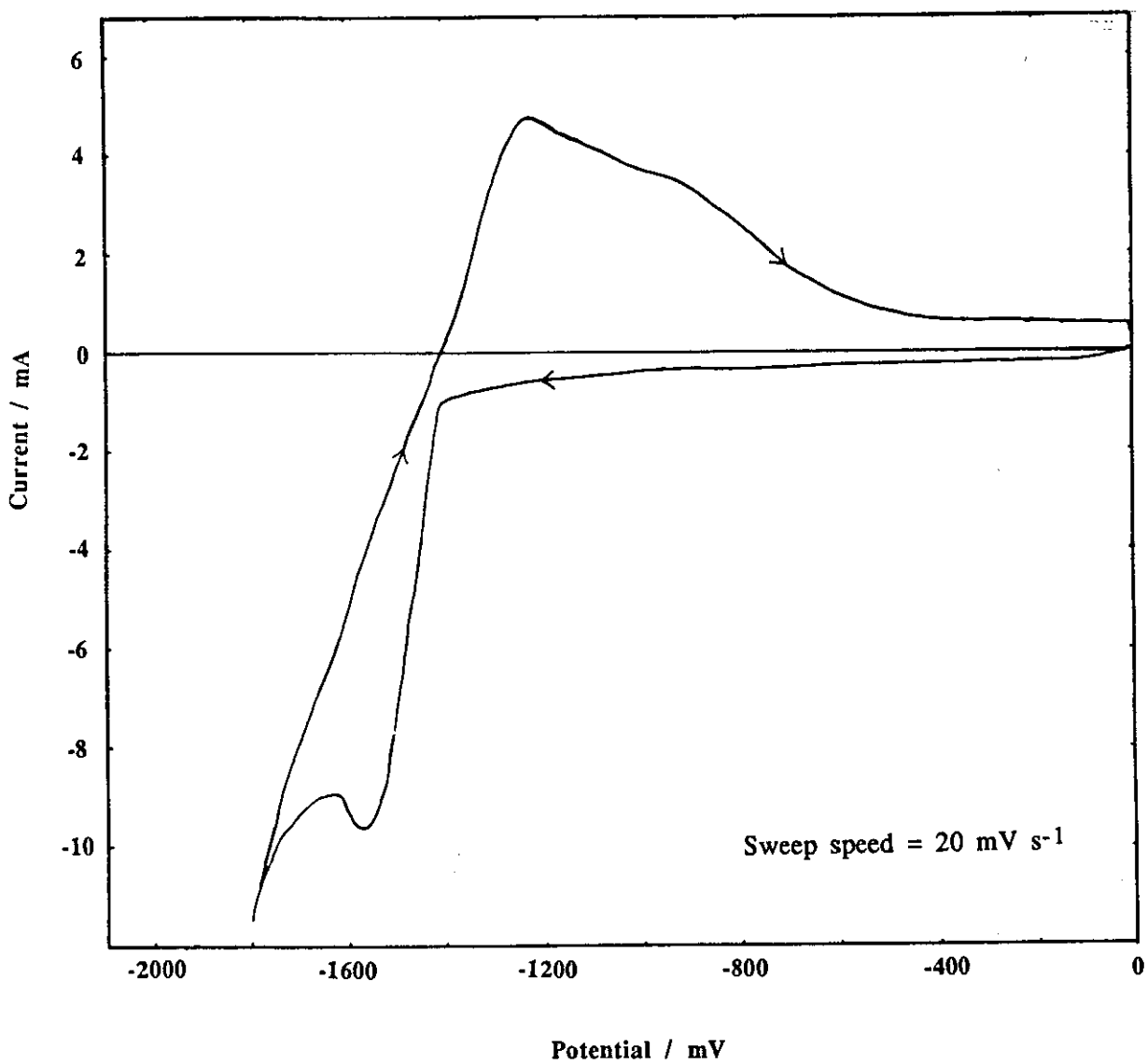

Figure 8.3.12. Cyclic voltammogram for pasted graphite electrode in 7M KOH electrolyte with addition of 20 gl^{-1} ZnO.

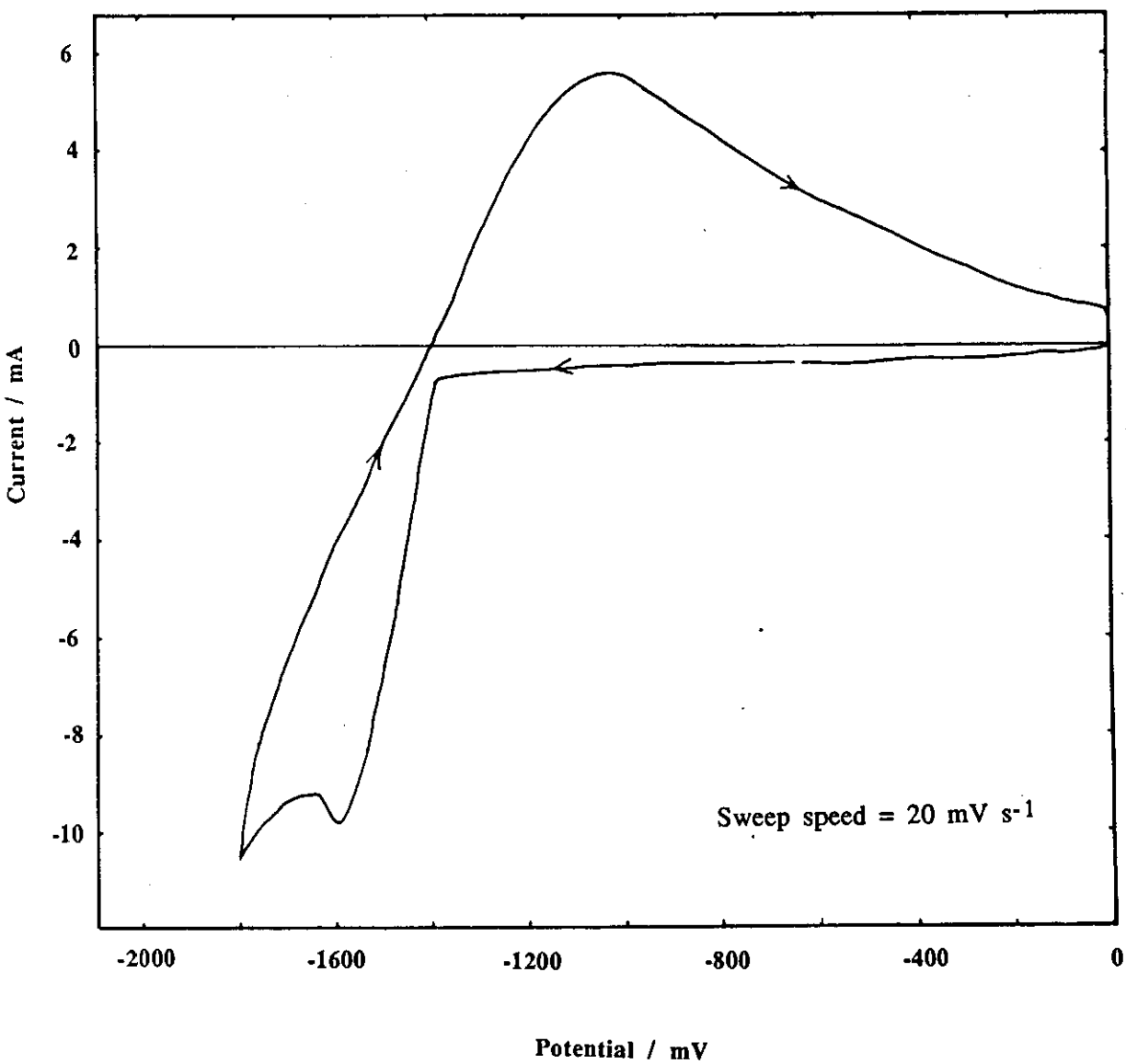

Figure 8.3.13. Cyclic voltammogram for pasted graphite electrode in 7M KOH electrolyte with addition of 40 gl^{-1} ZnO.

roughness or "porosity" causing an uneven potential distribution (with respect to the electrolyte) over the active area of the electrode. However, the important trend of a positive shift in deposition potential with increasing zinc oxide concentration was again evident.

The major consequences of this behaviour with regard to cell/battery performance can be summarised as follows. In a graphite modified, zinc-anoded system which undergoes some degree of dissolution on discharge (such as those employed by Duffield) the maximum concentration of zincate in the electrolyte, and consequently the largest area of uncovered graphite, will occur when the system is fully discharged. Upon recharge zinc deposition on the graphite will occur with a resultant decrease in dissolved zincate. This reduction in zincate increases the probability of concurrent hydrogen evolution from the graphite. However, since the zincate is depositing onto the graphite, the area available for hydrogen evolution is also reduced. Hence the relationship between zincate concentration and deposition potential is a favourable one with regard to the successful operation of graphite conductor-modified zinc anoded cells.

However, the same argument can also explain why the same electrode system proved unsuccessful in borate electrolyte. The above explanation assumes that there is enough soluble zinc species to entirely cover the graphite surface. Since the addition of borate actually reduces the solubility of zinc, and hence zincate, in solution this causes some graphite surface to be left exposed. It is from this surface that hydrogen evolution can occur.

The results obtained in these experiments can also help explain more fully the initial cycling behaviour (formation) of graphite modified electrodes as reported by Duffield et al [72-74]. The initial increase in capacity can be attributed to the progressive coverage of the graphite surface by electrodeposited zinc. This area diminishing the successive cycles until all the available

graphite is covered. The cell capacity then begins to fall with increasing cycle number as the efficiency of the zinc anode diminishes.

CHAPTER 9

CONCLUDING REMARKS AND SUGGESTIONS FOR FURTHER WORK

The anodic behaviour of zinc in alkaline electrolytes, with and without additives, has been studied by both galvanostatic and potentiostatic techniques.

The galvanostatic study has shown that cationic-zincate species are generally not as effective in reducing the time taken to passivate the electrode, as zinc anion species. This can be attributed to the limited solubility of the former in hydroxide solution, and thus does not give a real indication of their effectiveness when incorporated in the electrode mix, rather than the electrolyte.

Of the zinc anion species, it was noted that the concentration of additive in the electrolyte was critical - too much causing spontaneous passivation of the electrode surface, even at open circuit. Borate and chromate were found to be the most effective passivating agents. Auger analysis of the passivated surfaces suggests that two different mechanisms are occurring within these solutions. Borate addition was thought to cause a reduction in free hydroxyl species in solution which in turn, leads to a reduction of zincate solubility. In contrast, chromate addition caused passivation due to its strong oxidative and passivating nature.

Potentiostatic investigation of the most promising electrolytes yielded similar results, with the additive concentration again proving critical. Rotation of the electrode was found to have the effect of forcing the reaction away from a solid-state mechanism.

Long term cycling experiments performed with borate electrolytes revealed that the capacity of electrodes in these solutions was rather low. Increasing the surface area was a method of overcoming this. This was achieved incorporating C.M.C., P.V.A., or graphite into the electrode during its fabrication. P.V.A. was found to give the best results, as it retained an open structure in the electrode, even after cycling. This prevention of densification facilitated access of electrolyte to more of the electrode. Graphite proved ineffective as an additive due to excessive gassing during charging. This gassing is not problematic in systems where the graphite surface is covered with zinc such as that employed by Duffield, but in borate solution where zinc solubility is lower, exposed graphite remains.

Further work on this system is required to optimise both the electrolyte and electrode compositions. Gellation of the electrolyte as employed in primary systems could be one method to further reduce zinc species migration. To improve the electrode utilisation, selection of additives other than P.V.A. could be investigated. An alternative route could be to increase the hydroxyl ion concentration slightly. However, this would lead to higher solubilities and the possibility of dendrite growth etc. The use of one layer of microporous separator could be employed to mitigate this problem.

The overall conclusion to this work is that the system developed is capable of delivering reasonable capacity without the need for expensive separator systems. With further work it should mature into a worthy competitor to the nickel-cadmium system which has obvious environmental drawbacks.

References

1. A. Volta, Phil. Trans. Roy. Soc., 90 (1800) 403
2. J.F. Daniell, Phil. Mag., III, 8 (1836) 421
3. W. Grove, Phil. Mag., III, 15 (1839) 287
4. G. Leclanché, French Patent No., 71865 (1868)
5. G. Planté, Compt. Rend. Acad. Sci., 49 (1859) 402
6. F. Lalande and G. Chaperon, French Patent No., 143 644 (1881)
7. A. Dun and F. Hasslacher, British Patent No., 1862 (1887)
8. T. de Michalowski, British Patent No., 15 370 (1899)
9. W. Junger, Swedish Patent No., 15 567 (1901)
10. T.A. Edison, British Patent No., 20 072 (1901)
11. J.J. Drumm and Celia Ltd., British Patent No., 365 125 (1930)
12. H. André, Bull. Soc. Franc. Electriciens, 1 (1941) 132
13. J. McBreen, J. Electrochem. Soc., 119 (1972) 1620
14. K.W. Choi, D.N. Bennion and J. Newman, J. Electrochem. Soc., 123 (1976) 1616
15. K.W. Choi, D. Hamby, D.N. Bennion and J. Newman, J. Electrochem. Soc., 123 (1976) 1628
16. J. Hendrikx, W. Visscher and E. Barendrecht, J. Appl. Electrochem., 16 (1986) 175
17. C.M. Shepard and H.C. Langelan, J. Electrochem. Soc., 114 (1967) 8
18. R.Vignaud, Societetes Diels Wonder, Fr. Demande, F.R. 2 567 328
19. Lucas Industries Ltd., U.K. Pat. No. GB 2 054 252B (1983)
20. J.S. Dunning, D.N. Bennion and J. Newman, J.Electrochem. Soc., 118 (1971) 1251
21. H. Helmholtz, Wied. Ann., 7 (1879) 377
22. A. Gouy, J. Phys., 9 (1910) 457
23. D.L. Chapman, Phil. Mag., 25 (1913) 475
24. O. Stern, Zeit. Elektrochem., 30 (1924) 508
25. D.C. Grahame, Chem. Rev., 41 (1947) 1441
26. M.A.V. Devanathan, J. O'M. Bockris and K. Müller, Proc. Roy. Soc., A 274 (1963) 55
27. H. Gerischer, Z. Physik. Chem., 50 (1905) 641

28. W. Kossel, Nacht. Ges. Wiss. Gottingen Math. Physik. K.l., (1927) 135
29. I.N. Stranski, Z. Physik. Chem., 136 (1928) 259
30. F.C. Frank, Discuss. Faraday Soc., 5 (1949) 48
31. W.K. Burton, N. Cabrerà and F.C. Frank, Phil. Trans. Roy. Soc., A 243 (1951) 299
32. M. Fleischman and H.R. Thirsk, Electrochimica Acta, 2 (1960) 22
33. J.A. Harrison and H.R. Thirsk, "Electroanal. Chem., Vol. 5", A.J. Bard ed., Marcel Dekker Inc., New York, (1971) 67
34. L.A. Matheson and N. Nichols, Trans. Electrochem. Soc., 73 (1938) 193
35. J.E.B. Randles, Trans. Faraday Soc., 44 (1948) 327
36. A. Sevcik, Czech. Chem. Commun., 13 (1948) 349
37. R.S. Nicholson and I. Shain, Anal. Chem., 36 (1964) 706
38. V.G. Levich, "Physico-Chemical Hydrodynamics", Prentice Hall, Englewood Cliffs, (1962)
39. A. Fleischer and J.J. Lander eds., "Zinc-Silver Oxide Batteries", J.Wiley and Sons Inc., New York, (1971)
40. R.V. Bobker, "Zinc in Alkali Batteries", The Society for Electrochemistry, University of Southampton, (1973)
41. R.D. Armstrong and M.F. Bell, "Electrochemistry"; Specialist Periodical Reports, The Chemical Society, 4 (1974) 1
42. J. McBreen and E.J. Cairns, "Adv. Electrochem. Electrochem. Eng., Vol. 11", H. Gerisher and C.W. Tobias eds., J. Wiley and Sons Inc., New York, (1978) 273
43. J. McBreen, J. Electroanal. Chem. and Interfacial Electrochem., 168 (1984) 415
44. R.J. Brodd and V.E. Ledger, "Encyclopedia of Electrochemistry of the Elements, Vol. 5", A.J. Bard ed., Marcel Dekker Inc., New York, (1976)
45. D.P. Gregory, P.C. Jones and D.P. Redfern, J. Electrochem. Soc.,119 (1972) 1288
46. T.P. Dirkse and R. Timmer, J. Electrochem. Soc., 116 (1969) 162
47. R.N. Snyder and J.J. Lander, Electrochem. Tech., 3 (1965) 161
48. A. Himy and O.C. Wagner, Proc. 27th Power Sources Symp., (1976) 135

49. O.C. Wagner and A. Himy, Proc. 28th Power Sources Symp., (1978) 167
50. J. McBreen and E. Gannon, Electrochimica Acta, 26 (1981) 1439
51. J. McBreen and E. Gannon, J. Electrochem. Soc., 130 (1983) 1980
52. E.G. Gagnon, J. Electrochem. Soc., 133 (1986) 1989
53. E.G. Gagnon and B.S.Hill, J. Electrochem. Soc., 137 (1990) 377
54. D.M. McArthur, Paper 859054, 20th I.E.C.E.L. Proc. Miami (1985)
55. R.A. Sharma, J. Electrochem. Soc., 135 (1988) 1875
56. E.G. Gagnon and Y-M. Wang, J. Electrochem. Soc., 134 (1987) 2091
57. A. Charkey, European Patent No. 0048 009 (1981)
58. J. McBreen and E. Gannon, J. Power Sources, 15 (1985) 169
59. C. Biegler, R.L. Deutscher, S. Fletcher, S. Hua and R. Woods, J. Electrochem. Soc., 130 (1983) 2303
60. R.L. Deutscher, S. Fletcher and J. Galea, J. Power Sources, 11 (1984) 7
61. A.S. Berchelli and R.F. Chireau, U.S. Patent No. 4041 221 (1977)
62. A. Charkey, Proc. 26th Power Sources Symp., (1974) 87
63. J. Goodkin, Proc. 22nd Power Sources Symp., (1968) 79
64. A. Charkey, Power Sources 4 (1973) 93
65. Energy Research Corp., British Patent No.1 476 550 (1977)
66. A. Duffield, P.J. Mitchell, N. Kumar and D.W. Shield, J. Power Sources 15 (1985) 93
67. S.P. Poa and S.J. Lee, J. Appl. Electrochem, 9 (1979) 307
68. M. Cenek, O. Kouril, J. Sandera, A. Tousková and M. Calábek, Power Sources 6, (1977) 215
69. N.A. Hampson and A.J.S. McNeil, J. Power Sources, 15 (1985) 245
70. N.A. Hampson and A.J.S. McNeil, J. Power Sources, 15 (1985) 261
71. N.A. Hampson and A.J.S. McNeil, J. Power Sources, 15 (1985) 61
72. A. Duffield, Power Sources 11 (1987), 253
73. A. Duffield, PhD Thesis, Loughborough University of Technology, (1986)
74. A. Duffield, Chemistry and Industry, 2 (1988) 88

75. J. Sandera, A Touskova, M. Cenek and O.Kouril, 28th meeting I.S.E.,28 (1977) 381
76. J.A. Keralla and J.J. Lander, Electrochem. Technology, 6 (1968) 202
77. F. Mansfeld and S. Gilman, J. Electrochem. Soc., 117 (1970) 588
78. J.W. Diggle and A Damjanovic, J. Electrochem. Soc., 119 (1972) 1649
79. J.W. Diggle and A. Damjanovic, J. Electrochem. Soc., 117 (1970) 65
80. J. O'M Bockris, J.W. Diggle and A. Damjanovic, 1st Quarterly Report to NASA - contract NGR 39-010 002, (1969)
81. F. Mansfeld and S. Gilman, J. Electrochem. Soc., 117 (1970) 1154
82. I.N. Justinijanovic, J.N. Jovicevi and A.R. Despic, J. Appl. Electrochem., 3 (1973) 193
83. J.E. Oxley, NASA Report CR-377 (1966)
84. N.N. Flerov, J. Appl. Chem. (U.S.S.R.), 30 (1955) 1326
85. N.N. Flerov, J. Appl. Chem. (U.S.S.R.), 33 (1960) 134
86. A. Marshall and N.A. Hampson, J. Electroanal. Chem. and Interfacial Electrochem.,53 (1974) 133
87. J.S. Drury, N.A. Hampson and A. Marshall, J. Electroanal. Chem. and Interfacial Electrochem., 50 (1974) 292
88. J.D.H. Julian, U.K. Patent No. GB 2 083 683A, (1982)
89. M. Eisenberg, U.S. Patent No. 4 224 391 (1980)
90. G. Feuillade and P. Cord, U.S. Patent No. 3 849 199 (1974)
91. E.J. Carlson, U.S. Patent No. 4 273 841 (1981)
92. R.F. Thornton, U.S. Patent No. 4 247 610 (1981)
93. R.F. Thornton and E.J. Carlson, J. Electrochem. Soc., 127 (1980) 1448
94. J.T. Nichols, F.R. McLarnon and E.J. Cairns, Chem. Eng. Commun., 38 (1985) 357
95. P. Ruetschi, U.S. Patent No. 3 160 520 (1964)
96. T.P. Dirkse and R. Shoemaker, J. Electrochem. Soc., 115 (1968) 784
97. C. Cachet, Z. Chami and R. Wiart, Electrochimica Acta, 32 (1987) 465
98. E. Frackowiak and M.Kiciak, Electrochimica Acta, 33 (1988) 441

99. N.C. Cahoon, "The Primary Battery Vol. 2", G.W. Heise and N.C. Cahoon eds., J. Wiley and Sons Inc., New York, (1971)
100. J.T. Lundquist, J. Membrane Science, 13 (1983) 337
101. C.M. Rosser and R.A. Glinski, U.S. Patent No. 3 224 907 (1965)
102. C. Oberholzer, A.J. Salkin and E. Weiss, 2nd and 3rd Quaterly Reports to NASA contract NA 5-2860 (1963)
103. K.V. Lovell and L.B. Adams, Royal Military College of Science, Technical Note PD/25/81, (1981)
104. D.W. Sheibley, M.A. Mazo and O.D. Gonzalez-Sanabria, J. Electrochem. Soc., 130 (1983) 255
105. D.W. Sheibley, NASA Technical Memorandum, TM X-3199, (1975)
106. W.H. Philipp and C.E. May, NASA Technical Memorandum, TM X-3357, (1976)
107. D.W. Sheibley, NASA Technical Memorandum, TM X-3465, (1976)
108. I.A. Angres, W.P. Kilroy and J.V. Duffy, Proc. 28th Power Sources Symp., (1978) 162
109. C. Berger and F.C. Arrance, U.S. Patent No. 3 379 569 (1968)
110. O.C. Wagner, A. Almerini and R.L. Smith, Proc. 29th Power Sources Symp., (1981) 237
111. A. Himy and O.C.Wagner, U.S.Patent No.4 192 908, (1980)
112. Y. Sato, M. Kanda, H. Niki, M. Heno, K. Murata, T. Shirogami and T. Takamura, J. Power Sources, 9 (1983) 147
113. D.N. Bennion, "Review of Membrane Separators and Zinc-Nickel Oxide Batteriy Development", D.E. 83 011 663 (1980)
114. S. Aroueté, K.F. Blurton and H.G. Oswin, J. Electrochem. Soc., 116 (1969) 166
115. J.J. Smithrick, Proc. 15th Inter. Soc. American Inst. of Aeronautics and Astronautics, (1980) 1203
116. J. McBreen, E. Gannon, D.T. Chin and R. Sethi, J. Electrochem. Soc., 130 (1983) 1641
117. O.C. Wagner, Report No. 5, U.S. Army Electronics R and D Command, Fort Monmoth, (1982)
118. O.C. Wagner and A. Almerini, Proc. 31st Power Sources Symp., (1984) 255

119. M.H. Katz, T.C. Adler, F.R. McLarnon and E.J. Cairns, J. Power Sources, 22 (1988) 77
120. D.T. Chin and S. Venkatesh, J. Electrochem. Soc., 128 (1981) 1439
121. K. Appelt and K. Jurewicz, J. Power Sources, 5 (1980) 235
122. K. Appelt and K. Jurewicz, Electrochimica Acta, 27 (1982) 1701
123. L. Binder and K. Kordesh, Electrochimica Acta, 31 (1986) 255
124. M.B. Liu, G.M. Cook, N.P. Yao and J.R. Selman, J. Electrochem. Soc.,129 (1982) 913
125. O. Von Krusentierna, Power Sources 6 (1976) 303
126. Exide Management and Techonology Company, Annual Report for 1979 on Ni/Zn batteries for electric vehicle propulsion, ANL/OEPM-79-12, (1980)
127. N.A. Hampson and M.J. Tarbox, J. Electrochem. Soc., 110 (1963) 95
128. E.A. Schumacher, "The Primary Battery Vol. 1", G.W. Heise and N.C. Cahoon eds., J. Wiley and Sons, New York, (1971)
129. T.A. Friend, F. Gutmann, and T.W. Hayes eds., "Fuel Cells : Proc. 1st Australian Conf. Electrochem., Ch 3", Pergammon, New York, (1965) 673
130. R.C. Weast ed.,"C.R.C. Handbook of Chemistry and Physics, 65th Edition", C.R.C. Press Inc., Florida, 1985
131. N.A. Hampson, M.J. Tarbox, J.T. Lilley and J.P.G. Farr, J. Electrochem. Soc., 2 (1964) 309
132. R.N. Elsdale, N.A. Hampson, P.C. Jones and A.N. Strachan, J. Applied Electrochem., 2 (1964) 309
133. J.P.G. Farr and N.A. Hampson, J. Electrochem. Technology, 6 (1968) 10
134. M. Barack ed., "Electrochemical Power Supplies: Primary and Secondary Batteries", Inst. Elect. Engineers, London, Peter Peregrinues, (1980)
135. W. Morrison, U.S. Patent No., 975 885 (1910)
136. P.C. Morgan, Ph.D. Thesis, Loughborough University of Technology (1983)
137. N. Ingri, Acta Chem. Scand., 17 (1963) 581
138. F.A. Schneider and Z. Dominiczak, Power Sources 4 (1972) 115

139. T.P. Dirkse and N.A. Hampson, J. Electroanal. Chem. and Interfacial Electrochem., 35 (1972) 7
140. T.P. Dirkse and N.A. Hampson, Electrochimica Acta, 17 (1972) 135
141. J. O'M Bockris, Z. Nagy and A. Damjanovic, J. Electrochem. Soc., 119 (1972) 285
142. Y-C. Chang and G. Prentice, J. Electrochem. Soc., 131 (1984) 1465
143. M.W. Breiter, Electrochimica Acta, 15 (1970) 1297
144. M.W. Breiter, Electrochimica Acta, 16 (1971) 1169
145. L.M. Baugh, Electrochimica Acta, 24 (1979) 657
146. L.M. Baugh and A. Higginson, Electrochimica Acta, 30 (1985) 1163
147. L.M. Baugh and A.R. Baikie, Electrochimica Acta, 30 (1985) 1173
148. M.N. Hull, J.E. Ellison and J.E. Toni, J. Electrochem. Soc., 117 (1970) 192
149. R.D. Armstrong and G.M. Bulman, J. Electroanal. Chem. and Interfacial Electrochem.,25 (1970) 121
150. K. Huber, J. Electrochem. Soc., 100 (1953) 376
151. Z.Ya Nikitina, J. Appl. Chem. (U.S.S.R.) 31 (1958) 209
152. R.W. Powers and M.W. Breiter, J. Electrochem. Soc., 116 (1969) 719
153. M.C.H. McKubre and D.D. Macdonald, J. Electrochem. Soc., 128 (1981) 524
154. R.W. Powers, J. Electrochem. Soc., 116 (1969) 1652
155 P.L. Cabot, M. Cortés, F.A. Centellas, J. Garrido and E. Pérez, J. Electroanal. Chem. and Interfacial Electrochem., 201 (1986) 85
156. I. Sanghi and M. Fleischmann, Electrochimica Acta, 1 (1959) 161
157. G.S. Vozdvizhenskii and E.D. Kochmann, Russ. J. Phys. Chem., 39 (1965) 347
158. N.F. Harman, P.J. Mitchell and B. Buffham, "Electrochemical Engineering 1989", Inst. Chem. Eng. Symp. Series 112, Hemisphere Publishing Corp., New York, (1989) 177

159. M.G. Chu, J. McBreen and G. Adzic, J. Electrochem. Soc., 128 (1981) 2281
160. J. McBreen, M.G. Chu and G. Adzic, J. Electrochem. Soc., 128 (1981) 2286
161. G.T. Rodgers and K.J. Taylor, J. Electroanal. Chem. and Interfacial Electrochem., 167 (1986) 251
162. A.R. Despic and M.G. Pavloic, Electrochimica Acta, 27 (1982) 1539
163. R. Viswanathan, S. Sampath and H.V.K. Udupa, J. Mines and Metal Fuels, 9 (1961) 15, 34
164. C. Herring and M.H. Nichols, Rev. Mod. Phys., 21 (1949) 185
165. J.M. Baker and J.M. Blakeley, Surf. Sci., 2 (1972) 45

LIST OF SYMBOLS

A	Area or amperes
$A_{f,b}$	Arrhenius constant for forward/backward reaction
b	Tafel slope or backward reaction
C	Capacity of an electrode or concentration of a species
C_{dl}	Double layer capacitance
$C_{compact}$	Differential capacitance of compact layer
$C_{diffuse}$	Differential capacitance of diffuse layer
$C_{o,R}^{\infty}$	Bulk concentrations of oxidised/reduced species
$D_{o,R}$	Diffusion coefficient of oxidised/reduced species
E	Electrode potential on a suitable reference scale
$E^{\ominus}$	Standard electrode potential
F	Faraday's constant
f	Forward reaction
$G^{\ddagger}$	Activation energy
i	Current or current density
i_d	Diffusion limited current
$i_{f,b}$	Forward or backward current density
i_o	Exchange current density
$J_{subscript}$	Flux of species subscript
$k_{f,b}$	Potential dependent rate constants for forward and backward reactions
k_s	Specific rate constant at $E^{\ominus}$
$k^{\ominus}$	Standard rate constant
M	Mol, Molar
O	Oxidised species
q	Flux
R	Reduced species or gas constant
T	Temperature
t	Time
V	Volts
$\bar{v}$	Vector operation
x	Distance
z	Number of electrons

LIST OF SYMBOLS (Cont.)

α	Charge transfer coefficient
δ	Diffusion boundary layer thickness
ϕ	Electrostatic potential
η	Charge transfer overpotential
υ	Kinematic viscosity and sweep rate
ω	Angular frequency